University of Colorado, Boulder
CU Scholar

Civil Engineering Graduate Theses & Dissertations Civil, Environmental, and Architectural Engineering

Spring 1-1-2016

Advancement of Performance-Based Earthquake Engineering for RC Frame Buildings: Application to Retrofit Design and Consideration of Vertical Ground Motions

Cody Conroy Harrington
University of Colorado at Boulder, ccharrin@gmail.com

Follow this and additional works at: https://scholar.colorado.edu/cven_gradetds

 Part of the Construction Engineering Commons

Recommended Citation
Harrington, Cody Conroy, "Advancement of Performance-Based Earthquake Engineering for RC Frame Buildings: Application to Retrofit Design and Consideration of Vertical Ground Motions" (2016). *Civil Engineering Graduate Theses & Dissertations*. 50.
https://scholar.colorado.edu/cven_gradetds/50

This Dissertation is brought to you for free and open access by Civil, Environmental, and Architectural Engineering at CU Scholar. It has been accepted for inclusion in Civil Engineering Graduate Theses & Dissertations by an authorized administrator of CU Scholar. For more information, please contact cuscholaradmin@colorado.edu.

ADVANCEMENT OF PERFORMANCE-BASED EARTHQUAKE ENGINEERING FOR RC FRAME BUILDINGS: APPLICATION TO RETROFIT DESIGN AND CONSIDERATION OF VERTICAL GROUND MOTIONS

by

CODY C. HARRINGTON

B.S. California Polytechnic State University, San Luis Obispo

M.S. University of Colorado, Boulder

A thesis submitted to the

Faculty of the Graduate School of the University of Colorado in partial fulfillment

of the requirement for the degree of

Doctor of Philosophy

Department of Civil, Environmental, and Architectural Engineering

2016

This thesis entitled:
Advancement of Performance-Based Earthquake Engineering for RC Frame Buildings:
Application to Retrofit Design and Consideration of Vertical Ground Motions
written by Cody C. Harrington
has been approved for the Department of Civil, Environmental, and Architectural Engineering

_____
(Abbie Liel)

_____
(Keith Porter)

_____
(Petros Sideris)

_____
(Ross Corotis)

_____
(Siamak Sattar)

Date_____

The final copy of this thesis has been examined by the signatories, and we
find that both the content and the form meet acceptable presentation standards
of scholarly work in the above mentioned discipline

Harrington, Cody Conroy (Ph.D., Civil Engineering, Department of Civil, Environmental, and Architectural Engineering)

Advancement of Performance-Based Earthquake Engineering for RC Frame Buildings: Application to Retrofit Design and Consideration of Vertical Ground Motions

Thesis directed by Associate Professor Abbie B. Liel

ABSTRACT

Performance-based earthquake engineering (PBEE) provides a framework to quantitatively assess the seismic risks to buildings and explicitly consider building seismic performance in the design process. This thesis utilizes PBEE to enhance the understanding of the seismic performance of RC frame buildings by: (1) estimating the performance of buildings retrofit to standardized levels using existing retrofit design documents; (2) quantifying improvements in seismic performance possible through retrofit design; (and 3) evaluating the vulnerability of reinforced-concrete (RC) buildings to vertical ground shaking.

To evaluate the performance of retrofit RC frame buildings, a set of 3-, 6-, and 9 story RC frame buildings is designed to the Uniform Building Code of 1967 (International Conference of Building Officials, 1967). 1967 buildings are then retrofit to ASCE 41 standards (ASCE, 2013). The performance of each building is evaluated using a rigorous PBEE framework developed by the Pacific Earthquake Engineering Research (PEER) Center and damage observations are compared with ASCE 41 estimated damage levels. In many cases, retrofit buildings perform better than ASCE

41 performance definitions. In other cases, the performance of retrofit buildings appears to be consistent the ASCE 41's stated performance goal.

Subsequently, improvements in seismic performance from retrofitting are quantified though the identification of dimensionless indicators of retrofit effectiveness. Here, improvements in performance - i.e. retrofit effectiveness - are defined as reductions in collapse risk (quantified by the mean annual frequency of collapse) and earthquake-induced repair costs. The results demonstrate that a combination of strength-based and ductility-based indicators best describes improvements in mean annual frequency of collapse from seismic retrofitting. However, strength-based indicators (particularly those that relate strength capacity to the spectral demand) are correlated with reductions in earthquake-induced repair costs.

Finally, the vulnerability of ductile and nonducitle RC buildings to vertical ground shaking is quantified using PBEE methods. Building geometries include symmetric layouts and layouts that contain cantilever overhangs. Results show that the performance of buildings containing cantilevered sections is more impacted by vertical ground shaking than the performance of buildings with symmetric layouts. Furthermore, nonductile buildings are found to be more severely impacted by vertical ground shaking than ductile buildings.

DEDICATION

I would like to thank my Ph.D. advisor, Professor Abbie Liel, for her support and guidance. I feel extremely fortunate to have had the opportunity to work with such a dedicated, understanding, and knowledgeable individual. Her schedule is typically packed, yet she always made my research feel like a priority. She gave me the freedom to explore topics that I found interesting and gave me the opportunity to be involved with collaborative projects such as the Applied Technology Council Project 78. I came to Colorado for a Master's degree, the relationship I built with Dr. Liel during that time played a large part in my decision to pursue a Ph.D.

I would like to thank Drs. Bruce Ellingwood, Michael Mehrain, Keith Porter, Petros Sideris, Ross Corotis, Siamak Sattar, and Balaji Rajagopalan for their input to this thesis. Drs. Curt Haselton and Meera Raghunandan provided some of the building models that were used in the analysis of vertical ground motions.

The members of the ATC 78 project taught me a great deal about building code development and how to strike a balance between the complexity of academic research and the necessity for simplified analysis procedures for use in practice. The most brilliant ideas will rarely be used if they are too complex to apply efficiently. I would specifically like to thank Bill Holmes, Prof. Jack Moehle, Dr. Mike Mehrain, Dr. Bob Hanson, Peter Somers, Jon Heintz, and Christopher Rojahn for their guidance. I am grateful to the other members of the working group, Siamak Sattar, Travis Marcilla, Panagiotis Galanis, Carlos Arteta, and Pablo Parra. Skill I learned from working on this project served to greatly improve my personal research.

My officemates, Siamak Sattar, Meera Raghunandan, Derek Kozak, Yolanda Lin, Sarah Welsh-Huggins, Holly Bonstrom, Emily Elwood, Lan Nguyen, Karim Farokhnia, Rob Chace, and Travis Marcilla have made school-life relaxed and enjoyable. I am grateful to them for keeping the work environment light-hearted and for all the feedback they have provided during our research group meetings. It's been a pleasure to work with such a talented group of people and to have learned from their research. Living encased in a concrete block has helped developed long-lasting relationships that I'm not sure could been possible in an office "with a view".

I am forever grateful for the love and support I've received from friends and family along the way. My parents, Jack and Kit Harrington, have always valued education and done everything in their power to support me during my academic career. The time I spend with my sisters, Austyn and Brette, is a welcomed release from study. I always return feeling refreshed and motivated after being with them. They are amazing individuals whom I greatly admire. A special thanks to my girlfriend Jenny Lee. The passion and dedication she brings to teaching is inspiring and has helped motivate me, especially during the last few months. I cherish the time we spend together outdoors on weekends, or over meals at home. Her patience, compassion, and encouragement have been invaluable.

TABLE OF CONTENTS

LIST OF TABLES

LIST OF FIGURES

1 INTRODUCTION

Performance-based earthquake engineering (PBEE) differs from traditional, prescriptive design, such as load-and-resistance factor design (LRFD), in that PBEE evaluates structural performance at the system level, whereas prescriptive methods like LRFD primarily define performance at the component level. PBEE includes desired performance directly in the design process, thereby providing engineers with a framework to create designs that meet the needs and expectations of stakeholders, including clients, insurers, and governing jurisdictions. As developed by researchers in the past 15 years, PBEE is comprised of four phases: hazard analysis, structural analysis, damage analysis, and loss analysis. PBEE quantifies seismic hazard, building vulnerabilities, and expected losses probabilistically, facilitating risk-informed decision making (Porter, 2003). This dissertation assess the seismic risk of reinforced concrete (RC) buildings, specifically those that have been seismically retrofit, and when vertical ground shaking is included in the hazard analysis. These research topics are addressed through the use of advanced nonlinear modeling techniques and robust simulation methods. Results and recommendations are presented herein that aim to advance the current state of practice with respect to PBEE, especially applied to RC buildings.

In addition to this introductory chapter, this dissertation has four additional chapters. Chapters 2 and 3 are written as stand-alone works that are intended for publication. However, both chapters are based upon results from a common set of buildings. Therefore, referencing exists between sections concerning building design and modeling in chapters 2 and 3. Chapter 4 is an article that has been published in *Earthquake Engineering and Structural Dynamics*. Chapter

5 presents conclusions, limitations, and future work relevant to all previous chapters. Due to the format of this thesis, some content in introductory and background sections from different chapters may be repetitive.

Chapter 2 quantifies the performance obtained from retrofitting a set of buildings RC frame buildings to a standardized level. The performance is computed through a rigorous PBEE framework, and compared to approximate damage definitions for the standardized design performance level. ASCE 41-13 is the most widely used standard for seismic retrofit and is based upon the FEMA 356 (FEMA and ASCE, 2000) and FEMA 273 (Applied Technology Council, 1997) documents, which were the first documents to standardize PBEE for use in practice (Pekelnicky & Poland, 2012; Sattar & Hulsey, 2015; Porter, 2003). During an ASCE 41 evaluation and/or retrofit, a Performance Level (PL) is selected that best describes the desired global performance of a building. POs are defined by ASCE 41 at the system level, and include information such as the overall damage estimates, damage estimates for structural components, and damage estimates for nonstructural components conditioned on the design level earthquake. Despite the selection of a global performance objective, ASCE 41 calculations related to demand, capacity, and acceptance are carried out on a component-by-component basis. Furthermore, non-compliance with the selected global PO occurs when one or more components fail and global performance of the building is only assessed to obtain component demands.

To investigate retrofit buildings designed according to this standard, a set of 3-, 6-, and 9-story buildings is designed to the Uniform Building Code of 1967 (International Conference of Building Officials, 1967). These buildings exhibit deficiencies such as shear-critical columns, weak-

column to strong-beam arrangements, and overall weakness. The 1967 buildings are then retrofit according to ASCE 41 to comply with four distinct performance levels using steel or concrete jackets or fiber-reinforced polymer (FRP) wraps. Following the PBEE framework, the performance of the retrofitted buildings is assessed in terms of earthquake-induced repair costs, where a loss analysis is conducted in accordance with FEMA P-58 (FEMA, 2012). Significant variation in the performance of buildings retrofit to the same performance level is observed. In many cases, the performance of retrofit buildings is shown to be better than the damage estimates provided by ASCE 41 Section 2-3 and Table C2-3. However, the performance of some buildings match the ASCE 41 estimated damage levels, and none of the studied buildings perform worse than the ASCE 41 approximation This study provides a first step in estimating economic losses for a large set of RC frame buildings retrofit to ASCE 41 levels.

Chapter 3 steps away from standardized PBEE evaluation, seeking to identify characteristics of retrofit buildings – quantified through dimensionless retrofit indicators – that correspond with improvements in seismic performance. The same set of buildings developed in chapter 2 is leveraged in chapter 3. Retrofit indicators are intended to be simple measures that provide information on the benefits in collapse capacity and economic loss achievable through seismic retrofit. The considered retrofit indicators include improvement in strength and ductility through retrofitting, and design parameters that are indicative of deficiencies in 1967 buildings. The relationships between retrofit indicators and Decision Variables (DV) are evaluated. DVs considered in this study are mean annual frequency of collapse and annualized earthquake-induced repair cost. A combination of strength-based and ductility based indicators is found

effective when the DV is mean annual frequency of collapse. Strength-based indicators, particularly those that contain estimates of both seismic capacity and demand, are most related to improvements in annual repair cost though retrofitting. This research shows that a weak correlation exists between mean annual frequency of collapse and annualized repair costs (ρ = 0.38). This is an important finding because it suggests that retrofit designs that specifically focus on reducing mean annual frequency of collapse, or collapse risk, do not always mitigate earthquake induced repair costs. Therefore, it is important for resilient designs to consider both DVs independently in the design process.

Chapter 4 uses PBEE to evaluate the seismic vulnerability of RC structures when vertical ground motions are included as part of the hazard. This chapter quantifies ground motion parameters that are capable of predicting trends in building collapse due to vertical shaking, identifies the types of buildings that are most likely affected by strong vertical ground motions, and investigates the relationship between element level responses and structural collapse under multi-directional shaking. To do so, two sets of incremental dynamic analyses (IDA) are run on five nonlinear building models of varying height, geometry, and design era. The first IDA is run using the horizontal component alone; the second IDA applies the vertical and horizontal motions simultaneously. When ground motion parameters are considered independently, acceleration-based measures of the vertical shaking best predict trends in building collapse associated with vertical shaking. When multiple parameters are considered, Housner intensity (SI), computed as a ratio between the Housner intensity of the vertical (SI_V) and horizontal (SI_H) components of a record (SI_V/SI_H), predicts the significance of vertical shaking for collapse. The building with

extensive structural cantilevered members is the most influenced by vertical ground shaking, but all frame structures (with either flexural and shear-critical columns) are impacted. In addition, the load effect from vertical ground motions is found to be significantly larger than the nominal value used in U.S. building design.

2 LINKING ELEMENT-BASED EVALUATION AND RETROFIT STRATEGIES TO GLOBAL STRUCTURAL PERFORMANCE FOR RC FRAME BUILDINGS

2.1 Introduction

Performance-based earthquake engineering (PBEE) has emerged as a preferred method for seismic design and building rehabilitation. As opposed to load-and-resistance-factor design (LRFD) and other design strategies, PBEE explicitly defines a seismic performance objective based on the importance and occupancy of the structure and quantifies the future seismic risk for comparison with this objective. This approach allows the designer more control in terms of identifying an efficient design solution and risk mitigation strategy, providing meaningful metrics by which to assess the structure and design alternatives (Maison, Kasai, & Deierlein, 2009; Porter, 2003).

In the U.S., the most widely used and accepted standard employing PBEE for seismic evaluation and retrofit of reinforced-concrete (RC) buildings is ASCE/SEI 41-13 (ASCE, 2013), hereafter referred to as ASCE 41 (Sattar & Hulsey, 2015; Pekelnicky & Poland, 2012). ASCE 41 grew out of the FEMA 356 (FEMA and ASCE, 2000) and FEMA 273 (Applied Technology Council, 1997) documents, published in 2000 and 1997 respectively, which represented a first systematic effort to develop methods for PBEE that could be used in practice. ASCE 41 evaluates structural performance by comparing seismic demands to acceptance criteria (AC) for each element in the structure. The acceptance criteria depend on component ductility and strength. AC have been derived from experimental testing and analysis procedures based on principles of structural

dynamics, however, expert judgment is used when research is not available (Maison, Kasai, & Deierlein, 2009). AC are provided for many existing components, and have been updated over the three cycles of ASCE 41 publication. If ASCE 41 does not provide acceptance criteria for a building component, the analysist must prove the component behaves in a manner that complies with the selected performance level based on judgment.

The lack of data on the performance of retrofitted buildings during large scale seismic events in the U.S. drives us to study the performance of buildings retrofitted to standardized levels analytically. Furthermore, there has been a growing move toward evaluating design standards, to ensure they produce intended results. For example, the FEMA P-695 project concluded that modern-code designed buildings have less than 10% probability of collapse given the maximum considered earthquake (FEMA, 2009). Explicit definition of performance standards in this way aids in the development of code provisions for new structural systems and future code modifications.

In this study, 3, 6, and 9-story buildings are designed to the Uniform Building Code of 1967 (International Conference of Building Officials, 1967). Although nonductile RC frame buildings are only one category of existing building, they are potentially vulnerable, frequently considered as high risk or high priority candidates for retrofit, and often subject to ASCE 41 type analyses. A small set of 1967 buildings is analyzed, however the deficiencies contained in this buildings set such as shear critical columns, weak-column to strong-beam arrangements, and overall weakness are deficiencies that are commonly found in RC frame buildings constructed during this time. Each building is retrofit to meet ASCE 41 Collapse Prevention (CP), Life Safety (LS), and Immediate

Occupancy (IO) performance levels. In addition, multiple retrofit techniques are considered for each performance level: column jacketing using steel or concrete jackets, and wrapping columns in fiber-reinforced-polymer (FRP) wraps. These three local retrofit strategies are selected for this study because they improve structural characteristics, such as strength and ductility, with little impact to the architectural design of the structure. To assess the retrofit structures, structural responses, seismic-induced damage, and economic losses are estimated by nonlinear models and the FEMA P-58 methodology (FEMA, 2012). Structural performance metrics and estimated losses are then compared to the qualitative descriptions of the ASCE 41 Performance Levels (PL). This comparison serves to benchmark ASCE 41 PLs against analytical building responses, and provides a direct comparison between element-based retrofit strategies and anticipated global-level performance benefits.

2.2 Overview of ASCE 41 Evaluation and Retrofit Processes

ASCE 41 may be used for seismic evaluation and/or seismic retrofit. It is common for an ASCE 41 retrofit design to be performed if it is first shown that a building does not comply with a chosen PL during an ASCE 41 evaluation. A description of both processes and their similarities and differences is provided below.

2.2.1 ASCE 41 Evaluation Process

Unlike more traditional evaluation procedures, ASCE 41 is “performance based”, and the first steps in an ASCE 41 evaluation is to select a performance objective, and then define building performance levels. Performance objectives link the seismic hazard level with structural and

nonstructural performance. Certain ASCE 41 objectives requires that performance be evaluated at two hazard levels, with two distinct performance objectives (see Table 2-1).

Building performance levels are a combination of structural and nonstructural performance levels and represent discrete damage states a building could experience during an earthquake (ASCE, 2013). While building performance is a combination of the performance of the structural system and nonstructural system and contents, these are considered separately in an ASCE 41 evaluation with unique structural and nonstructural performance levels (FEMA, 1997).

The three main structural performance levels are Collapse Prevention (CP), Life Safety (LS), and Immediate Occupancy (IO); these are listed in order of increasing seismic resistance. According to the ASCE 41 Section 2.3, at the CP level, the structure is severely damaged and any additional deformation may cause instability leading to collapse. At the LS level, a moderate amount of damage has occurred, the structure's stiffness and strength have been reduced, but it retains significant deformation capacity. At the IO level, a limited amount of damage has occurred and the structure retains a significant amount of its initial strength and stiffness. Figure 2-1 presents an example of the ASCE 41 structural performance levels as they relate to the force-deformation response of ductile and nonductile structures. More detailed definitions of the structural performance levels are presented in subsequent sections. Four nonstructural performance levels are defined: Operational, Position Retention, Life Safety, and Not Considered.

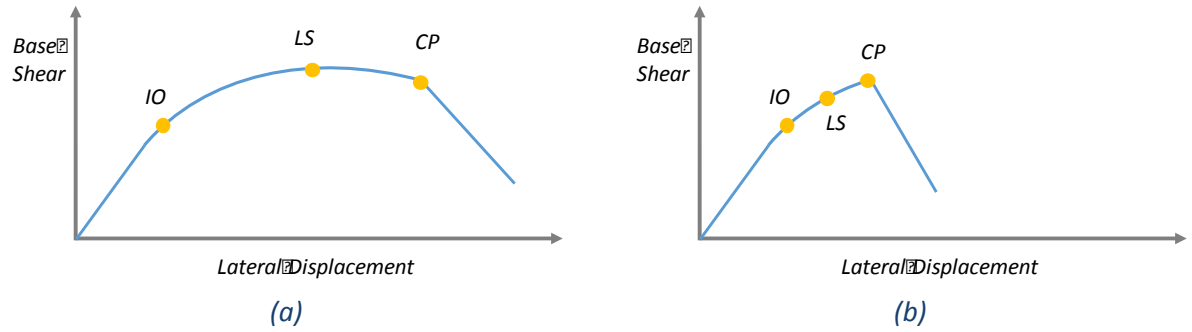

Figure 2-1 – ASCE 41 structural performance levels as they relate to structural deformation demands for (a) ductile structures and (b) nonductile structures

Next, the site seismic hazard is evaluated. In most cases the selected building performance objective dictates the level of shaking used in the analysis. For example, the Basic Performance Objective for Existing Buildings (BPOE) requires that the building be analyzed under two hazard levels: the BSE-1E motion (ground motion with probability of occurrence of 20% in 50 years at the site) and the BSE-2E motion (probability of occurrence of 5% in 50 years).

Three tiers of evaluation are permitted within ASCE 41. Tier 1 is a screening procedure in which the building is analyzed using a series of checklists that cover both structural and nonstructural components. Tier 1 procedures are meant to be easy to calculate, and therefore do not require the use of a computer model. Tier 2 procedures evaluate the potential deficiencies identified in Tier 1 in more detail by computing their demands and comparing them to capacities using acceptance criteria.

Tier 3 is a systematic calculation-based evaluation procedure. Tier 3 evaluations analyze the entire building in its current state. Deformation demands are computed using either linear static, linear dynamic, nonlinear static, or nonlinear dynamic procedures. The selection of an appropriate analysis procedure is based upon the structural geometry and building

characteristics. For example, static methods are not recommended for taller buildings where higher mode effects are important. In general, static procedures are intended to be more conservative than dynamic procedures and linear procedures are more conservative than nonlinear procedures. Computed demands are then compared against acceptance criteria for each building component; RC column and beam demands are typically quantified in terms of deformations. For a building to comply with an ASCE 41 performance level, all elements must satisfy these prescriptive acceptance criteria. The component limit states and modeling criteria have been developed based on test data, and several of the tables with modeling parameters and acceptance criteria for various components have been updated and improved in recent years, *e.g.* Elwood, et al. (2007). The remainder of this paper will consider the Tier 3 evaluation procedure because it is the least conservative procedure, and the one most commonly used in practice.

Historically, seismic retrofit of most building types (including RC frames) has been voluntary, leaving the engineer to decide which type of evaluation is performed. Often, this choice is dictated by economic limitations. Recently, Los Angeles passed a mandatory retrofit ordinance for older RC buildings (City of Los Angeles, 2015). ASCE 41 is listed as an accepted evaluation method, where buildings are required to meet or exceed requirements for the Basic Safety Objective to avoid triggering retrofit requirements. Tier 1, 2, and 3 evaluations are permitted, leaving the decision up to the engineer (SEAOSC, under review).

2.2.2 ASCE 41 Retrofit Process

The ASCE 41 retrofit process has many similarities with the evaluation process. First, a performance objective is set, building performance levels are defined, and the site hazard is analyzed. These steps are conducted as they are described in the section above.

During an ASCE 41 retrofit, only Tier 2 and Tier 3 procedures are permitted. Tier 2 procedures retrofit the deficiencies identified in a Tier 2 evaluation until they are shown to comply with the desired performance objective. As with the Tier 3 evaluation, the Tier 3 retrofit process is a systematic procedure that considers all elements in the structure. First, a preliminary retrofit scheme is selected and designed. The structural system is then analyzed through the same evaluation procedures, but with the building now including the retrofit measures. The retrofit scheme is modified until all building components are shown to comply with the desired performance objective.

2.3 Previous Studies that Evaluate the Performance Obtained from Designing to ASCE 41 Levels

Multiple studies have been conducted on particular aspects or sections of ASCE 41. What follows is a selection of studies that specifically examine analytical models or laboratory tests related to ASCE 41's building performance levels. Studies that evaluate the performance of buildings retrofit to ASCE 41 standards are important because of the limited number of observations of performance of buildings designed to ASCE 41 during large earthquakes. In addition, there is an inherent level of uncertainty in the ASCE 41 performance levels because of

the limited data from tests – which are themselves component or subassembly based - and post-earthquake reconnaissance is available for calibration. Therefore, it is difficult to show that buildings designed to unique performance levels behave in the manners described by ASCE 41 during design level shaking.

Maison, Kasai, and Deierlein (2009) performed an ASCE 41 evaluation of a full-scale 4-story welded steel moment frame building that was shaken to collapse on the E-Defense shake table. The building was evaluated for the CP performance level using linear and nonlinear procedures. ASCE 41 had mixed results when predicting the response of the laboratory test. However, the predictions generally fell on the conservative side, predicting collapse at lower intensities than were observed in the experiment. In terms of evaluation, the ASCE 41 linear dynamic procedure, nonlinear static procedure, and nonlinear dynamic procedures showed that the building failed the CP acceptance criteria when it was essentially linear-elastic. Therefore, the ASCE 41 CP performance level was shown to be very conservative, essentially predicting a collapse capacity of half that observed in the experiment. However, the same study found ASCE 41 to be an effective retrofit design tool because it correctly identified the deficient members that lead to collapse, therefore targeting the correct members for retrofit.

More recently, Sattar and Hulsey (2015) assessed the performance of a new, 4-story special RC frame building designed to ASCE 7 (ASCE, 2010) – the design standard for *new* buildings– using ASCE 41. The CP performance level was evaluated using a Tier 3 analysis. The assessment showed that the CP performance level for the new building was not met when the linear static procedure was used. However, the building was found to comply with the CP level

when the nonlinear dynamic procedure was used. This study indicates that the linear procedures in ASCE 41 are more conservative than the nonlinear procedures, due to their more simplified analysis techniques, and that the CP performance in ASCE 41 does not align with the performance level assumed in ASCE 7, *i.e*. is conservative in comparison to new design.

Harris and Speicher (2015) are also comparing seismic performance of an ASCE 7 code-compliant buildings and their performance as quantified using ASCE 41 analysis procedures. While Sattar and Hulsey (2015) focused on RC moment frames, Harris and Speicher (2015) investigated special steel moment frames, special concentrically-braced steel frames, and eccentrically-braced steel frames; a study of buckling-restrained braced frames is ongoing. It is difficult to link ASCE 7 with ASCE 41 because ASCE 41 component acceptance criteria are defined on a different basis than the seismic performance objective of ASCE 7, which aims to achieve less than 1% probability of collapse in 50 years (Luco, et al., 2007). Due to this inconsistency in the performance objectives of each document, the new steel buildings designed to ASCE 7 were shown to have difficulty satisfying the Basic Safety Objective in ASCE 41 (Harris & Speicher, 2015; Harris & Speicher, 2015). The authors propose that in order to link ASCE 41 with ASCE 7, future efforts should focus on what percentage of components needs to fail the CP criteria to achieve performance equivalent to that of modern buildings.

Results from the above studies suggest that some ASCE 41 evaluation methods are quite conservative. This conservatism stems in part from the element-based philosophy implemented in ASCE 41, in which the structure is said not to comply with a performance level if a *single* primary structural element does not satisfy the acceptance criteria. Some researchers believe

that, this “if one element fails, they all fail” approach is not representative of system level behavior as it neglects the effects of redundancy and load redistribution (Searer, Paret, & Freeman, 2008). In some ways, the idea of prescriptive, element-based acceptance criteria muddies the concept of performance-based engineering .

While most previous studies have focused on assessing ASCE 41 evaluation procedures, little work has been done to study the performance obtained from designing to ASCE 41 retrofit procedures. Complying with a performance objective does not necessarily mean an efficient retrofit design is achieved, where efficiency can be measured in terms of cost or seismic resistance of the structural system. In some cases, the cost of retrofitting to meet a desired performance objective may not be proportional to the benefit achieved. Pekelnicky and Poland (2012) argue that improving building performance by mitigating the most glaring deficiencies is more cost-effective. To address this issue, ASCE 41 allows existing buildings to be evaluated and retrofit to a seismic hazard with a return period lower than 5% in 50 years. However, evaluations are typically performed at two hazard levels, as shown in Table 2-1, where the larger hazard often governs the design.

2.4 Building Designs

In this study, a set of 3, 6, and 9-story, 5-bay, RC space frame buildings are designed to the 1967 Uniform Building Code (UBC). Frame geometries are shown in Figure 2-2; each space frame building has six such seismic resisting frames in each direction. Each 1967 building is then retrofit with concrete jacketing, steel jacketing, or fiber-reinforced polymer (FRP) to meet a

specified Basic Performance Objectives for Existing buildings (BPOE) defined in Table 2-1. Details of each retrofit design are presented below.

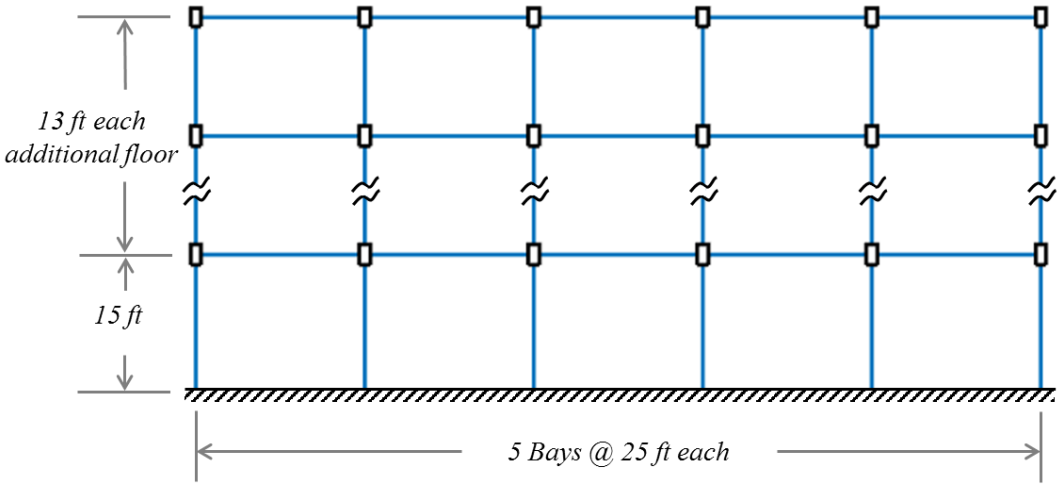

Figure 2-2 - Typical building elevation

RC space frame buildings are chosen for this study because they are common systems with design characteristics (i.e. strength and ductility) similar to other structural building types located in high seismic regions and are often retrofit due to their high seismic vulnerability. Heights of 3, 6, and 9-stories are chosen to represent low, mid, and high-rise RC fame buildings, while 5 bays are chosen based on the median number of bays for pre-1967 RC frames in the dataset of Los Angeles pre-1980 buildings compiled by The University of California, Berkeley and released by the *Los Angeles Times* (Lin II, Xia, & Smith, 2014). All buildings are located at a southern California site at 33.996°N, -118.162°W.

Table 2-1 - Performance Objectives used for seismic evaluation and retrofit

Performance Objective	*Structural Performance Level*	*Nonstructural Performance Level*	*Hazard Level*
BPOE for Risk Category I & II	CP	Not Considered	BSE-2E (5% /50 yrs)
	LS	Life Safety	BSE-1E (20% /50 yrs)
	LS	Not Considered	BSE-2E (5% /50 yrs)

BPOE for Risk Category IV	IO	Position Retention	BSE-1E (20% /50 yrs)

For simplicity, retrofit designs will henceforth be referred to by the structural performance level they satisfy. For example, a building that is said to comply with CP also has a nonstructural performance level that is not considered and is analyzed at the BSE-2E hazard level. Two LS structural PLs exist, which depend on the structure's risk category, as shown in Table 2-1. However, all pre-1967 buildings in this study comply with LS structural performance at the BSE-1E level before retrofit and therefore results for design level are not presented this study (a more detailed explanation is presented in subsequent sections).

2.4.1 1967 Buildings

A set of RC frame buildings is designed in accordance with loads in 1967 UBC (International Conference of Building Officials, 1967) and specifications in ACI 318-63 (ACI Committee 318, 1963). Loading is typical of an office building with a tar and gravel topping on the roof. For design purposes, internal element forces are calculated using beam equations as per 1967 UBC and the portal frame method, both typical of design practice during the 1960s. All elements are designed using Working Stress Design, the common design method in 1967, and transverse reinforcement consist of hooped, tied bars. The seismic design is based on the site in question and corresponds to Zone 3 in the 1967 UBC (the highest zone at that time). The buildings so-designed exhibit a number of common deficiency types. The considered building deficiencies include weak-first-stories, shear-critical columns, weak-column-strong-beam arrangements, and inadequate base shear strengths (*i.e.* overall weakness), as described in Table 2-2.

Table 2-2 - 1967 building properties

# Stories	# Bays	V_p/V_n [1]	M_c/M_b [2]	T_e [3] (sec)	V_y [4] (kips)	V_u [5] (kips)	Ductility[6]	$\mu_{strength}$ [7]	Deficiencies[8]
3	5	1.00	1.10	0.71	284	459	3.21	5.09	SC, WCSB, IS
6	5	1.10	1.02	0.99	577	744	2.68	4.54	SC, WCSB, IS
9	5	1.66	0.98	0.78	2507	2577	2.89	2.29	SC, WCSB

[1] - V_p is the maximum flexural capacity limited shear demand. V_n is the member shear capacity. V_p/V_n is calculated for each column and represents the expected failure mode. If $V_p/V_n \leq 0.6$ expected failure mode is flexure, $0.6 < V_p/V_n < 1.1$ failure mode is flexure-shear, and $V_p/V_n \geq 1.1$ member is expected to fail in shear. The building V_p/V_n is the average column V_p/V_n in the building weighted by axial load carried by each column.

[2] - M_c/M_b is the summation of the column expected flexural strengths over the summation of the beam expected flexural strengths in a story. The building M_c/M_b is the average story M_c/M_b.

[3] - T_e is the effective period as per Eqn. 7-27 of ASCE 41, calculated from pushover

[4] - V_y is the effective building yield strength as per Fig. 7-3 of ASCE 41, calculated from pushover

[5] - V_u is the ultimate building strength

[6] - *Ductility* is the building ductility capacity as per Eqn. 6-6 of FEMA P695, calculated from pushover

[7] - See Equation 3-2

[8] - *SC = Shear-critical Columns*
WCSB = Weak-Column-Strong-Beam arrangements - $M_c/M_b > 1.2$ at any joint
IS = Inadequate Strength (overall) - $\mu_{strength} > 4$

2.4.2 Retrofit Buildings

1967 buildings are subjected to an ASCE 41 Tier 3 evaluation and are then retrofit with concrete jacketing (Conc. J), steel jacketing (Steel J.), or fiber-reinforced polymer (FRP) wraps to meet the defined performance objectives shown in Table 2-1. Design parameters of the retrofit buildings are shown in Table 2-3. ASCE 41's Nonlinear Static Procedure (NSP) is used during the evaluation and retrofit because its visual nature provides a comparison between the original and retrofit building properties that helps eliminate design errors. Historically, the NSP has been the most commonly used evaluation procedure, however, modern advances in computing have led

to increased use of Nonlinear Dynamic Procedures (NDP) (Goel & Chadwell, 2008). This procedure is less conservative than the linear procedures, but studies have shown the NSP is slightly more conservative than the NDP and neglects higher mode effects important in taller buildings (Sattar & Hulsey, 2015; Goel & Chadwell, 2008).

Table 2-3 – Retrofit building properties

Retro. Meth.	*# Stories*	*PL*	*Haz.*	T_e *[sec]*	V_y *[kips]*	V_u *[kips]*	*Ductility*	$\mu_{strength}$
FRP	3	CP	BSE-2E	0.81	411	505	7.2	3.6
FRP	3	LS	BSE-2E	0.81	411	505	7.2	3.6
FRP	3	IO	BSE-1E	*FRP cannot provide required strength / stiffness*				
Steel J.	3	CP	BSE-2E	0.65	607	714	4.2	2.1
Steel J.	3	LS	BSE-2E	0.65	607	714	4.2	2.7
Steel J.	3	IO	BSE-1E	0.63	745	869	7.8	2.4
Conc. J.	3	CP	BSE-2E	0.52	625	747	5.5	2.9
Conc. J.	3	LS	BSE-2E	0.52	625	747	5.5	2.9
Conc. J.	3	IO	BSE-1E	0.50	836	875	23.6	2.3
FRP	6	CP	BSE-2E	1.08	724	817	4.3	3.3
FRP	6	LS	BSE-2E	1.08	724	817	4.3	3.3
FRP	6	IO	BSE-1E	*FRP cannot provide required strength / stiffness*				
Steel J.	6	CP	BSE-2E	0.90	965	1158	4.2	2.9
Steel J.	6	LS	BSE-2E	0.90	969	1155	4.1	2.8
Steel J.	6	IO	BSE-1E	0.81	1088	1214	21.4	2.4
Conc. J.	6	CP	BSE-2E	0.79	811	1032	3.4	3.7
Conc. J.	6	LS	BSE-2E	0.79	811	1032	3.4	3.7
Conc. J.	6	IO	BSE-1E	0.81	1088	1214	21.4	2.8
FRP	9	CP	BSE-2E	0.76	2491	2956	4.0	2.3
FRP	9	LS	BSE-2E	0.76	2491	2956	4.0	2.3
FRP	9	IO	BSE-1E	*FRP cannot provide required strength / stiffness*				
Steel J.	9	CP	BSE-2E	0.77	2980	3509	2.7	2.0
Steel J.	9	LS	BSE-2E	0.73	3020	3603	2.6	2.0
Steel J.	9	IO	BSE-1E	0.66	4827	6945	9.0	1.3
Conc. J.	9	CP	BSE-2E	0.71	3086	3586	2.5	2.0
Conc. J.	9	LS	BSE-2E	0.71	3086	3586	2.5	2.0
Conc. J.	9	IO	BSE-1E	0.55	5175	6000	25.8	1.4

Retrofit designs are conducted in the following manner. First, the 1967 building is evaluated as per ASCE 41, as illustrated in Figure 2-3a. Detailed descriptions of building models is presented in Section 2.5. Elements that are found to not comply with the acceptance criteria of the desired PL are retrofit, as illustrated Figure 2-3b. Retrofits are also designed to be symmetric about a frame's centerline (i.e., if an external column on the first story in frame-line 1 does not comply with the PL but the other first-story external column in frame-line 1 does, both are retrofit). An example is presented in Figure 2-3b. Beam shear failures are not considered in this study because this condition is relatively uncommon; therefore, only column deformation demands are compared against acceptance criteria based on the column's transverse reinforcement ratio, axial load ratio, and shear stress. The result is the creation of a ductile system with strong columns and weak beams through upgrades to columns. The retrofit building is then reevaluated, and newly identified non-compliant members are either retrofit, or the retrofit design is strengthened, as shown in Figure 2-3 c and d. This process is continued until all members are shown to comply with the desired PL, as shown in the example Figure 2-3 e and f. In cases where steel or concrete jackets were added to columns as the retrofit method, multiple iterations of the retrofit design were needed because the addition of jackets to one story often caused a weak story in the story directly above the retrofit (Figure 2-3 c and d).

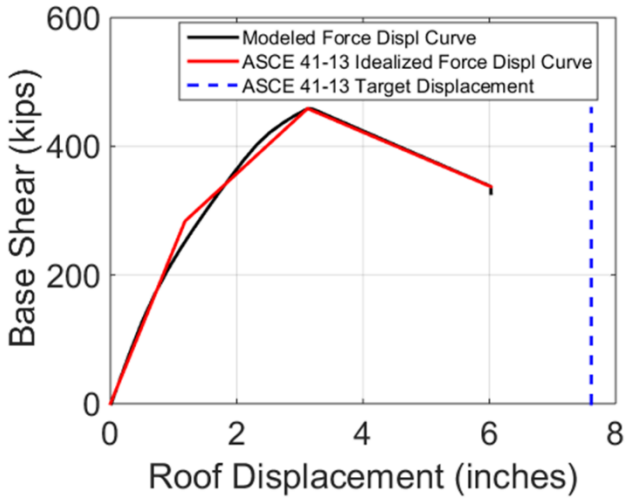
Modeled Force Displ Curve
ASCE 41-13 Idealized Force Displ Curve
ASCE 41-13 Target Displacement
Base Shear (kips)
Roof Displacement (inches)
0
200
400
600
0
2
4
6
8

(a)

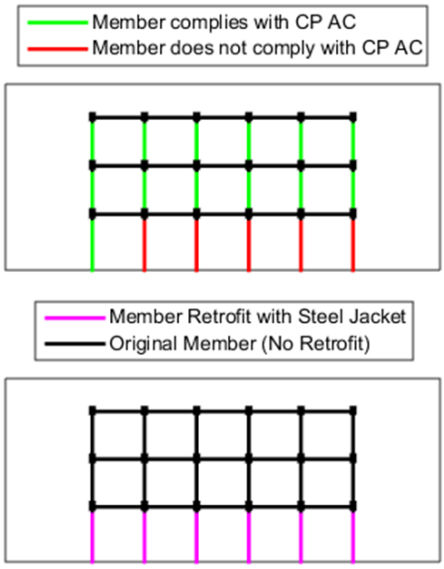
Member complies with CP AC
Member does not comply with CP AC
Member Retrofit with Steel Jacket
Original Member (No Retrofit)

(b)

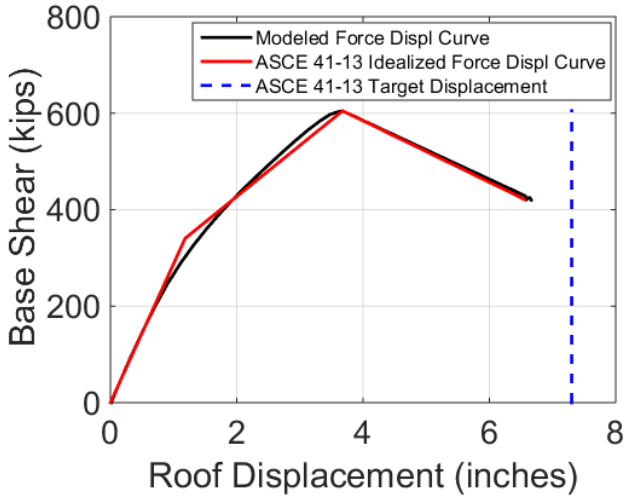
Modeled Force Displ Curve
ASCE 41-13 Idealized Force Displ Curve
ASCE 41-13 Target Displacement
Base Shear (kips)
Roof Displacement (inches)
0
200
400
600
800
0
2
4
6
8

(c)

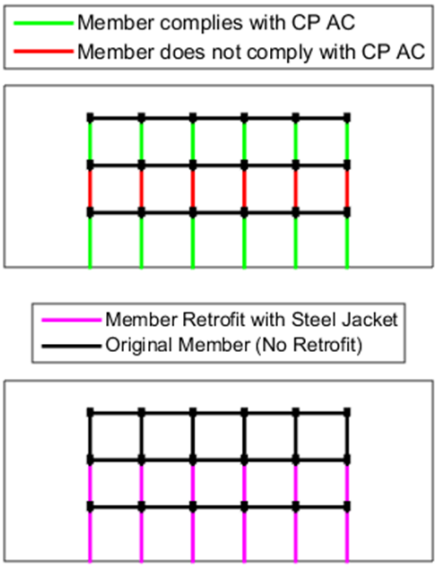
Member complies with CP AC
Member does not comply with CP AC
Member Retrofit with Steel Jacket
Original Member (No Retrofit)

(d)

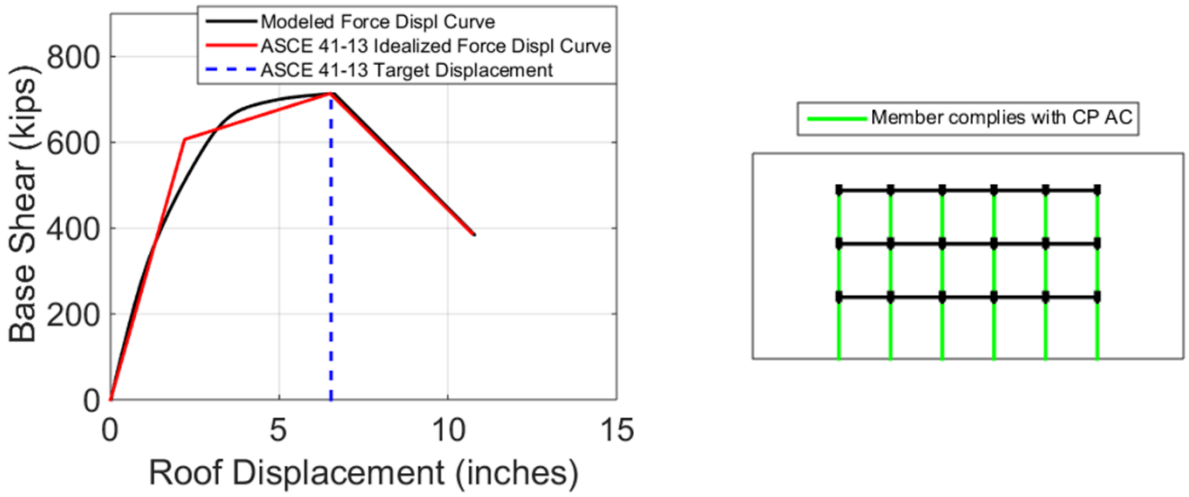

(e) *(f)*

Figure 2-3 - Retrofit design process for 3 story building retrofit with steel jackets to meet CP under the BSE-2E motion: (a) Evaluation of original 1967 building using the NSP; (b) Members that are found not to comply with CP acceptance criteria (AC) under BSE-2E and the retrofit scheme implemented to address these deficiencies; (c) Evaluation of structure after the first retrofit iteration; (d) Members that are not compliant with CP under BSE-2E, and the associated retrofit scheme; (e) Evaluation of the structure after the second retrofit iteration; (f) Showing that all members now comply with CP under BSE-2E.

During the design of the 27 building retrofits, some trends emerged. First, all 1967 buildings satisfy LS structural performance at the BSE-1E level without any retrofit. Secondly, in many cases, the designs for CP at BSE-2E and LS at BSE-2E are equivalent, as shown by the 3-story building retrofit to CP and LS using FRP wraps in Table 2-3. This is partially a product of the implemented retrofit design algorithm. In these cases, the first iteration of the retrofit design provides enough structural improvement to satisfy both CP at BSE-2E and LS at BSE-1E. This is more common in the 3-story models since there are fewer element that are candidates for retrofit, providing fewer opportunities for distinction in design approaches depending on PL.

To comply with ASCE 41, an analysis of the buildings that includes retrofit measures must be shown to comply with the selected performance criteria. If any of the retrofit measures fail to

comply with the acceptance criteria, the design must be altered. However, ASCE 41 does not provide acceptance criteria, or modeling parameters, for many types of retrofit measures, such as wrapping concrete columns in FRP or steel jackets, and minimal guidance is provided as to how these retrofit components should be evaluated (Alvarez & Brena, 2014; Brena & Alcocer, 2009; Kim & Hagen, 2014). This omission of guidance requires the engineer to use judgment. This judgment is one contributor to variability in the performance of structures retrofit to the same performance objective (Maison, Kasai, & Deierlein, 2009). Therefore, a novel solution was created that relates local retrofit designs to ASCE 41 acceptance criteria for RC columns.

For concrete jacket retrofits, the ASCE 41 acceptance criteria for RC columns are used for the retrofit member *(i.e.*, the jacketed member is treated as a traditional RC section and the transverse reinforcement ratio of the jacketed member and axial load ratio are computed using the total cross section of the jacketed member).

In retrofit designs where FRP wraps or steel jackets are applied to existing columns, the retrofit design is transformed into an equivalent transverse reinforcement design and the ASCE 41 acceptance criteria are used for the equivalent retrofit member. The concept of calculating an equivalent transverse reinforcement design for jacketed members was first presented by Alvarez and Brena (2014). To identify an equivalent transverse reinforcement design, the lateral confining stress provided by the jacket is computed. For steel jacketed members, the median lateral confining stress is computed as per Priestley et al. (1994) and for members wrapped in FRP the coning stress is taken from ACI 440.2R-08 (ACI Committee 440, 2008). The lateral confining stress provided by the jacket is then equated to the lateral confining stress equation for concrete in

Mander et al. (1998). By assuming #3 hooped bars, the spacing in an equivalent RC section required to produce the same confining stress as the jacket is obtained, and the equivalent transverse reinforcement ratio can be computed (Alvarez & Brena, 2014). The equivalent transverse reinforcement ratio is then used as input into the acceptance criteria tables for RC members provided in ASCE 41.

2.4.2.1 Design of Externally-Bonded FRP Wraps

There are many ways to strengthen an existing member, or to design a new member, using FRP (Bakis, et al., 2002). The most common retrofit application is through externally-bonded FRP jackets applied to existing members. FRP systems offer advantages over traditional retrofit systems due to their high tensile strength and lightweight, noncorrosive properties (ACI Comittee 440, 2008). Here, carbon fiber-reinforced polymer (CFRP) sheets are externally bonded to existing RC members by an adhesive, as shown in Figure 2-4a. Properties of a single ply of CFRP used in this study are provided in Table 2-4. Externally-bonded CFRP wraps are designed in accordance with ACI 440.2R-08 and design is for a complete wrap (i.e. wrap extends over the full height of the member). The lateral confining stress proved by the FRP wrap is calculated using the relation proposed by Lam & Tang (2003).

Table 2-4 – Properties of a single ply of an FRP wrap. Values are for QuakeWrap® VU18C Unidirectional Carbon Fabric.

Single Ply Property	*Value*
Nominal thickness	0.0399 in
Ultimate tensile strength	550 ksi
Rupture strain	0.0164
Tensile modulus of elasticity	33500 ksi

FRP wraps commonly consist of plies with unidirectional fibers. When plies are applied with the fibers oriented in the transverse direction, the shear strength of a member is increased; if plies are applied in the longitudinal direction, flexural capacity is improved. In this study, columns with FRP wraps are designed such that the shear capacity of the existing member is benefitted, and in most cases, addition of FRP wraps switches the member's governing failure mode from shear to flexure. The FRP also increases confinement. The FRP design is conducted iteratively, increasing each deficient member's shear capacity by increments of 20% until the design of each column complies with the desired PL. Many of the columns in the original building designs have V_p/V_n close to, or slightly above unity. Adding FRP wraps typically strengthens the components' shear capacities such that the expected failure mode becomes flexure, i.e. reducing V_p/V_n below 0.6. Overall, the addition of FRP wraps has minimal impact on component strength (because the flexural and shear strengths of the column before retrofit are similar; this would be different in components with V_p/V_n much greater than one), although ductility capacity is greatly improved. For all of the buildings analyzed in this study, the addition of FRP wraps alone could not provide enough benefit to strength and ductility to comply with IO (see Table 2-3), so retrofits only to LS and CP are considered here. In practice, retrofitting with FRP is often paired with other measures to increase strength and stiffness, such as the addition of shear walls, which assists in achieving compliance with more stringent PLs. However, this study does not consider such mixed retrofit strategies.

2.4.2.2 Design of Steel Jackets

A large number of existing columns in bridge and buildings structures have been retrofit using steel jackets (Priestley, Seible, & Calvi, 1996). Steel jackets can improve a member's flexural ductility, shear strength, and flexural strength simultaneously. For rectangular columns, rectangular or elliptical steel jackets may be applied. Rectangular steel jackets applied to rectangular columns are not recommended, as tests have shown them to be significantly less effective in improving flexural ductility than elliptical jackets (Sun, Seible, & Priestley, 1993). Additionally, the installation of rectangular jackets is more difficult because each side of the jacket must be epoxied to column, then all sides welded together. Elliptical jackets provide continuous confining action and are installed by welding two halves together, with the remaining void filled with normal strength concrete (Priestley, Seible, & Calvi, 1996). For these reasons, circular steel jackets are designed for the existing square columns in this study as presented in Figure 2-4b. Designs were performed following the procedures developed by Priestley et al. (1996) and lateral confining stresses for steel jacketed members are also calculated following these procedures (Priestley, Seible, & Calvi, 1996). Steel jackets are assumed to be made of A36 steel.

Steel jacket design is performed iteratively. First, a jacket is designed that reduces each deficient member's V_p/V_n to 0.6, effectively changing the failure mode from shear to flexure. If additional strength or ductility increases are needed, the jacket thickness is increase by $1/16^{th}$ of an inch (the minimum increment of thickness in U.S. steel plates). This process is repeated until the retrofit column is shown to comply with ASCE 41 acceptance criteria.

2.4.2.3 Design of Concrete Jackets

Concrete jacketing is the most commonly used method for upgrading the performance of deficient RC members in the U.S. because of its cost-effectiveness (Bousias, Spathis, & Fardis, 2004). This retrofit technique encases an existing RC member in a cast-in-place steel RC jacket, providing strength and ductility to the deficient member. Here, rectangular RC jackets are designed for deficient members following the design procedures proposed by Priestley, Seible, & Calvi (1996) and the requirements in ACI 318-14 (ACI Committee 318, 2014). A typical cross-section of concrete jacketed columns designed in this study is shown in Figure 2-4c. RC jackets are assumed to have concrete with a design compressive strength of 4 ksi and the transverse reinforcement design consists of hooped bars. During design, the contribution of the concrete in the jacket to shear strength is neglected as the bond between the jacket and the original member may be insufficient. The lateral confining stress provided by the concrete jacket is computed based on the equation presented by Priestley, Seible, & Calvi (1996).

The concrete jackets are designed iteratively by first adding a jacket with a No. 8 longitudinal bar placed in each corner (i.e. 4 bars in total). The thickness of the initial jacket is dictated by the size of the longitudinal rebar, transverse rebar, desired cover, and assuming a 1-inch cover between the outer face of the original column and the longitudinal rebar in the jacket. Based upon these constraints, the initial concrete jacket thickness is 4 inches. Next, the flexural strength of the retrofit column is computed and a transverse reinforcement design is provided to reduce the V_p/V_n to 0.6. If the initial design does not comply with the ASCE 41 acceptance criteria, the area of longitudinal steel in the jacket is increased or the thickness of the jacket is

increased by half an inch. This process is repeated until the designed column satisfies the acceptance criteria.

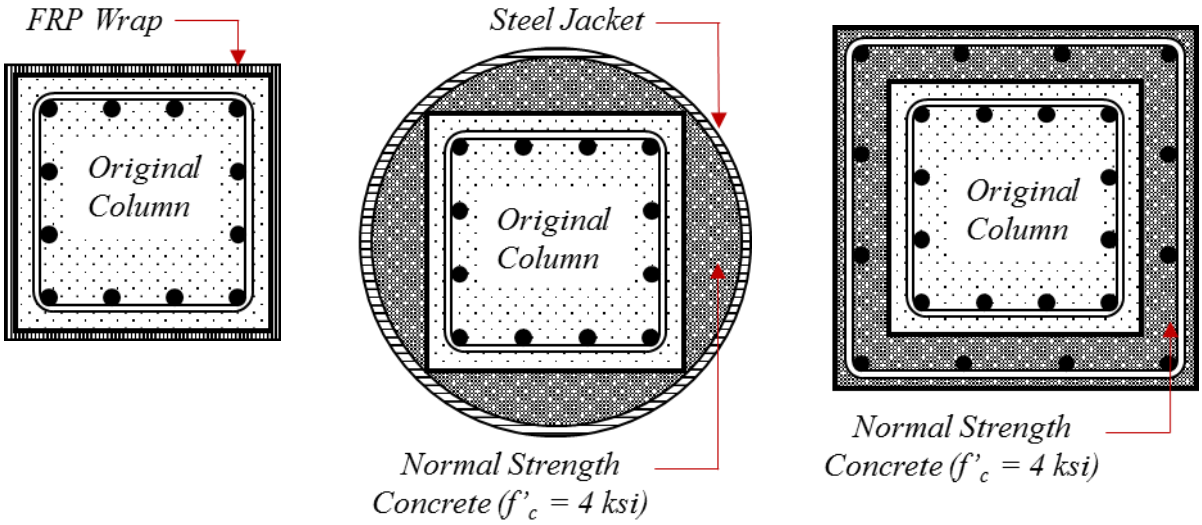

Figure 2-4 - Idealized cross-sections showing square columns retrofit with (a) FRP wraps, (b) circular steel jackets, and (c) rectangular concrete jackets

2.5 Numerical Modeling of Buildings

Two-dimensional nonlinear models capable of capturing important response characteristics and common failure modes are created in *OpenSEES* for the existing (1967) buildings and the retrofit buildings. ASCE 41 modeling parameters were not used in this study because that document does not provide modeling parameters for retrofit components. Therefore, modeling techniques were chosen that provide consistency between original and retrofit members. In practice, modeling of retrofit components relies heavily on judgment.

2.5.1 Modeling of Beam Elements

All beams are assumed to be flexurally-controlled. Layered force-based fiber elements, also called distributed plasticity elements, are used to capture phases of response that include: initial stiffness, concrete crushing, steel yielding, and steel buckling. The stress-strain relationship of concrete fibers is described by the modified Kent and Park model (Kent & Park, 1971); steel fibers are modeled using the relation proposed by Giuffre-Menegotto-Pinto (1983) and the onset of buckling and post-bucking behavior is determined using the model proposed by Dhakal and Maekawa (2002). A single force-based fiber element is used per beam and the regularized integration scheme presented by Scott & Hamutcuoglu (2008) is employed with five integration points per element, for which purpose the plastic hinge length is estimated using the relationship proposed by Paulay and Priestley (Scott & Hamutcuoglu, 2008; Paulay & Priestley, 1992).

2.5.2 Modeling of Column Elements

2.5.2.1 Existing Shear-Critical Columns

Shear-critical columns are commonly found in pre-1967 buildings. This study defines a shear-critical column as one with $V_p/V_n \geq 0.6$, because these columns are likely either to fail in shear or in flexure-shear (yielding followed shear failure) (Li, Elwood, & Hwang, 2014). For these cases, a layered fiber element is modeled in series with shear and axial springs. The material models in the fiber element are the same as those used for the beam, but buckling of the longitudinal steel rebar is not accounted for because the post-peak response of these type columns is governed by the shear spring response. The response of the shear and axial springs are described by shear and axial limit state materials (Elwood, 2004). In these materials, failure

surfaces are used to describe the onset of shear and axial failure. When the response of a member intersects the failure surface, the shear or axial strength and stiffness begin to degrade.

2.5.2.2 Existing Flexure-Critical Columns

Flexure-critical columns are those that exist in the 1967 buildings that have not been retrofit and have $V_p/V_n < 0.6$. These flexural columns are modeled in the same manner as beams.

2.5.2.3 Columns Wrapped in FRP

FRP wraps are designed and applied to the exterior of the existing column with uni-direction carbon fibers aligned in the transverse direction, altering the members' shear and axial strength as well as the confined concrete properties. To account for these effects, members retrofit with FRP are modeled by altering the original column's shear, axial and flexural response. For columns where the addition of FRP decreases V_p/V_n to less than 0.6, the shear and axial springs are removed and the member is modeled using regularized layered fiber element in the same way as flexure-critical columns and beams. The confined concrete model properties are adjusted, based upon the Mander et al. (1988) model, to account for the influence of the FRP wraps.

RC members jacketed in FRP wraps have many possible failure modes: 1) steel yielding followed by FRP fracture, 2) steel yielding followed by concrete compressive crushing (with FRP still intact), 3) concrete compressive crushing, 4) FRP peel-off at termination or cutoff point, 5) FRP peel-off initiated away from the ends due to inclined shear cracks in the concrete, 6) FRP peel-off at the termination point or at a flexural crack due to high tensile stresses in the adhesive, and 7) debonding at the FRP-concrete interface in areas of concrete surface unevenness or due

to faulty debonding (Bakis, et al., 2002). Failure mode 6 may be avoided by limiting the design tensile strain in the FRP to 0.008 and mode 7 may be avoided with proper quality control in construction (Bakis, et al., 2002), and are assumed to be avoided here by appropriate design. FRP wraps, and their unique failure modes, are not explicitly modeled. This simplification is judged to be adequate because failure modes 1 – 3 are modeled through alteration of the existing column model, and failure modes 4 and 5 do not necessarily contribute to lateral instability and collapse (Fakharifar, Chen, Dalvand, & Shamsabadi, 2015).

2.5.2.4 Steel-Jacketed Columns

1967 building members retrofit with steel jackets benefit from added confinement, strength, ductility, and energy dissipation capacity. Numerical models account for these benefits through explicit definition of the member cross-section. Here, additional fibers are added to the existing column cross-section that account for the geometry of the jacket. Fibers in the steel jacket are modeled using the relation proposed by Giuffre-Menegotto-Pinto (Filippou, Popov, & Bertero, 1983) and the fibers used to model concrete fill between the circular steel jacket and the existing column are modeled using the modified Kent and Park relationship (Kent & Park, 1971). The confined concrete model of the existing column is adjusted, based upon the Mander, et al. (1988) model, to account for the influence of the steel jacket.

Past research has shown that the use of adhesive anchor bolts is an effective measure for ensuring contact between the steel jacket and original RC member (Aboutaha, Engelhardt, Jirsa, & Kreger, 1996; Aboutaha, Engelhardt, Jirsa, & Kreger, 1999). Therefore, this study does not explicitly model the interface between steel jacket and original member, assuming this contact

is successfully provided through these methods. Additionally, past tests of steel jackets have been successful in retrofitting a shear-critical member to become flexurally governed. Therefore, shear failure of elements retrofit with steel jackets will not be considered, and shear and axial springs that are included in the original column model are removed from steel jacketed members.

2.5.2.5 Concrete-Jacketed Columns

Columns that are retrofit using concrete jackets must be able to reflect the improved performance (*i.e.* concrete confinement) as well as any additional failure modes RC jacketing may experience. Past research has shown that the effectiveness of RC jacketing depends upon the treatment of the surface of the original column, response of the interface between the original element and the RC jacket (Palieraki & Vintzileou, 2009), and the effects of preloading during retrofit (Vandoros & Dritsos, 2006). However, if properly implemented, members retrofit with RC jackets exhibit similar ductility, strength, and energy dissipation capacities to that of an equivalent monolithic specimen (Bousias, Spathis, & Fardis, 2004; Vandoros & Dritsos, 2006; Bousias, Biskinis, Fardis, & Spathis, 2007). Therefore, this study assumes retrofit members using RC jackets have properties equal to that of equivalent monolithic members with the same dimensions.

As was done for members retrofit with steel jackets, additional fibers are added to the existing cross-section that describe the jacketed member's geometry. Constitutive models of steel and concrete in the jacket are modeled in the same manner as beams, however, the constitutive model for unconfined concrete in the original, jacketed, column is updated to account for confining effects of the jacket based upon the Mander, et al. (1988) model.

2.5.3 Further Modeling Issues

Joints are modeled using panel zones of discrete size that contain elastic rotational springs at their center to account for shear flexibility and shear deformation. The effects of foundation flexibility and soil-structure interaction are neglected, and first-story columns are assumed to be fixed at their base. The defined seismic mass is representative of the weight of the building tributary to an internal space frame. Five percent Rayleigh damping is assigned to the first and third modes of each structure. Geometric nonlinearities, or P-Δ effects, are accounted for in the geometric transformation through use of *OpenSEES* "PDelta" coordinate transformation.

2.6 Performance Assessment Framework

Probabilistic seismic damage and loss assessments are performed for all buildings using the Seismic Performance Prediction Program (SP3) software (Haselton Baker Risk Group), a web tool largely based on the FEMA P-58 methodology (FEMA, 2012). The loss assessment framework can be categorized into four components: hazard analysis, structural analysis, damage analysis, and loss analysis.

2.6.1 Hazard Analysis

During hazard analysis the site specific earthquake hazard is characterized considering the type, geometry, and relative distance of all nearby faults and local site conditions. This study defines the ground motion intensity measure as the spectral acceleration measured at the effective fundamental vibration period of the building, $S_a(T_1)$. The effective fundamental period is computed from an idealized force-displacement curve as per ASCE 41 Section 7.4.3.2.5. All

buildings are located at a southern California site (33.996°N, -118.162°W) that is not subject to near-fault directivity effects. The site-specific hazard curve, shown in Figure 2-5, is calculated based upon the U.S. Geological Survey hazard maps and assuming Site Class D soil (Petersen, et al., 2008).

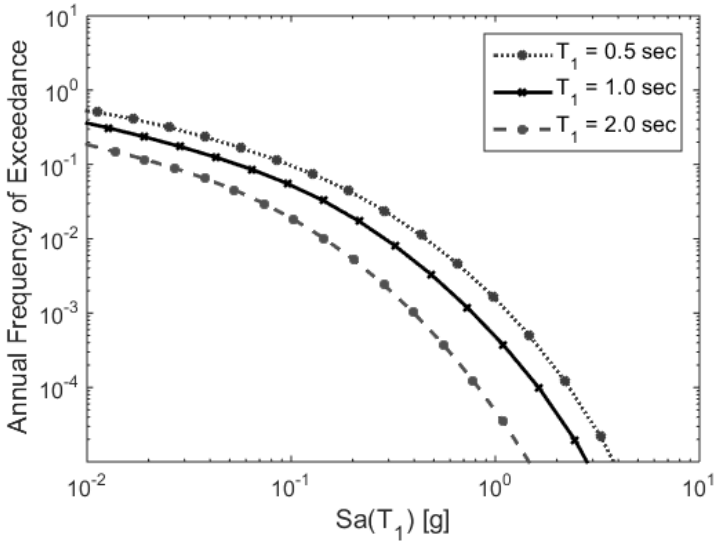

Figure 2-5 – USGS probabilistic seismic hazard curves for the L.A. site (33.996°N, -118.162°W)

2.6.2 Structural Analysis

In the structural analysis, each building's response is traced through nonlinear time history analysis. Conditional estimates of Engineering Demand Parameters (EDP) are obtained at increasing levels of seismic intensity. In this study, EDPs are quantified in terms of story drift ratios (SDR) and peak floor accelerations (PFA). EDPs are measured during nonlinear dynamic multistripe analysis (Jalayer & Cornell, 2009). Five hazard levels are considered, with the following probabilities of exceedance: 50% in 50 years, 20% in 50 years, 10% in 50 years, 5% in 50 years, 2% in 50 years. Eleven two-component records are chosen to represent each stripe

(hazard level) based on recommendations in FEMA P-58. The motions are selected using the Conditional Mean Spectra (CMS) method (Baker, 2011), based on the southern California site.

The collapse capacity of each building, measured in terms of spectral acceleration, is assessed through Incremental Dynamic Analysis (IDA) using the FEMA P-695 far-field ground motion set (Vamvatsikos & Cornell, 2002; FEMA, 2009). During IDA, the structural response is measured up to collapse, where collapse may occur when (1) lateral instability resulting from large flexural deformations in beams and columns, (2) the total story shear capacity degrades to its residual capacity, or (3) the story vertical load demand exceeds the total column axial capacity in that story. Collapse mode (1) is commonly referred to as sideway collapse and is the expected failure mode in ductile frames. It is taken here as the spectral level at which the IDA curves decrease to 20% of their initial slope. Non-ductile buildings commonly collapse by modes (2) and (3) (Baradaran Shoraka, Yang, & Elwood, 2013). Residual story shear capacity is the sum of the individual column residual shear capacities, taken to be 5% of their ultimate shear strength. Column axial (gravity-load bearing) capacities are computed using the axial limit surface proposed by Elwood (2004), which varies as a function of drift demand through the analysis. Due to convergence of the numerical solution algorithm, collapse modes (2) and (3) are also triggered if more than 75% of columns in a story degrade to their residual shear capacity or fail axially. Table 2-5 presents collapse capacities, and mean annual frequencies of collapse ($\lambda_{collapse}$) for all of the buildings analyzed in this study.

Table 2-5 – Collapse capacities of buildings that have not been retrofit and those retrofit to ASCE 41 standards

Retro. Meth.	*# Stories*	*PL*	*Design Haz.*	*Median Sa,col (T_1) [g]*	*$\sigma_{LN\ (Sa,\ col)}$*	*$\lambda_{collapse}$ [x 10^{-4}]*	*P(col) in 50 yrs [%]*
None	3	N.A.	N.A.	1.11	0.27	15	7.0
None	6	N.A.	N.A.	0.93	0.34	10	5.0
None	9	N.A.	N.A.	1.17	0.31	10	4.9
FRP	3	CP	BSE-2E	2.44	0.30	2	1.2
FRP	3	LS	BSE-2E	2.44	0.30	2	1.2
FRP	3	IO	BSE-1E	*FRP cannot provide required strength / stiffness*			
Steel J.	3	CP	BSE-2E	1.72	0.30	6	3.1
Steel J.	3	LS	BSE-2E	1.92	0.30	7	3.1
Steel J.	3	IO	BSE-1E	1.99	0.41	5	2.5
Conc. J.	3	CP	BSE-2E	2.06	0.29	6	2.8
Conc. J.	3	LS	BSE-2E	2.06	0.29	6	2.8
Conc. J.	3	IO	BSE-1E	2.96	0.35	2	0.9
FRP	6	CP	BSE-2E	1.26	0.26	3	1.3
FRP	6	LS	BSE-2E	1.26	0.26	3	1.3
FRP	6	IO	BSE-1E	*FRP cannot provide required strength / stiffness*			
Steel J.	6	CP	BSE-2E	1.27	0.34	5	2.3
Steel J.	6	LS	BSE-2E	1.36	0.21	4	1.9
Steel J.	6	IO	BSE-1E	1.81	0.38	4	1.9
Conc. J.	6	CP	BSE-2E	1.36	0.35	7	3.3
Conc. J.	6	LS	BSE-2E	1.36	0.35	7	3.3
Conc. J.	6	IO	BSE-1E	2.86	0.38	1	0.6
FRP	9	CP	BSE-2E	1.44	0.38	10	5.1
FRP	9	LS	BSE-2E	1.44	0.38	10	5.1
FRP	9	IO	BSE-1E	*FRP cannot provide required strength / stiffness*			
Steel J.	9	CP	BSE-2E	1.57	0.30	5	2.5
Steel J.	9	LS	BSE-2E	1.57	0.30	4	2.2
Steel J.	9	IO	BSE-1E	3.70	0.19	1	0.5
Conc. J.	9	CP	BSE-2E	1.58	0.23	6	3.2
Conc. J.	9	LS	BSE-2E	1.58	0.23	6	3.1
Conc. J.	9	IO	BSE-1E	3.56	0.19	3	1.3

2.6.3 Damage Analysis

During damage analysis, damage to building components is probabilistically computed using empirically derived fragility functions, representative of the probability individual components experience discrete damage states as a function of the EDPs. Damage states correspond with repair efforts to restore a component to its original state. In addition to component damage, damage due to structural collapse and residual drift are computed based on probabilistic structural capacity models.

Architectural layouts and associated contents for each building in this study are representative of a commercial office building, with an assumed replacement cost per square foot of $230. Since 1967 buildings and retrofit buildings are assumed to have the same cost per square foot and all buildings have the same floor plan, total building replacement cost is only a function of number of stories. In this study the replacement cost of 3-, 6-, and 9-story buildings is $10,781,250.00, $21,375,000.00, and $32,062,500.00 respectively.

Inventories of structural and nonstructural components based on the lateral load resisting systems and building design era are used to estimate each building's seismic losses. Nonstructural component inventories were assembled using the SP3 default components for buildings constructed in 1967. Table 2-6 provides a list of the components present in all buildings.

Most of the fragility functions are defined directly from the library provided in SP3 based on FEMA P-58. Fragility functions are derived empirically and relate the probability that a component is in or exceeds a specified damage state as a function of engineering demand that

the component is most sensitive to. Engineering demand parameters include inter-story drift, peak floor accelerations, and residual drift. Damage states for each component require unique repair actions, and the consequence of a damage state is quantified in terms of repair cost or repair time. However, FEMA P-58 and SP3 do not contain fragility functions for members retrofit with FRP, steel, or concrete jackets. Here, any component that has been seismically retrofit using FRP wraps, steel jackets, or concrete jackets is assigned the fragility function for an Ordinary Moment Frame (OMF) with weak joints and beam flexural response. In these systems, columns are flexurally-governed and damage tends to concentrate in beams and joints. Therefore, damage states for OMFs are reasonable substitutes for RC subsystems where the columns have been jacketed because the damage patterns are similar. However, the cost associated with repair of OMF systems and locally retrofit systems may differ. The fragility function for OMFs differs from the fragility function used for pre-1967 non-conforming columns in that damage occurs at higher drift demands and concentrates in beams and joints as opposed to columns.

Table 2-6 - Example of damageable structural and nonstructural components used in 3-story building retrofit to CP. The EDP column identifies which demand parameter governs the response of the component. The only items that differ between this and the other 3-story buildings are the structural components.

Category	*Component*	*EDP*	*Quantity*
Interior finishes	Curtain Walls	SDR	325
	Concrete tile roof	PFA	42
	Wall Partition, Type: Gypsum with wood studs,	SDR	48
	Non-monolithic precast concrete stair assembly with concrete stringers and treads with no seismic joint	SDR	6
	Wall Partition, Type: Gypsum + Wallpaper	SDR	6
	Raised Access Floor, seismically rated.	PFA	36
	Precast Concrete Panels 4.5 inches thick	SDR	24
	Precast Concrete Panels 4.5 inches thick	PFA	24
	Suspended Ceiling	PFA	96
Lighting	Recessed lighting in suspended ceiling	PFA	705
	Independent Pendant Lighting	PFA	72
	Traction Elevator	PFA	2
Plumbing	Cold Water Piping	PFA	1
	Hot Water Piping - Small Diameter Threaded Steel	PFA	8
	Hot Water Piping - Large Diameter Welded Steel	PFA	1
	Sanitary Waste Piping - Cast Iron w/bell and spigot couplings, SDC C,	PFA	3
	Sanitary Waste Piping - Cast Iron w/bell and spigot couplings, SDC C	PFA	3
	Chiller - Capacity: 100 to <350 Ton - Vibration isolated equipment that is not snubbed or restrained	PFA	2
HVAC	HVAC Galvanized Sheet Metal Ducting	PFA	3
	HVAC Galvanized Sheet Metal Ducting	PFA	1
	Air Handling Unit	PFA	2
Fire	Fire Sprinkler Water Piping	PFA	9
	Fire Sprinkler Drop Standard Threaded Steel	PFA	3
Electric	Motor Control Center	PFA	2
	Low Voltage Switchgear	PFA	3
Structural	Non-conforming MF, weak columns and strong joints, Conc Col & Bm = 24" x 24", Beam both sides*	SDR	48
	Non-conforming MF, weak columns and strong joints, Conc Col & Bm = 24" x 24", Beam one side*	SDR	24
	ACI 318 OMF with weak joints and beam flexural response, Conc Col & Bm = 24" x 24", Beam both sides**	SDR	96
	ACI 318 OMF with weak joints and beam flexural response, Conc Col & Bm = 24" x 24", Beam one side**	SDR	48

*Un-retrofit columns

**Retrofit columns

2.6.4 Loss Analysis

During loss analysis damage measures are related to Decision Variables (DV) through probabilistic models. DVs are measures such as repair cost, downtime, and fatalities. This study utilizes building repair cost as the primary decision variable, which is a function of damage to structural components, damage to nonstructural components, global collapse, and residual drift. In cases where the building collapses or experiences unrepairable residual drifts, the cost of demolition is included in the estimated repair cost.

2.7 Comparison of ASCE 41 Performance Levels and Simulation Results

Qualitative descriptions of approximate limiting levels of structural and nonstructural damage are provided by ASCE 41 in Section 2.3 and in Table C2-3. The damage descriptions provided by ASCE 41 are estimates. On average, damage is expected to be less than the approximate ASCE 41 limiting damage level, and variations among buildings designed to the same PL are expected. (ASCE, 2013). It should be noted that ASCE 41 does not specify if damage estimates are provided at seismic hazard levels for new buildings (i.e. BSE-1N and BSE 2-N) or at hazard levels for existing buildings (i.e. BSE-1E and BSE 2-E). The author assumes damage estimates provided by ASCE 41 are meant to represent the general damage states of a PL and are applicable at both new and existing buildings hazard levels. Here, qualitative damage descriptions provided by ASCE 41 are compared to damage observations from the simulation results, while acknowledging a reasonable level of variability is inherent in the ASCE 41 definitions.

2.7.1 Global Performance

ASCE 41 descriptions of approximate global damage are broad. During a BSE-2E event, structures designed to CP are estimated to have “severe overall damage”; during a BSE-1E level event structures designed to LS, and IO are estimated to have “moderate” and “light” overall damage, respectively. The following metrics from the simulations of the retrofit buildings are used to quantify overall damage: median repair cost at design level shaking, and annualized repair cost.

2.7.1.1 Global Performance Quantified in Terms of Median Repair Cost at the Design Level Intensity

Median repair costs are quantified at the design level event for direct comparison with ASCE 41’s performance estimates. For original buildings and those designed to CP, the design level event is at the BSE-2E level (5% in 50 years). The design level event for buildings designed to LS and IO is taken to be the BSE-1E level (20% in 50 years). It should be noted that all unretrofit 1967 building models in this study were shown to comply with LS at BSE-1E. Therefore, the following results present performance estimates for buildings designed to comply with LS at the BSE-2E level.

Median repair cost estimates for the original buildings at the design level of shaking (i.e. those that have not been retrofit) range from 65% to 87% of the building replacement cost. Figure 2-6 shows a clear trend, indicating that as the design PL increases in seismic resistance (*i.e.* from CP to IO), the median repair cost decreases. For retrofit buildings, normalized median repair cost

estimates are as follows: 40% – 75% for building designed to CP; 10% – 50% for LS; 5% – 18% for IO.

In a relative sense, the ASCE 41 overall damage estimates (provided in ASCE 41 Section 2-3 and Table C2-3) align with the observed trends; damage in buildings designed to CP is more severe than those designed to LS, and even more severe relative to those designed to IO. Evaluating the ASCE 41 overall damage estimates in an absolute sense is problematic as it is difficult to quantify descriptors such as “severe”. For building owners, the descriptive damage estimates provided by ASCE 41 are subjective.

In addition to median repair cost decreasing with the more ambitious design PL used in the retrofit, the difference in median repair cost for buildings designed to the same PL also decreases. Specifically, the results show that more variation in terms of median repair cost exists in buildings designed to CP or LS, than in buildings designed to IO. In part, this is due to the larger range of possible designs improvements an engineer may make to comply with CP as opposed to IO. For example, in the 3 story building retrofit with FRP wraps, only the ductility of the original model is significantly improved in order to meet CP. When the same building in retrofit with steel jackets, both lateral strength and ductility capacity are improved. This difference in structural characteristics can lead to variations in structural response under design level shaking. These variations in structural response will influence component damage in the loss analysis and cause variations in median repair cost estimates. However, the acceptance criteria for IO are more stringent than those for CP, requiring that the retrofit designs often provide significant

improvements to both strength and ductility, leading to more uniform structural responses under design level shaking.

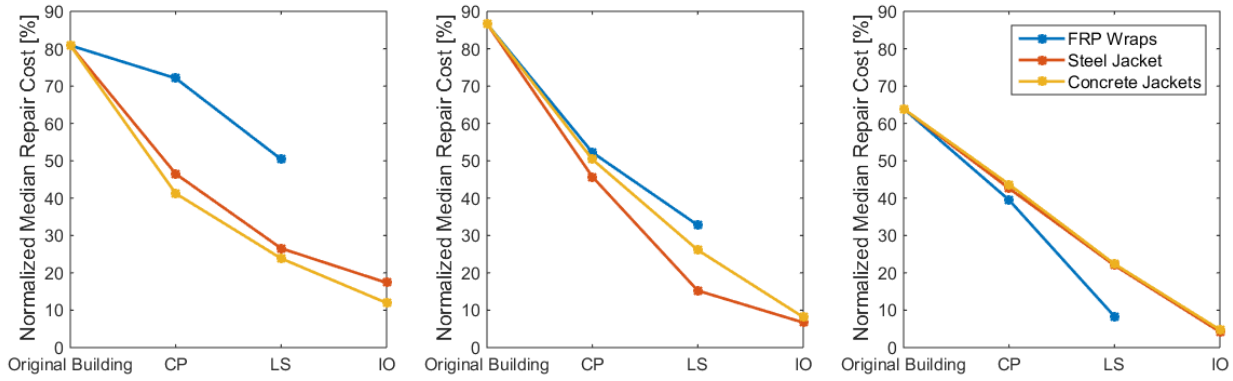

Figure 2-6 - Median repair costs normalized by the total building replacement cost at design level shaking (i.e. BSE-2E for original buildings and CP, and BSE-1E for LS and IO) for (a) 3-story buildings, (b) 6-story buildings, and (c) 9-story buildings

2.7.1.2 Global Performance Quantified in Terms of Annualized Repair Cost

Compared to loss predictions at the design level shaking, annualized repair cost estimates provide a more complete picture of the building's seismic risk by accounting for all ground shaking intensities, weighed by their probabilities of occurrence. More frequently occurring, small intensity events have a significant contribution to annualized loss because annualized loss is the convolution of the mean repair cost conditioned on the hazard intensity and the mean occurrence rate of the hazard. Typically, losses at lower seismic hazards are heavily influenced by nonstructural damage. While it is important to consider structural response under design level shaking, many building owners base their decision to repair or demolish a building after an earthquake based on economics. For example, approximately 60% of concrete buildings were demolished following the Canterbury Earthquakes, many of which were generally good-

performing buildings by modern code standard (Elwood, Marquis, & Kim, 2015). Defining performance goals at a single hazard level ignores a vast majority of events in which buildings are damaged, and demolitions or rehabilitations may occur. Yet, while ASCE 41 addresses loss at lower level hazards by requiring engineers to consider two hazard levels to meet basic safety performance objectives (see Table 2-1), the hazard levels are evaluated independently, with the more stringent design governing the result

Figure 2-7 presents annualized repair cost estimates for the original and retrofit buildings in this study. Annualized repair cost is reported as a fraction of the total building replacement cost. Ranges of annualized repair cost are: 0.4% to 1.2% for original buildings, 0.2% – 0.8% for buildings retrofit to CP, 0.2% – 0.8% for LS, and 0.1% - 0.3% for IO. Whereas Figure 2-6 previously showed that there is a clear difference between buildings retrofit to CP and LS in terms of repair costs conditioned on the design level earthquake, when annualized repair costs are used as the performance metric, there is little difference between the majority of models retrofit to CP and LS; many buildings designed to meet CP, also satisfy LS, or the designs are very similar. Figure 2-7 also shows that, for 1967 buildings, the number of stories is inversely related to the annualized repair cost. This trend is exhibited because damage tends to concentrate in a few stories (commonly the first story) because of the shear-critical nature of the columns and weak-column-strong-beam arrangements, thus concentrating damage in a relatively smaller fraction of the building for taller structures. In addition, the normalized repair costs for buildings with more stories are lower due to the large building replacement costs.

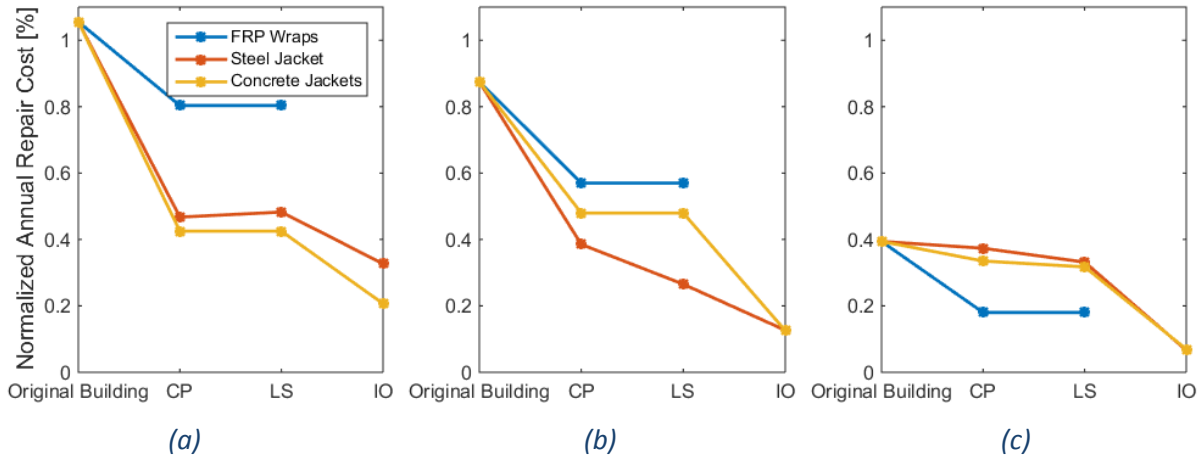

Figure 2-7 – Annualized repair cost for original and retrofit buildings of (a) 3-stories, (b) 6-stories and (c) 9-stories.

Figure 2-8 compares annualized repair cost estimates for 1967 buildings retrofit to ASCE-41 PLs with annualized repair cost estimate for modern buildings. Here, annualized repair costs associated with modern structures is reported from Welsh-Huggins and Liel (under review) because the hazard curve used to calculate annualized repair cost matches the hazard curve in this study, allowing for a direct comparison (Welsh-Huggins & Liel, under review). Based upon Figure 2-8, the following observations can be drawn about the ASCE 41 damage estimates as they relate to modern building performance:

- The annualized repair costs for retrofit buildings that comply with CP and LS are generally larger than those for modern RC frames analyzed by Welsh-Huggins and Liel (under review).
- Annualized repair costs for IO compliant buildings are generally less than the annualized repair cost for buildings designed to modern code standards.

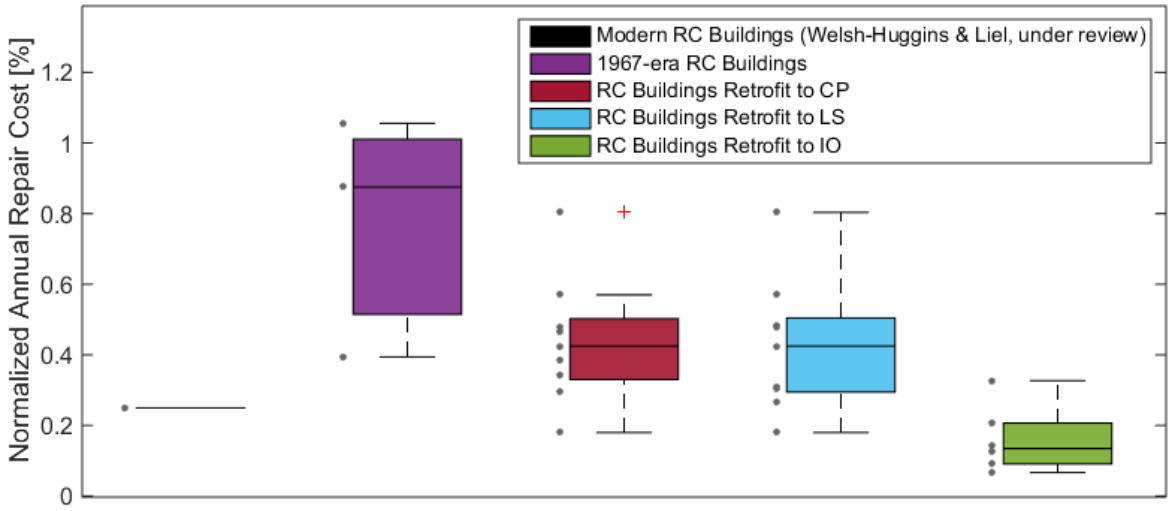

Figure 2-8 - Annualized repair cost statistics for a modern RC frame (taken from Welsh-Huggins and Liel, Under Review), nonductile 1967 RC frames, and nonductile RC frames retrofit to meet CP, LS, and IO

2.7.2 Performance of Structural Components

Damage to structural components conditioned on design PL is provided by ASCE 41 in terms of 1) general damage estimates in ASCE 41 Table C2-3 and 2) damage estimates specific to structural classification in ASCE 41 Table C2-4. What follows is a detailed comparison of the damage observations to structural components from this study and the damage estimates provided by ASCE 41 at the system and component levels. Again, it should be noted that ASCE 41 damage estimates are approximate levels of limiting damage and variability in damage levels is expected.

2.7.2.1 Evaluation of Structural Damage Defined at the System Level

Table 2-7 summarizes ASCE 41's structural damage estimates, in terms of reductions in strength and stiffness and residual drift after a building has been subjected to a design level event. Buildings designed to CP are estimated to sustain significant structural damage, and be

near collapse. Buildings designed to LS are estimated to experience significant reductions in strength and stiffness such that continued occupancy of the building is unlikely, while buildings designed to IO should retain a majority of their original strength and stiffness.

Table 2-7 - ASCE 41 damage estimates for structural components during design level shaking (reproduced from ASCE 41-13 Table C2-3)

PL	*Approximate Damage to Structural Components*
CP	Little residual stiffness and strength to resist lateral loads, but gravity load-bearing columns and walls function. Large permanent drifts. Some exits blocked. Building is near collapse in aftershocks and should not continue to be occupied.
LS	Some residual strength and stiffness left in all stories. Gravity-load-bearing elements function. No out-of-plane failure of walls. Some permanent drift. Damage to partitions. Continued occupancy might not be likely before repair. Building might not be economical to repair.
IO	No permanent drift. Structure substantially retains original strength and stiffness. Continued occupancy likely.

Damage to structural systems in evaluated in this study through nonlinear dynamic and static analyses. First, a building is analyzed dynamically under seismic excitation with the spectral acceleration of the record corresponding to the design level event. After dynamic analysis, a pushover analysis is conducted of the building in its damaged state and the structural characteristics (*i.e.* V_y, V_u, ductility) are computed.

Figure 2-9 shows pushovers for the 3-story building retrofit to CP (Figure 2-9a) and IO (Figure 2-9b) using steel jackets before and after a design level event occurs. Comparing Figure 2-9 a and b shows that the retrofit designed to CP experiences much larger reductions in strength and stiffness than the structure designed to IO. In addition, the building designed to CP sustains

residual drifts which are not present in the IO building. These findings are representative of the results for the entire building set.

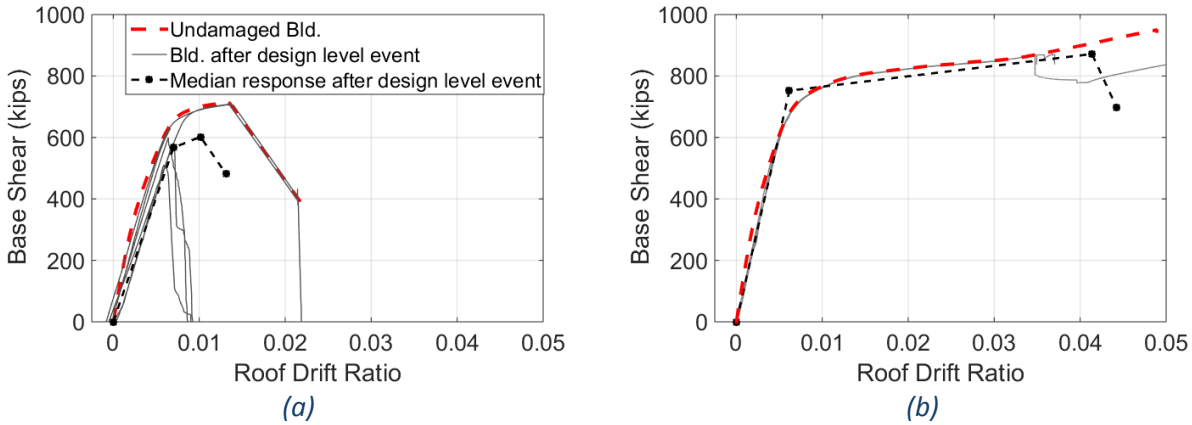

Figure 2-9 - Pushover results of the 3-story building retrofit to (a) CP and (b) IO using steel jackets, where the pushover is conducted after being subjected to design level shaking.

Figure 2-10 shows the effect of design level shaking on building strength and stiffness for the entire building set by plotting response characteristics (obtained from results like those in Figure 2-9) for each building after design level shaking. These results indicate that a building designed to the CP level retains 60% of its original stiffness, 80% of its yield strength, and 70% of its ultimate strength on average. ASCE 41 estimates that buildings designed to CP will have "little residual stiffness and strength to resist lateral loads" (see Table 2-7). This damage description predicts more damage than observed during simulation, although considerable variation in post-dynamic strength exists for the buildings analyzed. In one case, a structure retrofit to comply with CP only retained 20% of its strength after experiencing a design level event. For cases such as this, the ASCE 41 damage descriptor matches the simulated performance. For buildings retrofit to the LS level, on average, a building retains 75%-85% of its original strength and stiffness after a design level event. These numbers are in good agreement with ASCE 41 approximate damage

definitions, which state that some residual strength and stiffness remains in all stories. For buildings designed to IO, the original strength is left unaltered by a design level event, and 80% of the stiffness is retained. These numbers appear to be consistent with the ASCE 41 structural damage descriptions associated with IO in Table 2-7.

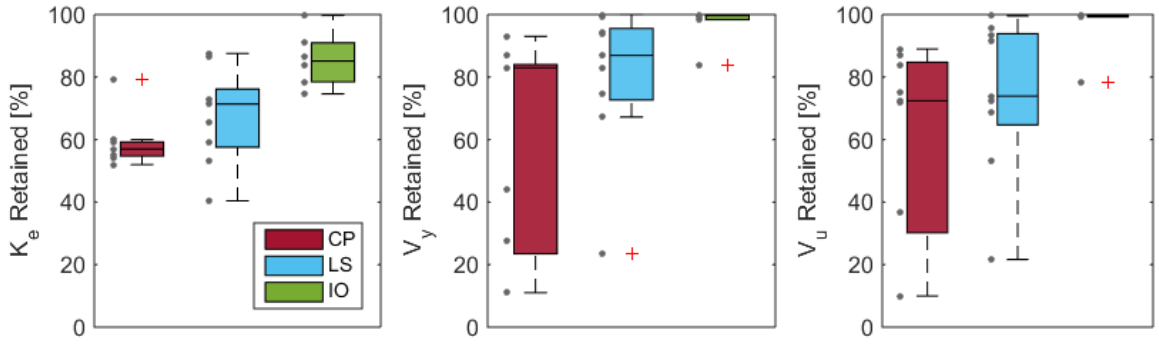

(a) *(b)* *(c)*

Figure 2-10 – Percent of (a) effective stiffness, (b) yield strength, and (c) ultimate strength retained after experiencing design level shaking for each building. Boxplots account for variability in ground motions and in buildings, where 25th and 75th percentiles are indicated by top and bottom edges of the box. The central mark in the box shows the median value and whiskers extend to most extreme value not considering outlier.

ASCE 41 approximate damage estimates indicate that large permanent drifts may occur in buildings designed to CP and, for the CP compliant retrofit buildings in this study, permanent interstory drifts ranged from 0.1% to 0.4%. Furthermore, ASCE 41 indicates that some permanent drifts may occur in buildings designed to LS, and that permanent drifts are not estimated to occur. No significant permanent drifts were observed in buildings designed to achieve LS. For buildings that comply with IO standards, residual drifts observed during the in this study are negligible.

2.7.2.2 Evaluation of Structural Damage Defined at the Component Level

ASCE 41 Table C2-4 provides more detailed damage estimates based on building type. Table 2-8 compares ASCE 41 damage descriptions for primary elements in concrete frames with

the most damaged components identified from simulation in this study. ASCE 41 does not provide damage estimates for retrofit members.

For buildings retrofit to comply with CP, the damage approximated by ASCE 41 is opposite of the damage observed in the simulation results. ASCE 41 estimates that damage will concentrate in ductile elements, and limited damage will occur in non-ductile columns. However, the simulation predicts that the remaining non-ductile columns are the most likely to be damaged element in buildings retrofit to CP, regardless of the retrofit method (*i.e.* steel jacketing, concrete jacketing, or FRP wraps). Such retrofit designs are permitted by ASCE 41 so long as they have sufficient strength to resist a design level event, but Table 2-8 clearly shows that damage pattern in these buildings differs from the damage pattern approximated by ASCE 41. The same trends are true for buildings retrofit to LS, however, the amount of damage to non-ductile components in the simulation results is less than that observed in buildings retrofit to CP.

For buildings designed to IO in this study, most designs required retrofits to all columns in the building. Since there are no fragility functions for retrofit members, the ACI Ordinary Moment Frame (OMF) fragility was used in the loss analysis. While this is technically only valid for members retrofit with RC jackets, the characteristics of the fragility such as strong columns and weak beams, also apply to members retrofit with steel jackets. For buildings designed to this PL, there is good agreement between ASCE 41 damage definitions and the observed damage from simulation. Damage is primarily occurring in beams, and yielding, cracking and spalling are minimal.

Table 2-8 – Most damaged structural components during design level event, comparing simulation and ASCE 41 approximation (reproduced from ASCE 41 Table C2-4 for primary elements in concrete frame buildings). In the analysis, as the component having the highest contribution to structural repair cost during design level shaking is identified as "most damaged".

PL	*ASCE 41 Approximate Damage to Structural Components*	*Most Damaged Structural Component from Analysis*	*Damage State (DS) for Most Damaged Structural Component from Analysis*
CP	Extensive cracking and hinge formation in ductile elements. Limited cracking or splice failure in some non-ductile columns. Severe damage in short columns.	Unretrofit 1967 moment frames with weak columns and strong beams	**DS2**: Concrete Crushing: slabs, beams or joints. Spalling of beam, column or joint cover concrete exposes longitudinal reinforcement or strength loss initiates in laboratory testing. Exhibits concrete spalling that exposes longitudinal steel or crushing of core concrete
LS	Extensive damage to beams. Spalling of cover and shear cracking in ductile columns. Minor spalling in non-ductile columns. joint cracks.	Unretrofit 1967 moment frames with weak columns and strong beams	Either: **DS1:** Concrete Cracking: beams, joints or possibly. Residual concrete crack widths exceed 0.06in. (1.5 mm). Column exhibits residual crack widths that require epoxy or **DS2** (see definition for DS2 above)
IO	Minor cracking. Limited yielding possible at a few locations. Minor spalling of concrete cover.	ACI 318 Ordinary Moment Frame (OMF) with weak, flexurally controlled, beams (i.e. moment frames that have been retrofit)	**DS1:** Beams or joints exhibit residual crack widths > 0.06 in. No significant spalling. No fracture or buckling of reinforcing.

2.7.3 Performance of Nonstructural Components

ASCE 41 requires compliance with a combination of structural and nonstructural performance levels as described in Table 2-1. Three nonstructural performance levels are defined: Positon Retention, Life Safety, and Not Considered. At the BSE-1E level, nonstructural performance must meet Life Safety standards in combination with LS structural performance.

However, here, existing 1967 buildings were shown to comply with this nonstructural performance level and did not require retrofit. Moreover, at the BSE-2E hazard level, ASCE 41 does not require consideration of nonstructural performance. As a result, comparing buildings retrofit to CP and LS structural performance levels (in both retrofit levels nonstructural performance is not considered) in Figure 2-11 shows that no noticeable improvement in nonstructural performance is observed when designing to the more stringent structural performance leave. Effectively, if nonstructural performance is not explicitly considered in the design, one cannot assume annualized nonstructural repair costs will improve with increasing the structural performance.

Buildings designed to IO structural performance must comply with Position Retention nonstructural performance. To consider the impact of nonstructural performance here, buildings designed to IO at the BSE-2E level are investigated with upgraded nonstructural components. In these buildings, existing nonstructural component fragilities were replaced with seismically-rated fragilities wherever possible to represent the upgrade of nonstructural components in the retrofit. We note however that nonstructural repair cost is dominated by damage to partition walls and cladding, components, which were not seismically upgraded during loss analysis. ASCE 41 requires that these components be able to resist force demands resulting from design level shaking, however, this was not performed for this study. Nevertheless, this approach does provide an estimate of the effect of reduced nonstructural vulnerability during the loss estimation.

Figure 2-11 presents nonstructural and total annualized repair cost estimates for the IO-designed buildings. Improvement in the annualized repair cost due to nonstructural components in models designed to meet IO structural performance and position retention nonstructural performance are negligible, despite the fact that repair cost estimates in these models are based upon seismically rated nonstructural fragilities. Displacement demands and repair costs associated with drift sensitive nonstructural components are lower in stronger buildings such as those designed to IO. However, acceleration demands and repair costs associated with acceleration sensitive nonstructural components are larger in stronger buildings. Differences in repair costs due to acceleration sensitive and drift sensitive nonstructural components can offset one another (Ramirez, et al., 2012; Takahashi & Shiohara, 2004) In addition, buildings designed to IO fail by a sideway mechanism in which damage is distributed throughout beams in all stories and at the base of first story columns. In buildings designed to CP or LS, damage typically concentrates in a single story. The distributed damage pattern and deformed shape of buildings designed to IO leads to nonstructural component damage in multiple stories. EDPs are lower in buildings designed to IO than in those designed to CP or LS, but this is counteracted by nonstructural damage distributed thought multiple stories. The results also demonstrate that nonstructural repair costs in buildings designed to IO dominate the total annualized repair cost as opposed to buildings designed to CP or LS in which repair cost is dominated by damage to structural components. Therefore, emphasis on reducing nonstructural damage is of greater importance to these structures.

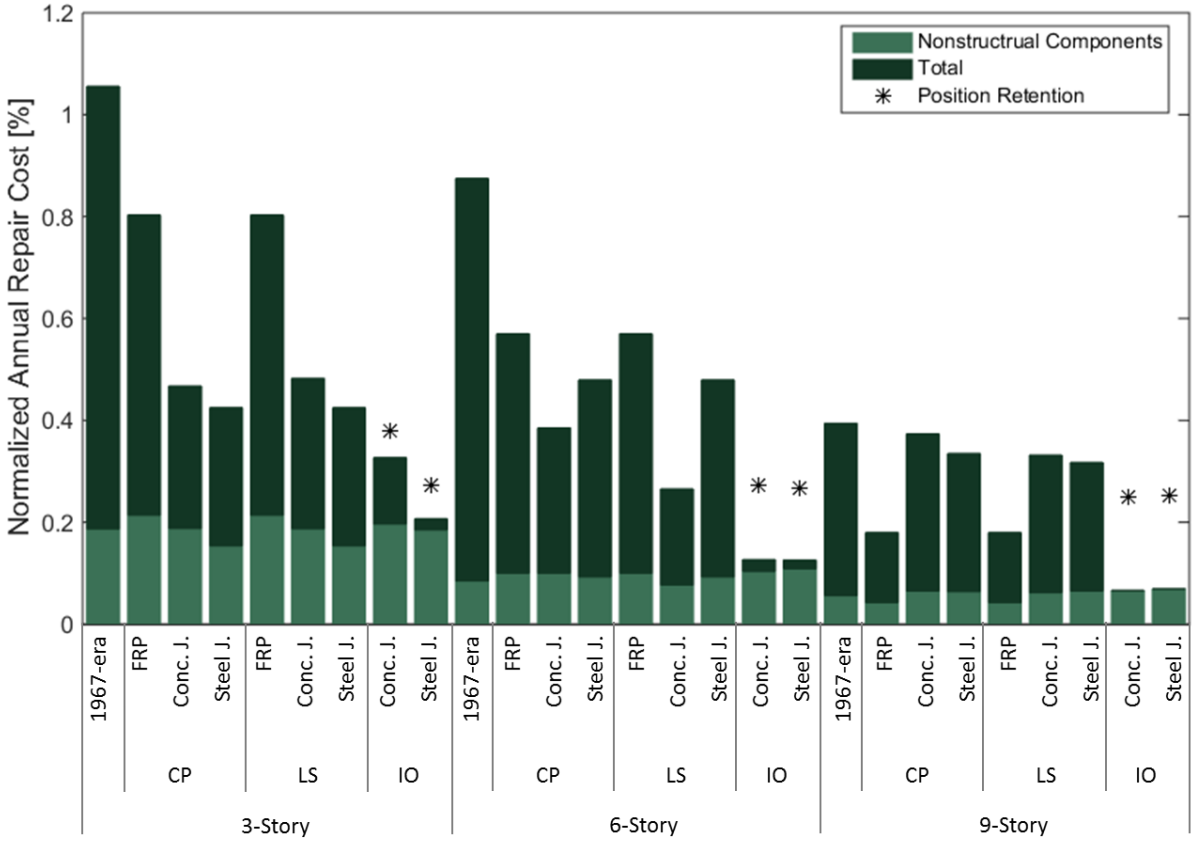

Figure 2-11 - Contribution of nonstructural losses to total annualized repair cost. Asterisk indicates IO retrofit building has been designed to comply with Position Retention nonstructural performance.

2.8 Results and Discussion

This study provides performance estimates for RC frame buildings that are retrofit to ASCE 41 defined PLs. Performance observations are compared to ASCE 41 approximate damage levels for buildings designed to CP, LS, and IO standards. 3-, 6-, and 9-story RC buildings are designed to the 1967 UBC and then retrofit with FRP wraps, steel jackets, or concrete jackets to comply with ASCE 41 CP, LS, and IO performance levels. In total, 36 retrofit designs are considered. Building performance is simulated through nonlinear time history analysis and associated losses are estimated following the FEMA P-58 methodology.

2.8.1 Retrofit Building Performance

2.8.1.1 Overall Performance

This study provided quantitative estimates of building performance in terms of earthquake induced repair cost for a set RC buildings retrofit to ASCE 41 standards as summarized in Table 2-9. ASCE 41 provides qualitative, approximate damage estimates for CP, LS, and IO. The performance observations in Table 2-9 are more detailed than performance estimations in ASCE 41 and therefore provide researchers and practicing engineers with meaningful metrics by which to assess approximate performance of buildings retrofit to ASCE 41 levels.

Trends in overall damage indicate that PLs are internally consistent when evaluated at the design level event (i.e. damage during design level shaking decreases as the design PL is increased from CP to LS and IO). For the majority of structures analyzed in this study, retrofit designs that comply with CP comply with LS without further improvements, as seen by the similarities in annual repair costs between buildings designed to CP and LS in Table 2-9. Furthermore, all 1967 RC frames analyzed in this study are shown to comply with LS performance when evaluated using the BSE-1E motion (i.e. that with 20% probability of occurrence in 50 years). While only RC frames are considered in this study, the acceptance criteria for this PL are liberal, especially when used to analyze a building at a hazard level as low as the BSE-1E.

ASCE 41 overall damage estimates generally align with damage results from this study. However, a few cases are identified where the damage simulated in this study is less than the approximate limiting damage levels listed by ASCE 41. For example, annualized repair costs of the retrofit buildings in this study are compared to annualized repair cost for a modern 4-story

RC building analyzed at the same site by Welsh-Huggins and Liel (under review). Some buildings retrofit to CP were found to have slightly more damage than the modern building analyzed by Welsh-Huggins and Liel (under review), while others had less damage. However, ASCE 41 estimates that CP compliant buildings may have significantly more damage than modern buildings.

The study also shows that buildings designed to CP or LS levels have a larger possible range of estimated repair costs than buildings designed to comply with IO. This occurs because acceptance criteria for CP and LS are more relaxed than in IO, allowing for a broader range of retrofit design solutions. For buildings retrofit to IO standards, both strength and ductility typically need to be improved and all columns within the buildings are typically retrofit leading to a more uniform performance for this PL.

Table 2-9 - Overall performance results

	ASCE 41 Estimates (Sa = Sa, design)		*Simulation Results*	
PL	*Overall Damage*	*Damage compared to modern RC frames*	*Normalized Median Repair Cost (Sa = Sa, design)*	*Normalized Annual Repair Cost*
CP	severe	significantly more damage	40% - 75%	0.2% - 0.8%
LS	moderate	somewhat more damage	10% - 50%	0.2% - 0.8%
IO	light	less damage	5% - 18%	0.07% - 0.3%
Modern Buildings	-	-	-	0.25%

2.8.1.2 Performance of Structural Components

Structural performance is evaluated using two approaches. Damage to structural systems is first assessed by subjecting buildings to design level shaking in dynamic analysis, then calculating remaining building capacities after shaking has ceased through pushover. Based on assessments of reductions in strength and stiffness after design-level shaking, the results show that ASCE 41 damage estimates for structural systems are in good agreement with buildings in this study retrofit to meet LS and IO performance, indicating buildings designed to these levels retain a significant amount of their original strength and stiffness after experiencing a design level event. However, less damage is observed in buildings designed to CP (showing the buildings retain 60% of their original stiffness, 80% of their yield strength, and 70% of their ultimate strength on average) than approximated by ASCE 41. These results also show that buildings designed to less restrictive PLs (i.e. CP and LS) contain a significant amount of dispersion in the capacities of the damaged in its damaged state. This is due to varying degrees of nonlinear behavior recorded during dynamic analysis resulting from record-to-record variation. Buildings designed to IO experience negligible nonlinear behavior during design level shaking and therefore less dispersion is measured in their post-dynamic capacities.

Damage to individual structural components is also assessed during loss analysis and compared with approximate damage patterns from ASCE 41. Simulation results show that damage in buildings designed to the IO level is limited and is concentrated in beams and joints. This observation is in good agreement with ASCE 41 expectations. Damage in buildings designed to CP and LS concentrates in the moment frames in which the columns have not been retrofit.

Damage in these moment frames occurs in the beams, columns, or joints. This result is contrary to ASCE 41 defined damage pattern where damage is expected to concentrate in ductile components. In buildings designed to CP or LS standards, the undesirable failure mechanism may not warrant extreme concern so long as the strength provided by the retrofit design sufficiently lowers the collapse risk of the building.

2.8.1.3 Performance of Nonstructural Components

Two nonstructural performance levels are considered: Position Retention and Not Considered. Nonstructural components are not explicitly considered during the retrofit design process or modeled during numerical simulation. However, in buildings designed to Position Retention standards, nonstructural component fragilities are updated to seismically-rated components whenever possible. If the nonstructural performance level is Not Considered, component fragilities are representative of nonstructural components typically found in 1967 buildings.

Building that are designed with nonstructural performance Not Considered do not see any reduction in nonstructural repair costs with increasing structural performance from retrofit. Indeed, buildings that have not been seismically retrofit have repair costs due to nonstructural components that are equivalent to those estimated for buildings retrofit to comply with CP and LS performance levels. Therefore, if nonstructural performance is not explicitly considered during the design one cannot assume an improvement in structural performance through retrofit design will reduce nonstructural damage. Furthermore, nonstructural damage in IO buildings designed to comply with Position Retention nonstructural performance do not have reliable reductions in

nonstructural repair costs compared to buildings that do not consider nonstructural performance.

3 QUANTIFYING IMPROVEMENTS IN SEISMIC PERFORMANCE POSSIBLE THROUGH RETROFIT OF RC MOMENT FRAMES

3.1 Introduction

A significant amount of damage and collapse has occurred in older, potentially nonductile, reinforced concrete (RC) moment frame structures in past earthquakes. For example, during the recent 2016 Meinong Earthquake in Taiwan, around 10 RC buildings collapsed (Tu, 2016). As a result, older concrete structures pose a high seismic risk to occupant life safety, with probabilities of collapse that may be substantially larger than other structures, particularly modern code-conforming construction (Liel, Haselton, & Deierlein, 2011). The most feasible approach for improving the seismic performance of older RC buildings is through retrofit. Recently, Mayor Garcetti of Los Angeles, proposed the most aggressive seismic safety regulations in California history; these regulations specifically target older concrete structures, requiring the retrofit of hundreds of such buildings within the next 30 years (Lin II, Xia, & Smith, 2014). Other U.S. cities are considering similar legislation.

In the U.S., seismic retrofit design is primarily conducted following an accepted standard such as ASCE 41 (ASCE, 2013), though voluntary retrofits may be designed without use of a standard or through partial adherence to a standard. Common to all standard-based retrofit designs is the goal of achieving a predefined level global performance (*i.e.* Performance Levels in ASCE 41, or the traditional retrofit goal of designing to 75% of modern code levels). However, the cost of retrofitting to satisfy a standard-based performance objective may not appropriately

consider the relative costs and benefits of specific retrofit decisions and actions (Pekelnicky & Poland, 2012). While standard-based approaches seek to design retrofits that mitigate the most glaring seismic deficiencies, they may not do so in the most cost-effective manner. Furthermore, standard-based retrofit designs are typically conducted considering one or two hazard levels and commonly ignore the seismic response at lower intensities which have been shown to have a high contribution to annualized loss (Ramirez, et al., 2012).

Currently, it is unclear how benefits and shortcomings of different rehabilitation methods compare, in terms of global performance, because capacity and fragility models for retrofit structures are rare. In part, this is due to limited observations on the performance of retrofit buildings in large earthquakes and a lack experimental research. The vast majority of previous research has been focused on describing the effect of rehabilitation methods on element level responses such as strength, stiffness, and ductility. Though this research is paramount for building a database from which constitutive relationships are obtained and applied to component models, it does not answer questions related to structural level response benefits from retrofit or serve as a decision tool for the relevant stakeholders. To empower the stakeholder with tools to aid in the selection of the efficient retrofit techniques, conditioned on type of building deficiency and desired performance objective, global retrofit metrics are needed that quantify the effect of individual rehabilitation methods on structural level performance measures. In particular, there is a need to compare system level effects across rehabilitation techniques.

This study systematically quantifies the benefits of retrofitting RC frames at the structural level through the identification and definition of dimensionless structural indicators that are

strong predictors of retrofit effectiveness. Effectiveness is defined as the improvement in collapse capacity and expected seismic loss achieved through retrofit. For example, structural indicators quantifying the change in strength and deformation capacity associated with retrofit action are considered. Structural indicators are identified through a performance-based engineering framework that accounts for main sources of uncertainty related to seismic hazard, building vulnerability, and loss. This study evaluates set of retrofitted RC buildings to identify effective structural indicators. The set of RC buildings is designed to contain a wide range of performances possible through retrofitting to standard levels. While indicators are derived based on this limited set of buildings, the author theorizes the performance of other structures retrofit to standardized levels should be contained within this set.

First, a set of buildings is designed in accordance with loads in 1967 Uniform Building Code (UBC) and specifications in ACI 318-63 (International Conference of Building Officials, 1967; ACI Committee 318, 1963). These buildings exhibit common deficiencies in older concrete structures, including weak-stories, shear-critical columns, weak-column-strong-beam arrangements, and inadequate base shear strengths (i.e. overall weakness). Buildings are then retrofit with concrete jacketing, steel jacketing, or fiber-reinforced polymer (FRP) wraps according to the U.S. standard for seismic evaluation and retrofit, ASCE 41-13 (ASCE, 2013). Each of the deficient and retrofit buildings are assessed through the performance-based earthquake engineering (PBEE) framework. Nonlinear models of each building are created in OpenSEES and time-history analysis is performed to quantify the mean annual frequency of collapse ($\lambda_{collapse}$) and relevant Engineering Demand Parameters (EDP) under the Design Basis Earthquake (DBE). Dollar losses

associated with repair of earthquake-induced damage are quantified using the FEMA P-58 methodology (FEMA, 2012) to estimate annualized repair costs and median repair costs for the DBE. Through comparison of mean loss estimates for retrofit and un-retrofit building models, structural indicators that quantify retrofit effectiveness in protecting life safety and preventing future losses are defined.

3.2 Improving the Seismic Performance of Older RC Buildings Through Rehabilitation of Column Deficiencies: Previous Research

In the U.S., research on local seismic rehabilitation has been directed at upgrading deficiencies in columns, beam-column connections, and slab-column connections. Beams and wall elements are generally considered to be less critical or less vulnerable, and therefore have not been researched as extensively (Moehle, 2000). Column response in frame buildings may be controlled by axial load, flexure, shear, or bond length. Modern seismic design practice considers flexure to be the desirable failure mode (Moehle, Hooper, & Lubke, 2008). Furthermore, columns should not undergo the majority of inelastic deformation within a frame system. Research into rehabilitation of column deficiencies has been concerned with improving column properties to meet these expectations. This study examines structural improvements from retrofitting columns with concrete, steel, or FRP jackets. Selected research that describes experimental tests or design procedures pertaining to each of these retrofit techniques is highlighted below.

3.2.1 Concrete Jacketing of Deficient RC Members

Concrete jacketing is the most commonly used method for upgrading the performance of deficient RC members in the U.S. because of its cost-effectiveness (Bousias, Spathis, & Fardis, 2004). This retrofit technique encases an existing RC member in a cast-in-place steel RC jacket, with the goal of enhancing strength and ductility of the deficient member.

Seven cantilever columns with inadequate lap-splice lengths, four with smooth bars and hooked ends and three with ribbed bars and straight ends, were tested by Bousias *et al.* (2004). Each column was retrofit with an RC jacket and cyclically tested to failure. In this study, RC jacketing was found to increase the flexural strength capacity in all members to the level of that of an equivalent monolithic column. RC jacketing of columns with smooth bars and hooked ends drastically improved deformation capacity and energy dissipation to levels equivalent to that of monolithic columns. However, in columns with ribbed bars and straight ends, RC jacketing improved deformation capacity, but could not restore deformation capacity and energy dissipation to that of a monolithic column. Supplementing the work from (Bousias, Spathis, & Fardis, 2004) with additional data from the literature, Bousias *et al.* (2007) developed expressions for yield moment, yield drift, secant stiffness, and ultimate drift of RC jacketed columns under cyclic loading with or without lap splices at the base of the original column. The derived expressions produce parameters that are presented as a ratio of the corresponding quantities of an equivalent monolithic member.

A majority of research conducted on seismic retrofitting using RC jackets tests members that are constructed under zero axial load conditions. However, in practice, the retrofit column

is responding under service loads (*i.e.* preloading) at the time of instillation of the RC jacket. Vandoros and Dritsos (2006) examined the effect of preloading on the cyclic performance of columns retrofit with RC jackets. Four cases of testing were considered: 1) the original column without retrofit, 2) an equivalent monolithic column (*i.e*. whose cross-section equals that of the retrofit column), 3) the original column retrofit under a zero load condition, and 4) the original column retrofit under an axial load of 75% of its ultimate capacity when computed with zero moment. For specimens retrofit under service loads, preloading was found to increase strength and deformation capacities as well as helps the specimen to dissipate more energy because of the additional compressive stresses in the jacket during the time of installation (Vandoros & Dritsos, 2006).

Recently Chalioris *et al.* (2014) tested 20 beams designed to fail in shear either prior to, or immediately after flexural yielding. Specimens were loaded to near failure, then repaired with a thin layer of three-sided high-strength self-compacting concrete. Specimens that had been repaired and retrofitted were shown to have increased strength and ductility compared to the original members. Additionally, analytical models were created to predict the response of retrofit members (Chalioris, Thermou, & Pantazopoulou, 2014).

3.2.2 Steel Jacketing of Deficient RC Members

In the retrofit of existing RC members with steel jacketing, the existing member is encased in a rectangular or elliptical steel section that provides shear strength, and ductility due to added confinement, without significantly increasing the member's cross-sectional area (Bett, Klinger, & Jirsa, 1988). To experimentally test this technique, three short RC columns were tested by Bett

et al. (1988) with and without retrofit by rectangular steel jacketing filled with shotcrete. Columns were tested under cyclic lateral loading. Columns without retrofit were governed by shear failure due to the small shear span to depth ratio. After retrofit, columns exhibited significant increases in stiffness and strength, both flexural and shear, due to jacketing. Jackets were able to provide enough shear capacity to resist the shear corresponding to the formation of plastic hinges at column ends, effectively shifting the governing failure mode of the members from shear to flexure and improving deformation capacities.

Studies conducted by Aboutaha *et al.* (1996; 1999) also examined the response of deficient RC members retrofit with steel jackets. Eleven large-scale tests were performed on columns designed to ACI 318-56 and ACI 318-63 standards with inadequate lap splices in the longitudinal reinforcement, and subsequently retrofit with rectangular steel jackets. Cyclic tests indicated that thin rectangular steel jackets combined with adhesive anchor bolts are effective retrofit measures. Design guidelines for retrofitting inadequate lap splices with rectangular steel jackets are also presented (Aboutaha, Engelhardt, Jirsa, & Kreger, 1996). In a separate study, eleven large-scale columns with inadequate shear resistance were retrofit with steel jackets and tested under quasi-static monotonic and cyclic loading. Steel jackets were found to be effective retrofit measures for improving the deformation capacity and strength of shear-critical columns. Furthermore, shear-critical columns retrofit with steel jackets exhibited large deformation capacity and high-energy dissipation (Aboutaha, Engelhardt, Jirsa, & Kreger, 1999).

3.2.3 Wrapping Deficient Members with FRP

There are many ways to strengthen an existing RC member, or to design a new member, using FRP (Bakis, et al., 2002). However, the most common retrofit application is through externally bonded FRP jackets applied to existing members. FRP systems offer advantages over traditional retrofit systems due to their high tensile strength and lightweight, noncorrosive properties (ACI Comittee 440, 2008). Here, we consider FRP sheets that are externally bonded to existing RC members by an adhesive. These sheets can be oriented with the fibers longitudinally to increase flexural strength, or with fibers oriented in the transverse direction to increase confinement and shear strength.

To examine the effect of externally bonded FRP wraps oriented in the transverse direction on concrete confinement, Mirmiran & Shahawy (1997) performed uniaxial compression tests on 9 concrete-filled FRP tubes, and results were compared with available confinement models. A significant increase in flexural strength and deformation capacity was recorded in concrete confined by FRP. Unlike steel-encased concrete, the hardening response of FRP encased concrete is bilinear up until failure. The monotonic response consists of three regions: 1) an initial response similar to plain concrete, since the lateral expansion of the core is insignificant, 2) a transition zone is entered as microcracks increase in the concrete and the FRP tube exerts a lateral pressure on the core to counteract stiffness degradation of the concrete, and 3) the FRP tube becomes fully active activated and the stiffness stabilizes around a constant value, which is dependent upon the stiffness of the FRP tube, until failure.

Eight specimens with inadequate transverse reinforcement were tested by Ilki *et al.* (2004) under cyclic lateral loads. Four of the specimens exhibited inadequate lap splices, and four had continuous longitudinal rebar. In each of these two groups, one specimen was tested as the reference, two were retrofit with different thicknesses of carbon fiber reinforced polymer (CFRP) jackets aligned in the transverse direction, and one previously damaged specimen was retrofit using CFRP jacketing, also aligned in the transverse direction. Significant improvement of strength and deformation capacity due to CFRP jacketing was observed in all specimens. In members with continuous longitudinal reinforcement, CFRP jacketing provided sufficient confinement to help prevent longitudinal rebar buckling. In specimens with inadequate lap splices, CFRP jackets limited transverse displacements, delaying loss of strength due to bar slip.

3.3 Relationship Between Changes in Retrofits' System-Level Structural Characteristics and Seismic Performance Improvements: Previous Research

The vast majority of studies that report changes in structural properties (*i.e.* strength and ductility) resulting from seismic retrofits either focus on element level improvements, as described above, or are the published results of seismic retrofits performed by design firms. Few studies link incremental changes in structural performance with incremental improvements in estimated loss. What follows is a selection of studies that connect seismic resistance with seismic performance.

Though a cost-benefit analysis, Liel and Deierlein (2013) evaluated the economic benefits of various retrofit strategies. Based on analytical results of 8 non-ductile RC frames and 8 retrofit

RC frames, retrofitting produced a positive rate of return valued at 10% to 30% of the building replacement cost when damage and repair costs were considered. The cost of retrofits is generally more expensive than this valuation, however, and therefore, retrofitting was not found to be cost-effective when based on the reduced risk of damage and repairs. However, when benefits associated with reduced fatality risks are considered, retrofitting can produce a rate of return greater than 60% of the building replacement cost, which may be cost-effective given typical retrofit costs (Liel & Deierlein, 2013).

In a similar study, Smyth et al. (2004) evaluated the effectiveness of three retrofit strategies for a RC frame apartment in Turkey through cost-benefit analysis. Expected benefits and discounted damage of the 3 retrofit schemes was compared, showing that a full shear wall retrofit structure performed better than the partial shear wall retrofit structure and braced frame retrofit structure. Additionally, all 3 retrofit schemes where shown to be desirable options as opposed to not retrofitting based upon expected time-dependent damage estimates (Smyth, et al., 2004).

While not directly dealing with estimated losses, Thermou and Elnashai (2006) qualitatively compared the effect of different retrofit strategies on structural strength, stiffness, and ductility. Thermou and Elnashai propose comparing retrofit schemes at the structural level in terms of strength, stiffness, and ductility because they are the three most important seismic parameters in assisting designers in decision making to satisfy performance objectives (Thermou & Elnashai, 2006).

Tesfamariam and Goda, 2015 assessed the seismic risk of a 4-story nonductile RC building located in Victoria, British Columbia, Canada through the performance-based engineering framework. The seismic hazard considered mainshock-aftershock sequences representative of a magnitude 9 Cascadia subduction earthquake. Annual repair costs were found to increase 1-4% when aftershocks were included in the analysis, showing that the effect of aftershocks on overall seismic loss is relatively minor. Additionally, assumptions regarding damage states related to demolition had a significant impact during loss assessment (Tesfamariam & Goda, 2015).

3.4 Design of 1967 RC Frame Buildings

Here, a set of 3-, 6-, and 9-story non-ductile RC space frame structures is designed according to the Uniform Building Code of 1967. All buildings are located at a site in Los Angeles, California (33.996°N, -118.162°W). Common deficiencies for non-ductile buildings developed for this study include: shear-critical columns, weak-column-strong-beam arrangements, and overall weakness in strength. The 1967 buildings are then retrofit using local rehabilitation techniques to standards set forth in ASCE 41 (ASCE, 2013), the most commonly used document for retrofit design of RC frames in the U.S. Local rehabilitation techniques considered in this study address column deficiencies through wrapping columns in FRP, or encasing the column in a steel or concrete jacket. Local retrofits are designed to comply with ASCE 41 Collapse Prevention (CP), Life Safety (LS), and Immediate Occupancy (IO) performance levels. For a more detailed description of the design of 1967 buildings and retrofit designs please refer to Section 2.4.

3.5 Nonlinear Modeling and Structural Performance

The seismic response of buildings designed in this study is assessed through the use of two-dimensional nonlinear models analyzed using the *OpenSEES* platform. Nonlinear component models are selected that are capable of capturing significant response characteristics and failure modes for the original and retrofit structures. Table 3-1 provides a list of the element models used for primary structural components making up the original and retrofit 1967 buildings.

In fiber – also called distributed plasticity - models, the stress-strain relationship of concrete fibers is described by the modified Kent and Park model (Kent & Park, 1971); steel fibers are modeled using the relation proposed by Giuffre-Menegotto-Pinto (Filippou, Popov, & Bertero, 1983) and the onset of buckling and post-bucking behavior is determined using the model proposed by Dhakal and Maekawa (2002). When the governing failure mode is flexure, a single force-based fiber element is used per flexural element and the regularized integration scheme presented by Scott & Hamutcuoglu (2008) is employed with five integration points.

Nonlinear dynamic analysis is performed to characterize probabilistic relationships between seismic intensity measures (IM) and engineering demand parameters (EDP). EDPs, quantified in terms of peak floor accelerations, story drift ratios, and residual drifts, are computed through multi-stripe analysis. Five stripe levels are considered that have probabilities of occurrence equal to 50%, 20%, 10%, 5%, and 2% in 50 years. 11 two-component records (22 horizontal records total) are run at each stripe level, where records are selected using conditional mean spectra as a target (Baker J. W., 2011). The collapse capacity of each building is estimated through use of Incremental Dynamic Analysis (IDA) (Vandoros & Dritsos, 2006). Mean annual

frequencies of collapse are calculated by integrating the collapse fragility with the probabilistic site hazard curve. For a more complete description of the simulation models used in this study please refer to Section 2.5.

Table 3-1 - Element models and associated responses used for primary structural components

Component	*Element Model(s)*	*Responses Captured*
• 1967 columns	layered fiber element in series with shear and axial springs	elastic behavior; steel yielding; steel buckling; concrete crushing; concrete tensile failure; column shear failure and subsequent column axial failure
• FRP wrapped columns • Steel jacketed columns • Concrete jacketed columns • Beams	layered fiber element	elastic behavior; steel yielding; steel buckling; concrete crushing; concrete tensile failure
• Joints	elastic panel	elastic behavior

A comparison of the retrofit designs for the 3-story building designed to comply with ASCE-41 CP performance is presented in pushover responses in Figure 3-1a. The FRP retrofit approach employed here adds ductility capacity to the structure, while having a negligible effect on strength. Steel and concrete jackets improve both strength and ductility. Despite the lack of strength increase, the building retrofit with FRP wraps has the highest collapse capacity (Figure 3-1b). A multistory failure mode occurs in the building retrofit with FRP wraps, where the first story yields in flexure then the second story fails in shear. In the buildings retrofit with steel and concrete jackets, the added strength in the first two retrofit stories creates a weak story in the third floor which then fails in shear. This phenomenon is discussed in detail in later sections. Similar patterns are observed for buildings of different heights.

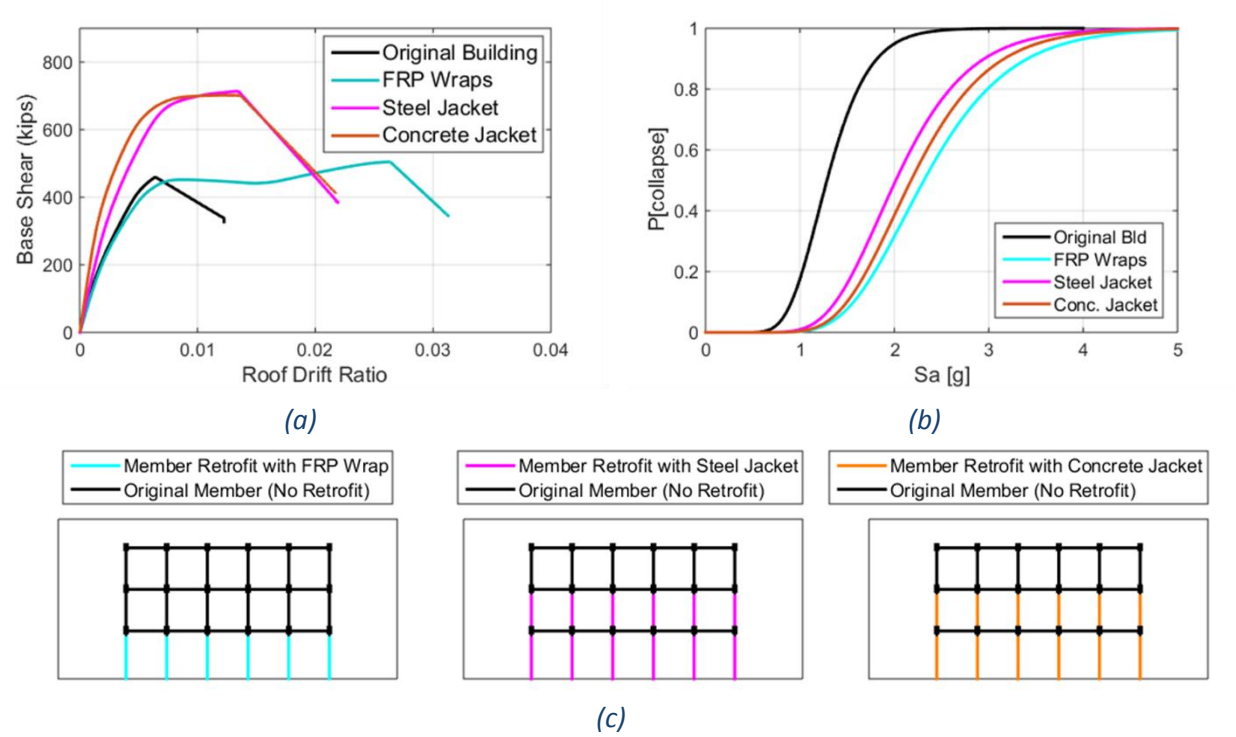

Figure 3-1 - (a) Pushover results, (b) collapse fragilities, and (c) retrofit designs for 3-story buildings retrofit to comply with ASCE 41 CP performance level.

3.6 Loss Estimation Methodology

Probabilistic loss analysis quantifies the damage and associated loss a structure is expected to sustain given a unique seismic hazard level. Loss analysis is performed using the Seismic Performance Prediction Program (SP3) software (Haselton Baker Risk Group, n.d.), a web tool largely based on the FEMA P-58 methodology (FEMA, 2012). In this study, loss is quantified as the estimated repair cost to restore a damaged structure to an undamaged state. Median loss estimates are presented at five hazard levels and account for variability related to hazard, building vulnerability, and component fragilities. Annual loss estimates are computed as the convolution of the median repair cost conditioned on hazard intensity and the hazard's mean rate of occurrence. Annual loss estimates are presented in terms of the average yearly dollar

amounts needed to repair earthquake damage. Repair costs are normalized by the total building replacement cost where the replacement cost of a 3-, 6-, and 9-story building is $10,781,250.00, $21,375,000.00, and $32,062,500.00 respectively. A detailed explanation of the loss estimation methodology and how it is implemented in this study can be found in Section 2.6.

3.7 Strength Indicators to Quantify Improvements in Seismic Performance Through Seismic Retrofit

Historically, base shear strength has played a substantial role in the seismic design of new buildings. Design codes since the mid 1920's have used design base shear as one of the main structural demand parameters for design of buildings in seismic areas. However, adding strength to the structural system may not always be a central part of retrofit design. For example, strong buildings that contain shear-critical columns may be retrofit by wrapping columns in FRP to improve ductility while having a negligible impact on strength.

What follows is an evaluation of the relationship between the strength of retrofit and un-retrofit 1967 buildings and seismic loss, measured in terms of repair cost. In the following results, yield strength and ultimate strength are quantified by fitting a bilinear approximation to the nonlinear pushover cure as per ASCE 41-13 section 7.4.3.2.4 (ASCE, 2013). Since yield strength is computed from an idealized force-displacement curve, it is an "effective" yield strength. Figure 3-2 presents effective yield strength, V_y, and ultimate strength, V_u, as they are calculated using an idealized force-displacement curve.

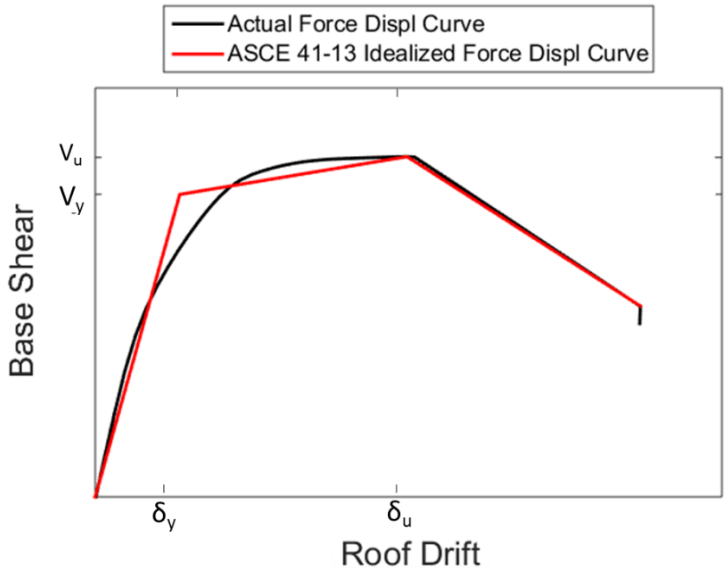

Figure 3-2 - Pushover results and idealized force-displacement curve for 3-story building retrofit to CP standards using concrete jackets

Two metrics are used to quantify the strength of a retrofit design. Equation 3-1 defines the normalized strength parameter, calculated as the strength of the retrofit frame under consideration, divided by the strength of the original, un-retrofit, frame.

$$Normalized\ Parameter = \frac{Parameter\ in\ the\ retrofit\ building\ under\ cosideration}{Parameter\ in\ the\ original\ building} \quad \text{Equation 3-1}$$

For example, Normalized V_y is the yield strength of the considered structure divided by the yield strength of the corresponding un-retrofit 1967 building. Additionally, a measure of the absolute building strength is quantified through $\mu_{strength}$ (ASCE, 2013). $\mu_{strength}$ is calculated by Equation 3-2 where S_a is the 5% damped elastic spectral acceleration at the building's fundamental period, corresponding to shaking intensity with 5% in 50 years likelihood of occurrence, V_y is the effective yield base shear strength as shown in Figure 3-2, and W is the structural weight. $\mu_{strength}$ is thus a ratio of demand to capacity, and larger $\mu_{strength}$ values indicate

weaker buildings. It should be noted that $\mu_{strength}$ is similar to the yield reduction factor, R, in modern design codes (ASCE, 2010).

$$\mu_{strength} = \frac{S_a}{V_y/W} \qquad \textit{Equation 3-2}$$

Strength is used in lieu of stiffness because strength has historically been more prevalent in seismic design. However, trends identified in the following sections for strength also reflect impacts of changes in stiffness because the two parameters are highly correlated. For the building analyses in this study, the correlation coefficient between yield strength and effective stiffness is 1.0 – because they are calculated based on an idealized force-displacement curve shown in Figure 3-2 - and the correlation coefficient between ultimate strength and effective stiffness is 0.96, where effective stiffness is measured as the stiffness of the bilinear pushover approximation.

3.7.1 Relationship Between Strength and Collapse Resistance

The relationship between increased strength provided by retrofit design and mean annual frequency of collapse is presented in Figure 3-3, showing that increases in strength due to seismic retrofitting generally lead to decreases in the mean annual frequency of collapse. However, the significant scatter and low R^2 values in Figure 3-3 signify that $\lambda_{collapse}$ is not well correlated with strength increase provided by retrofitting. Furthermore, stronger buildings (*i.e.,* those with lower $\mu_{strength}$ values) tend to have smaller mean annual frequency of collapse, though this is true not all buildings. For example, the 3-story building with $\mu_{strength}$ between 3 and 4 has a lower mean annual frequency of collapse than many buildings with lower $\mu_{strength}$ values. This building is one

that has been retrofit to meet ASCE 41 CP performance using FRP wraps. In this study, FRP sheets are externally bonded to the exterior face of the existing column with fibers aligned in the transverse direction, significantly increasing the building's ductility capacity, but having negligible impact on strength. Therefore, using measures of strength exclusively to predict improvements in collapse capacity through retrofit design do not work in cases such as this. Instead, the combination of improvements in strength and ductility provided by a retrofit scheme must be considered.

From a design perspective, this study emphasizes that a combination of strength and ductility capacity is important for mitigating collapse risk. For example, if the strength of a system is increased through retrofitting, the ductility demand on that structure decreases, reducing the need for significant ductility capacity. Conversely, in systems with reduced strength, the ductility demand is large. Therefore, the ductility capacity must be large to resist the demand. The collapse risk of a structure can therefore be mitigated by reducing ductility demand by increasing the strength of the systems, or by providing enough ductility capacity to resist the ductility demand.

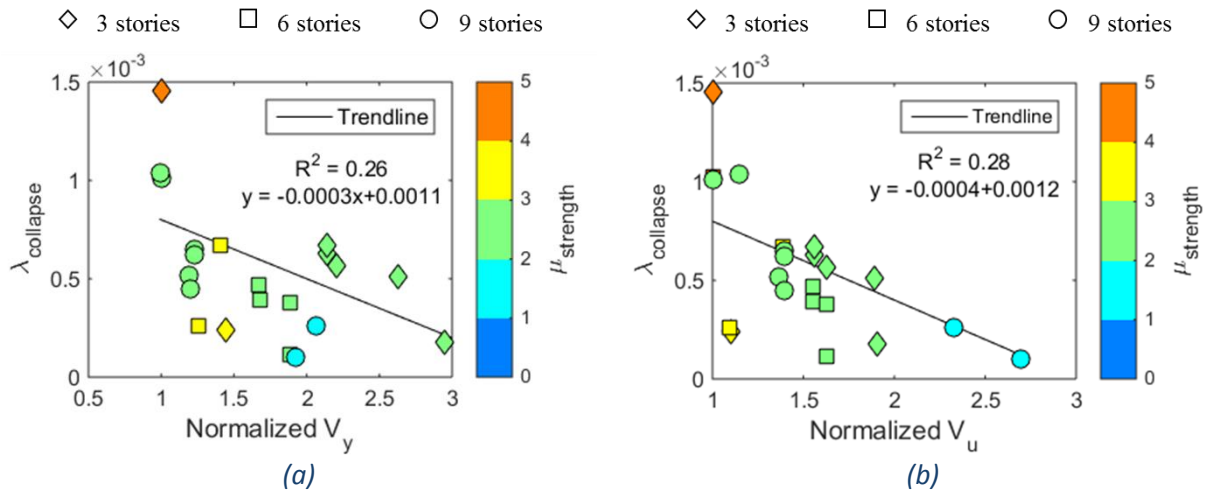

Figure 3-3 - Effect of relative (a) yield strength increase and (b) ultimate strength increase through retrofit design on Mean Annual Frequency of Collapse. $\mu_{strength}$ is calculated using Sa = Sa_{DBE}.

3.7.2 Relationship Between Strength and Estimated Seismic Loss

The impacts of altering the yield strength of the structure through seismic retrofit on median repair cost conditioned on hazard level is presented in Figure 3-4; similar trends are observed with respect to ultimate strength. As the normalized strength is increased during the retrofit design, median repair cost decreases for all hazard levels. This trend is valid for all building heights, as shown by Figure 3-4 a, b, and c. This result is intuitive because increasing yield strength improves the seismic resistance of structural components (reducing structural losses), reduces drift demands (reducing drift-sensitive nonstructural losses), and increases the collapse capacity (reducing collapse losses). However, repair costs in acceleration-sensitive nonstructural components tend to increase at low spectral values when nonlinear behavior is minimal or has not occurred, though the increase is small in comparison to the cost savings in other building components.

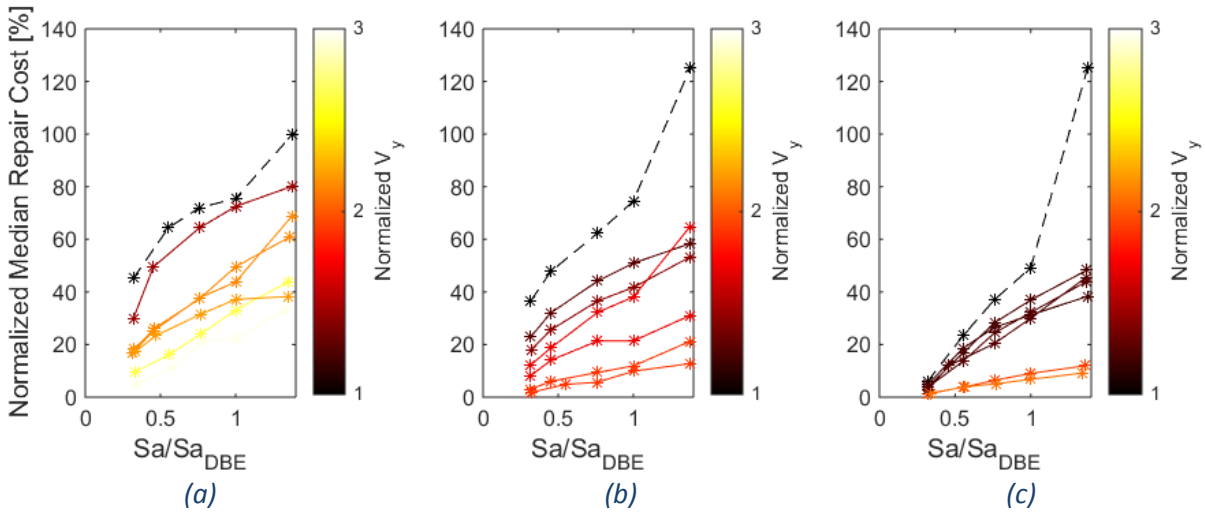

Figure 3-4 - Impact of normalized V_y on median repair cost normalized by total building replacement cost, as a function of spectral acceleration normalized by spectral acceleration of the DBE for (a) 3- (b) 6- and (c) 9-story buildings. Dashed lines indicate 1967 buildings that have not been seismically retrofit. Solid lines indicate 1967 buildings that have been seismically retrofit.

"Annualized" repair costs provide a more complete representation of seismic vulnerability, by combining repair cost estimates from discrete hazard levels based on their probabilities of occurrence. Figure 3-5 a and b present annualized repair cost estimates for varying levels of normalized yield and ultimate strength, where each point in the plot represents a single building. On average, as yield strength and ultimate strength is increased through retrofit design, annualized repair cost is reduced.

In Figure 3-5 absolute strength is quantified through the $\mu_{strength}$ parameter, represented by the color of each data point. Figure 3-5 considers five ranges of $\mu_{strength}$, where $\mu_{strength}$ values close to one are very strong buildings (relative to the level of design shaking) and expected to behave close to elastically; $\mu_{strength}$ values greater than four are exceptionally-weak buildings. Four regions (I- IV) are identified in Figure 3-5 a and b. These regions group buildings based on

their $\mu_{strength}$ value and correspond to a range of annualized repair costs. These regions are independent of building height, retrofit method, and normalized yield and ultimate strength, signifying that the $\mu_{strength}$ value of both 1967 buildings and seismically retrofit buildings is an effective predictor of annualized repair costs. Here, $\mu_{strength}$ is calculated using the spectral acceleration at the fundamental period of the building resulting from a ground motion with 5 percent probability of occurrence in 50 years at the Los Angeles site of interest. If a different hazard was used to calculate $\mu_{strength}$, the results would be similar because each buildings $\mu_{strength}$ would change in a consistent manner however, the precise values of repair cost that correspond to specific level of $\mu_{strength}$ would vary.

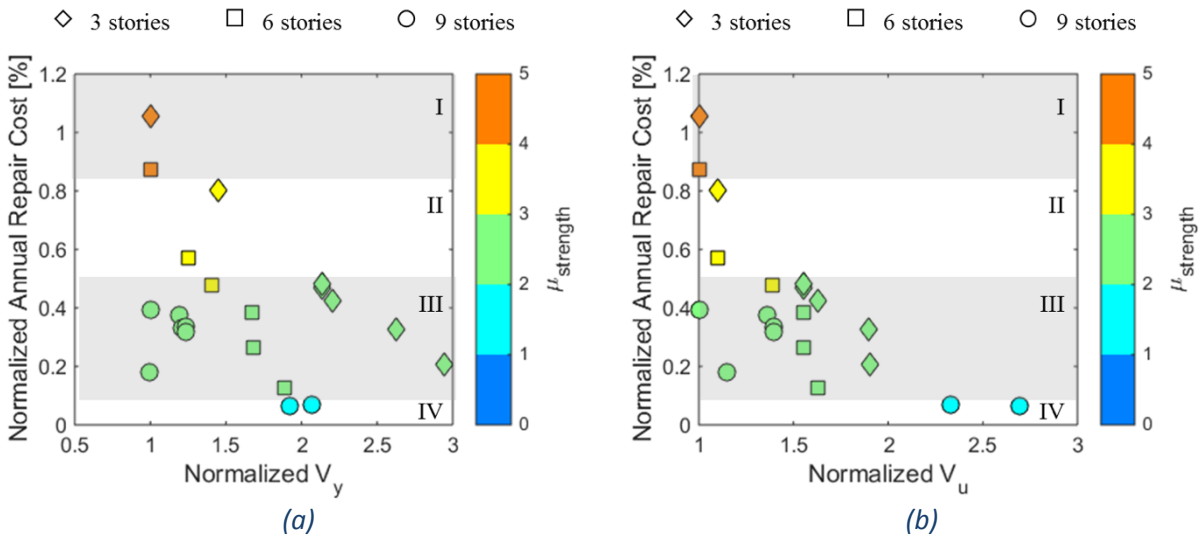

Figure 3-5 - Effect of relative (a) yield strength and (b) ultimate strength increase through retrofit design on annualized repair cost. $\mu_{strength}$ is calculated using Sa = Sa_{DBE}.

To further investigate the relationship between $\mu_{strength}$ and estimated repair cost, annualized repair cost is plotted against $\mu_{strength}$ in Figure 3-6. $\mu_{strength}$ and annualized repair cots appear to be linearly related, though significant scatter exists for $\mu_{strength}$ values between 2 and

3, where the most data points exist. The scatter observed in Figure 3-6 shows that while $\mu_{strength}$ identifies general trends in annualized repair cost, it is not a precise measure (R^2 = 0.72).

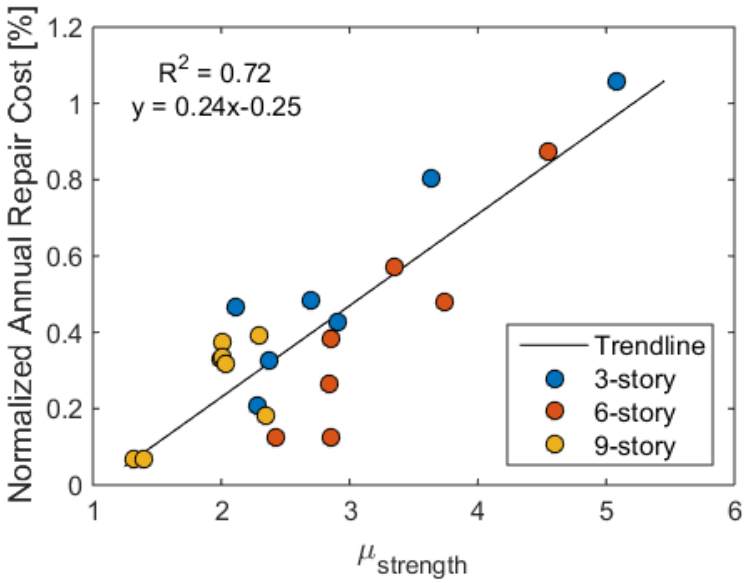

Figure 3-6 - Effect of $\mu_{strength}$ on annualized repair cost for retrofit and original RC frame buildings.

3.7.3 Summary: Strength Indicators

In this section, strength (measured in terms of increased strength provided by a retrofit design and as absolute building strength) is evaluated as an indicator for seismic performance. When strength is used as an indicator of collapse resistance, mean annual frequency of collapse was lower in buildings retrofit to larger strengths on average. However, there were some exceptions to this finding such as buildings retrofit with FRP wraps in which ductility is improved and strength is relatively unaffected yet mean annual frequency of collapse is decreased. These findings indicate that strength and collapse resistance are related, but combinations of strength and ductility are likely better indicators of collapse capacity. The combination of strength and

ductility as it relates to improves in seismic collapse resistance is presented in subsequent sections.

Results also show that strength can be used as an effective indicator for estimated annualized repair costs. Damage to a building and associated repair costs can be mitigated through increased strength in the following ways:

- Capacities of retrofit structural components are increased, such that loss fragilities are reduced
- Drift demands on structural and drift sensitive nonstructural components are decreased
- The collapse capacity of the structure is increased

Absolute strength, measured in terms of $\mu_{strength}$, provides a measure by which expected repair costs can be estimated. Here, buildings were binned into four distinct regions according to their $\mu_{strength}$ values and associated repair costs were assigned. This provides a possible method by which to assess the benefit a retrofit design provides in terms of economic loss.

3.8 Deformation Capacity Indicators to Quantify Improvements in Seismic Performance Through Retrofit Design

One of the primary deficiencies in 1967 buildings is limited deformation capacity. Often, columns lack ductile detailing and are shear-critical. Local retrofit techniques can improve member deformation capacity and, by extension, system level ductility. The effect of ductility on seismic performance is embedded in modern design. Modern codes, such as ASCE 7 and ACI 318, attempt to maximize ductility in RC frames through requirements of ductile detailing provisions

(e.g. requiring strong-column-weak-beam arrangements to spread inelastic behavior to multiple stories and provisions that provide adequate transverse reinforcement to avoid shear failure) (Moehle, Hooper, & Lubke, 2008). Additionally, capacity design ensures the expected building failure mode is ductile. This design philosophy stems from the idea that ductility assists the structure in sustaining multiple cycles of inelastic response. Additionally, failure is less sudden than non-ductile failure modes, therefore providing occupants with more time to evacuate. This section examines the relationship between improved ductility capacity at the system level and seismic collapse capacity and estimated earthquake-related repair costs. Here, ductility capacity is calculated from a nonlinear static analysis as per Eqn. 6-6 of FEMA P695.

3.8.1 Relationship Between Deformation Capacity and Collapse Resistance

The relationship between ductility and collapse capacity, measured in terms of the mean annual frequency of collapse, is presented in Figure 3-7. Figure 3-7 a shows the relationship for all buildings analyzed in this study. In general, increasing system ductility through retrofit design (i.e. normalized ductility) leads to decreases in mean annual frequency of collapse. Decreases in collapse risk are most effective until normalized ductility exceeds 4, or the absolute ductility of a building is raised above 8.

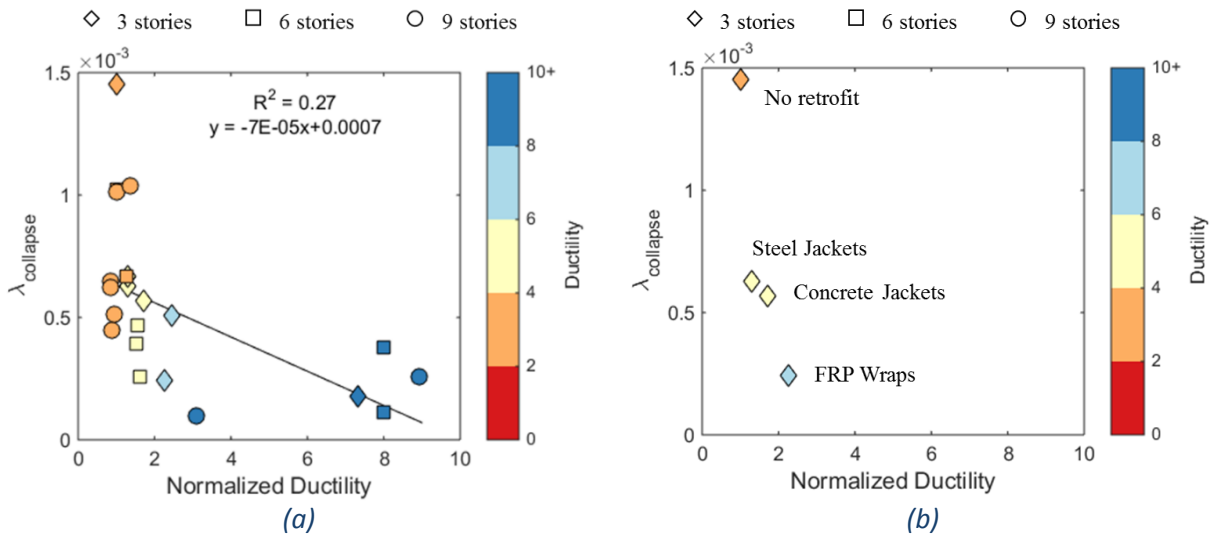

Figure 3-7 - Effect of ductility on building seismic collapse resistance for (a) all buildings analyzed in this study and (b) 3-story building retrofit to comply with ASCE 41 CP performance

While general trends can be observed in Figure 3-7a, the vast range of building characteristics (i.e. strengths, failure modes, etc.) makes it difficult to make detailed observations on the effect of ductility on building collapse risk. The effects of increasing system ductility on mean annual frequency of collapse shown in Figure 3-7b is more obvious. Interestingly, the building retrofit with FRP wraps (the most ductile building) has the lowest collapse risk, despite the fact that the buildings retrofit with steel and concrete jackets are stronger, as shown in Table 3-2. This finding is observed for other buildings of similar strengths analyzed in this study and highlights the importance of providing adequate ductility through retrofit design, particularly in buildings that are expected to behave nonlinearly, to limit collapse risk.

Table 3-2 – Selected capacities for 3-story buildings retrofit to comply with ASCE 41 CP performance

Retrofit Type	$\mu_{strength}$	*Ductility Capacity*	$\lambda_{collapse}$ *[x* 10^{-4}*]*
None	5.1	3.2	15
FRP Wraps	3.6	7.2	2
Steel Jackets	2.1	4.2	6
Concrete Jackets	2.9	5.5	6

3.8.2 Relationship Between Deformation Capacity and Estimated Seismic Loss

Figure 3-8 presents annualized repair costs as a function normalized ductility capacity. Normalized ductility is the ductility capacity of the retrofitted structure normalized by the ductility capacity of the 1967 building without retrofit. The tenuous relationship ($R^2 = 0.24$) shows that increasing ductility through retrofit design can reduce annualized repair costs. However, there appears to be no relationship between ductility capacity and annualized repair cost.

Figure 3-8b presents the relationship between ductility and annualized repair cost for the 3-story building retrofit to comply with ASCE 41 CP performance using either FRP wraps, steel jackets, or concrete jackets. Here, the most ductile building (retrofit with FRP) experiences higher annualized losses than retrofit designs with lower ductility. This trend was observed in different buildings retrofit to either LS or CP and in buildings of different heights. This finding strays from modern design philosophies in which providing ductility is a major concern. The primary reason that ductility and annualized repair cost are not strongly related is that damage from lower intensity events, in which the structure may remain elastic or exhibit slight nonlinear behavior, contribute significantly to annualized repair cost. Essentially, damage from lower intensity events in which collapse is not a concern are more related to the structure's elastic or early inelastic behavior than to the structure's ductility capacity and damage during events with spectral accelerations near the structure's collapse capacity is controlled by a combination of strength and ductility (as explained in detail in later sections). Retrofit designs that provide ductility without having a significant impact on strength will have higher losses at lower hazard levels

because drift demands will be larger. Increased drift demands cause damage and economic loss in both structural and nonstructural components.

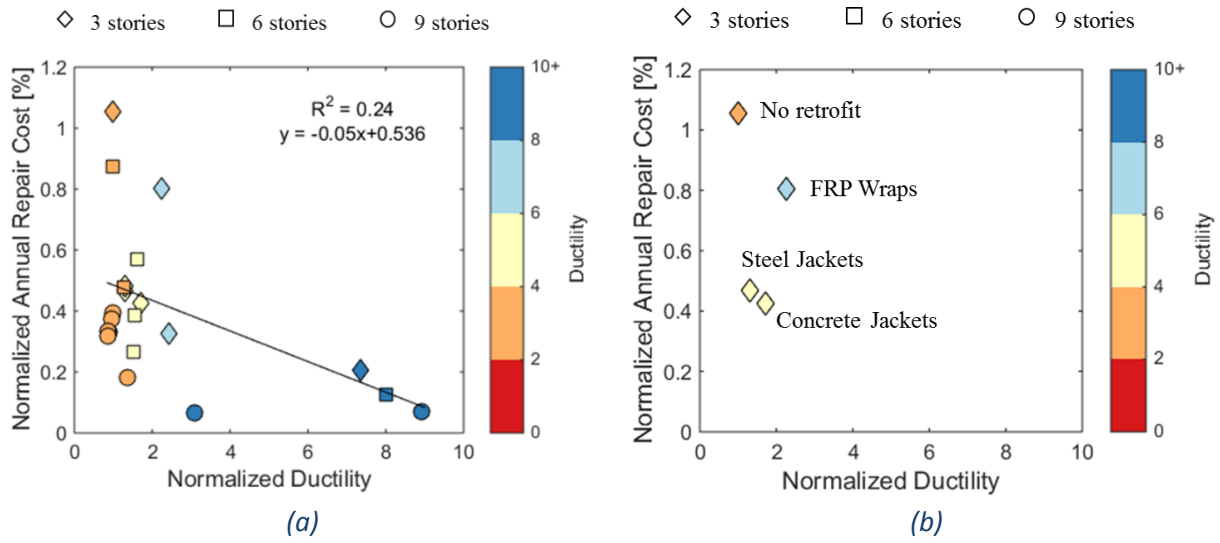

Figure 3-8 - Effect of normalized and absolute ductility capacity on annualized repair cost for (a) all buildings analyzed in this study and (b) 3-story building retrofit to comply with ASCE 41 CP performance

A new term is defined here that compares the structure's expected displacement demand to its effective yield displacement, thereby providing a displacement-based measure that gauges the extent of expected nonlinear behavior in a structure. This new term, δ_{DCR}, is defined in Equation 3-3. δ_{DCR} provides a measure of the ductility demand as opposed to traditional ductility which is a measure of capacity.

$$\delta_{DCR} = \frac{\delta_D}{\delta_y} \qquad \textit{Equation 3-3}$$

In Equation 3-3, δ_y is the effective yield displacement of the structure measured form an idealized bilinear force-displacement curve. δ_D is the expected displacement demand at

measured at the full height of the building, as calculated by Equation 3-4, taken directly from ASCE 41 (ASCE, 2013):

$$\delta_D = C_0 C_1 C_2 S_a \frac{T_e^2}{4\pi^2} g \qquad \textit{Equation 3-4}$$

Here, Co, C1 and C2 are factors that modify the spectral displacement to account for the difference between single and multi-degree of freedom systems, effects of inelasticity and pinched hysteresis. Precise definitions are provided in ASCE 41 (ASCE, 2013). It should be noted that δ_{DCR} can be rearranged and presented as:

$$\delta_{DCR} = \frac{\delta_D}{\delta_y} = C_0 C_1 C_2 \mu_{strength} \qquad \textit{Equation 3-5}$$

The relationship between δ_{DCR} and annualized repair cost is explored in Figure 3-9. Here, δ_{DCR} is computed using the spectral acceleration of the DBE (Sa_{DBE}). A strong linear relationship between δ_{DCR} and annualized loss (correlation coefficient, $\rho = 0.89$) is seen in Figure 3-9. This linear relationship is independent of the number of stories or retrofit technique. The reason δ_{DCR} is a good predictor of annualized repair cost is because δ_{DCR} provides a measure of the extent of nonlinear behavior. For example, buildings with δ_{DCR} close to unity are expected to respond with limited nonlinear behavior under the level of ground shaking considered. Therefore, during lower intensity ground motions that have a large contribution to annualized loss, the structure's response will remain well within the elastic range, limiting damage to structural components and reducing damage to nonstructural components that are sensitive to drift demand. This

relationship is important because it provides a link between design parameters and annualized loss that could be used to define building performance levels.

We note also that the color of the data points in Figure 3-9 represents the ductility capacity of each building. There is a lack of an obvious trend between ductility capacity and annualized repair cost, supporting the conclusion that two parameters are unrelated. More generally, annualized repair cost is not highly related to the collapse capacity of the building, and therefore is better predicted through indicators that quantify the extent of expected nonlinear behavior in a structure.

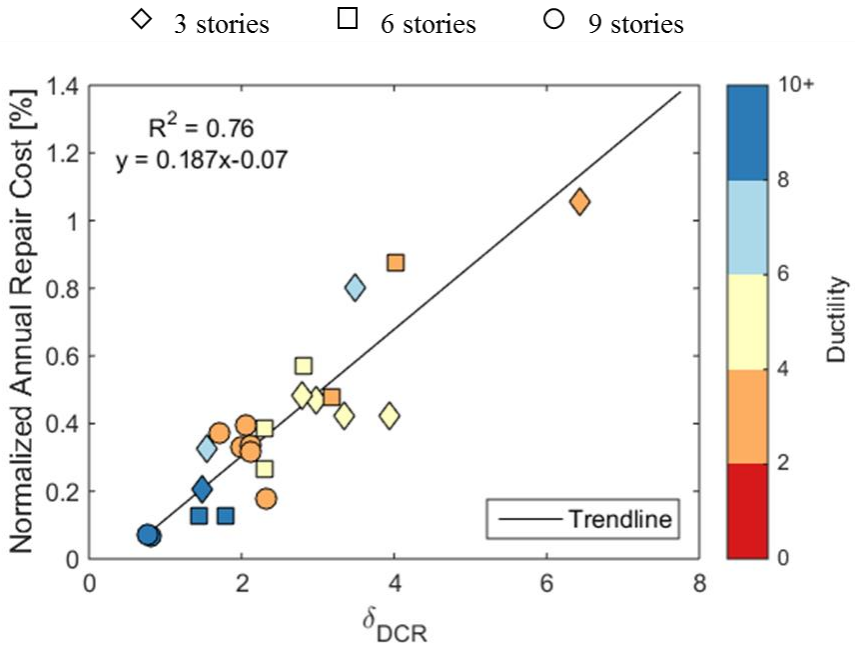

Figure 3-9 - Effect of δ_{DCR} on annualized repair cost. δ_{DCR} is computed using the spectral acceleration corresponding to the hazard level with probability of occurrence equal to 5 percent in 50-years.

3.8.3 Summary: Deformation Capacity Indicators

In this section, deformation capacity was examined as an indicator of seismic collapse risk and expected annualized loss. When ductility capacity is used to measure deformation capacity,

competing observations emerge. On one hand, increasing system ductility decreases collapse risk as shown in Figure 3-7b. However, Figure 3-8b shows that increasing ductility without increasing strength can lead to higher annualized losses because story drifts tend to be larger in these systems. Therefore, when considering ductility improvements through retrofit design, one must separately evaluate the effects on collapse resistance and expected loss.

3.9 Interaction of Strength and Ductility Capacity Indicators to Quantify Improvements in Seismic Performance Through Retrofit Design

The interaction of design variables, particularly as they relate to mean annual frequency of collapse, have been shown to be of potential importance in previous sections on strength and ductility (Galanis & Moehle, 2015). Strength and ductility capacity play crucial roles in seismic design, however, their interaction and tradeoffs are rarely discussed.

Figure 3-10 presents the strength and ductility capacity of each building analyzed in this study, and their associated mean annual frequency of collapse and annual repair costs. The worst performing buildings are the pre 1967 buildings that have not been seismically retrofit, shown in purple. These buildings have high $\mu_{strength}$ values, signifying they are weak relative to the design spectral acceleration, and have low ductility capacities. These two design parameters are associated with large mean annual frequency of collapse and annual repair costs. Conversely, the best performance is observed in retrofit buildings with low $\mu_{strength}$ values and high ductility capacities.

The results for two buildings that have been seismically retrofit are bolded in green and labeled *i* and *ii* in Figure 3-10. Building *ii* is strong, with $\mu_{strength}$ of approximately 1.3, with medium ductility capacity. The other building, *i*, is weaker, with $\mu_{strength}$ around 3.0, but has substantial ductility capacity. These combinations of design parameters, high strength and medium ductility capacity, or medium strength with high ductility capacity, lead to similar collapse capacities, highlighting the complementing interaction of these two design parameters with regards to collapse risk. With respect to annual repair costs, the weaker building, *i* experiences 80% higher losses. As shown in previous sections, repair cost is more correlated with strength than with ductility. Another example of strength and ductility complementing each other is shown by the dashed lines in Figure 3-10 labeled *a* and *b*. Here the difference in strength between the two buildings is less drastic than in buildings *i* and *ii*. The stronger building, building *b*, has a higher mean annual frequency of collapse because it has minimal ductility capacity. Yet, both buildings have the same annualized repair cost.

These results emphasize that deficiencies in one design parameter can be compensated for by supplying additional capacity in the other. This relationship is of increased importance when the decision variable is mean annual frequency of collapse because the building collapse fragility is dependent upon its ductility capacity. The interaction between strength and docility remains significant, but is of less importance when the decision variable is annualized loss, because it is primarily controlled by lower intensity earthquakes. In these lower intensity earthquakes, ductility capacity is not particularly important because the building remains elastic, and limited nonlinear behavior is observed.

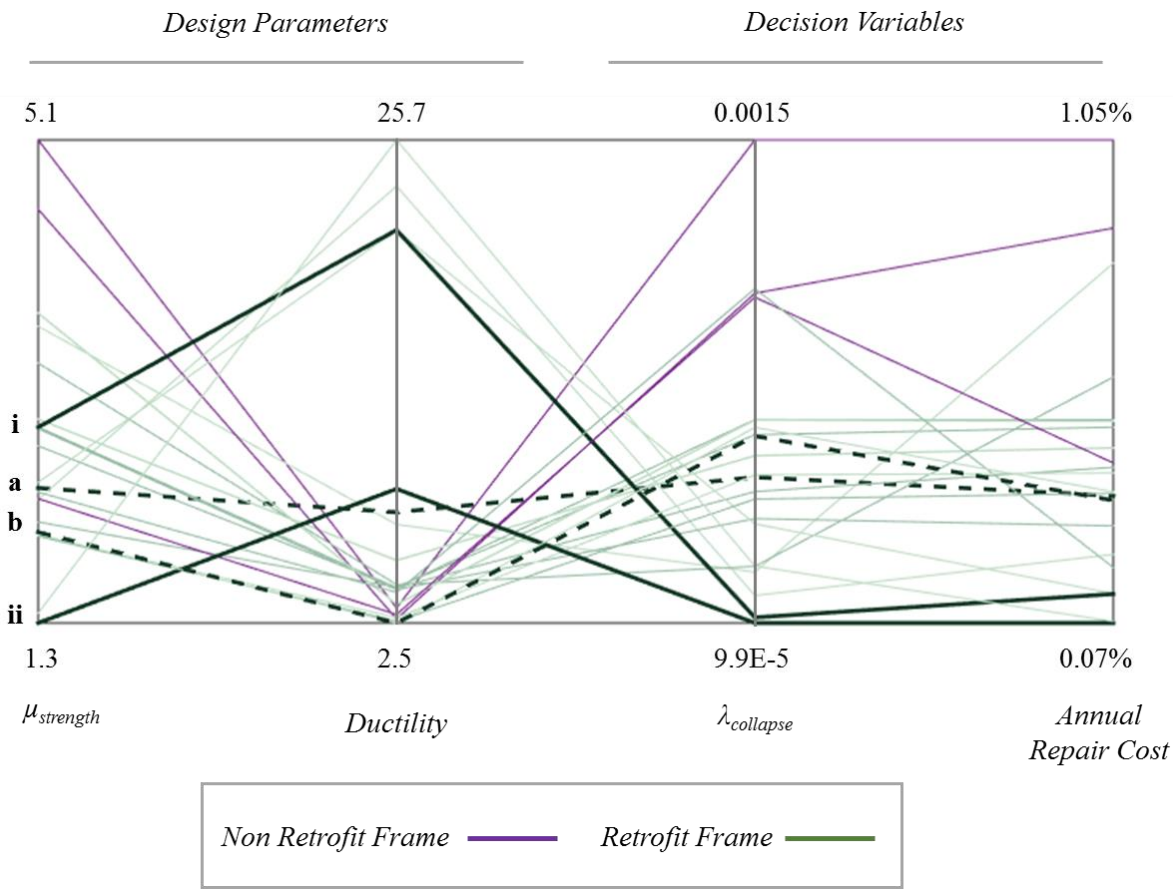

Figure 3-10 - Interaction of strength and ductility capacity and its effect on collapse risk and annual repair costs shown on a parallel coordinate plot.

3.10 Deficiencies in Existing RC Buildings as Indicators to Quantify Improvements in Seismic Performance Through Retrofit Design

3.10.1 Shear-Critical Columns

In 1967 buildings, the expected failure mode of the columns often governs the building collapse mechanism. The parameter V_p/V_n can be used to describe the expected failure mode of a column, where V_p is the maximum flexural capacity limited shear demand (*i.e.* the shear demand that produces an end moment equal to the column's flexural capacity) and V_n is the member shear capacity. V_p/V_n is computed on a column-by-column basis and represents the

expected failure mode. If $V_p/V_n \leq 0.6$ expected failure mode is flexure, $0.6 < V_p/V_n < 1.1$ failure mode is flexure-shear, and $V_p/V_n \geq 1.1$ member is expected to fail in shear (Li, Elwood, & Hwang, 2014). Here, we compute the building V_p/V_n as the average column V_p/V_n in the building weighted by axial load carried by each column, so columns at lower stories have a higher contribution to the building V_p/V_n (Sattar & Liel, under review). Often, retrofit designs for RC frame buildings aim to improve the ductility capacity of shear-critical columns, effectively lowering the V_p/V_n ratio. There are two motivations for doing this: 1) shear-critical elements have smaller drift capacities than flexural elements with equal axial load ratios in ASCE 41 (ASCE, 2013) and are therefore more likely to be identified as problematic, and 2) shear and subsequent axial failure in columns can lead to sudden collapse and may pose a high threat to occupant life safety.

Figure 3-11a presents building V_p/V_n as it relates to annualized repair cost. To isolate the effect of V_p/V_n on mean annual frequency of collapse, a selected subset of buildings analyzed in this study are presented that have similar $\mu_{strength}$ values. Buildings contained within the selected subset have 3-, 6-, and 9-stories, some have not been retrofit, while others have been retrofit with FRP wraps or concrete jackets. In Figure 3-11a, buildings with columns that are expected to fail in flexure have a lower mean annual frequency of collapse than buildings with columns that are expected to fail in shear (Sattar & Liel, under review). Columns that fail flexurally typically have more ductility capacity than those that fail in shear (Liel, Haselton, & Deierlein, 2011). Therefore, V_p/V_n is a proxy for element ductility. Increased component ductility enhances resistance against collapse by providing additional deformation capacity after initial yielding that is absent in non-ductile or shear-critical elements

Figure 3-11b presents the relationship between building V_p/V_n and annualized repair cost. There is little correlation between V_p/V_n and annualized loss, primarily because V_p/V_n does not provide any measure of expected nonlinear behavior for a given hazard level. V_p/V_n simply describes the mode in which failure is expected to occur, it does not measure when damage or failure will occur. Therefore, a shear-critical building can have lower annualized repair cost than a flexure critical building if its response is less nonlinear at all hazard levels.

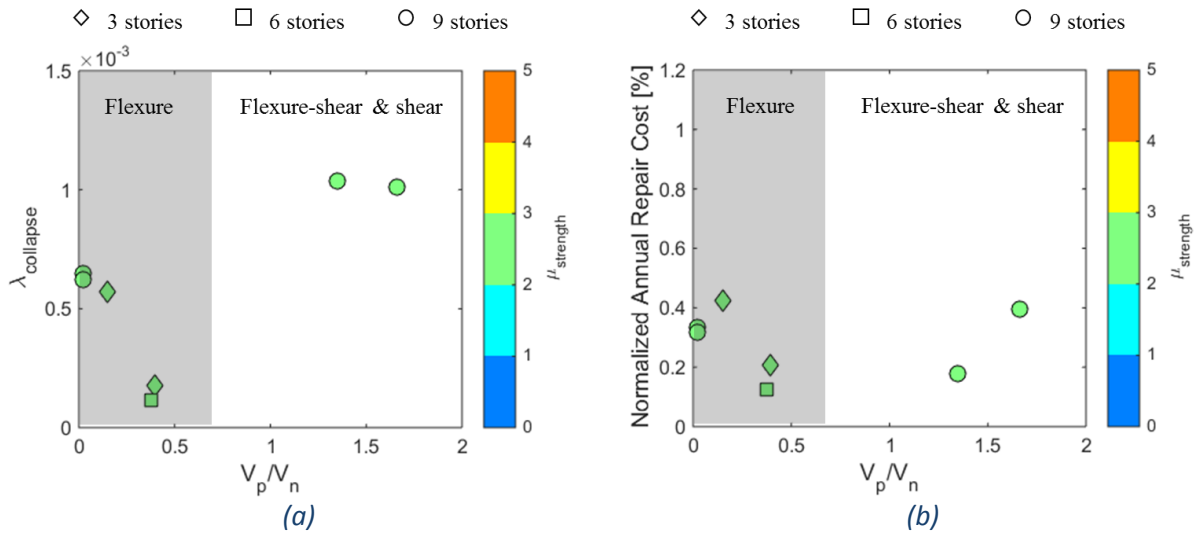

Figure 3-11 - Effect of building V_p/V_n on (a) mean annual frequency of collapse and (b) annualized repair cost. A selected subset of buildings is presented for which $2 \leq \mu_{strength} \leq 3$.

3.10.2 Column-to-Beam Strength

The effect of column-to-beam strength on the seismic performance of RC frames has been studied by many researchers (Galanis & Moehle, 2015; Sattar & Liel, under review). Buildings with strong column to weak beam (SCWB) arrangements have been shown to have higher seismic collapse capacities than weak-column-strong-beam arrangements because these systems avoid localized failure mechanisms and attain a higher energy dissipation capacity though a distributed

mechanism (Haselton, Liel, Deierlein, Dean, & Chou, 2011; Ramirez, et al., 2012). As a result, modern seismic design provisions limit the minimum SCWB such that M_c/M_b is greater than or equal to 1.2 at each joint (ACI Committee 318, 2014). Here, at the story level, M_c/M_b is quantified as the summation of the column expected flexural strengths over the summation of the beam expected flexural strengths in a story (ATC, 2015). The building M_c/M_b is the average story M_c/M_b. This definition differs slightly from that proposed by ACI 318 in which M_c/M_b is computed on a joint-by-joint basis. M_c/M_b is computed on a story basis instead a joint basis as this formulation is consistent with static analysis of a full building and is more representative of the formation of a story mechanism.

Figure 3-12a relates column-to-beam strengths, measured in terms of building M_c/M_b, and mean annual frequency of collapse. Figure 3-12 presents results for a subset of buildings with similar strengths to isolate the effects of building M_c/M_b. Buildings with high M_c/M_b distribute damage to throughout multiple stories leading to a higher energy dissipation capacity and, therefore, reduced mean annual frequencies of collapse. M_c/M_b and mean annual frequency of collapse generally follow a linear relation for M_c/M_b between 1.0 to 2.25 ($R^2 = 0.71$).

Figure 3-12b presents annualized repair cost estimates as a function of M_c/M_b. Here, M_c/M_b does not appear to influence annualized repair cost as indicated by the lack of a clear trend in the data ($R^2 = 0.13$). The following two reasons are identified that explain why repair cost and M_c/M_b are unrelated:

- Repair cost due to collapse and repair cost due to nonstructural damage offset each other as M_c/M_b is varied as explained by Ramirez el al. (2012) and summarized in the following paragraph.
- M_c/M_b is a measure of capacity. Damage is dictated by how large the seismic demand is relative to the capacity, as shown in previous sections by δ_{DCR} and $\mu_{strength}$. Looking at M_c/M_b by itself ignores the demand side. This suggests that measures of capacity are not sufficient to predict trends in repair costs, and measures that quantify demand and capacity are more informative.

Ramirez el al. (2012) examined the effect of M_c/M_b on median repair cost for 4-story ductile RC moment frames. Nine buildings were analyzed with M_c/M_b values ranging from 0.4 to 3.0. At the design spectral acceleration, median repair costs due to collapse was found to significantly decrease as M_c/M_b increased from 0.4 to 1.2, however, total median repair cost remained approximately equivalent for all M_c/M_b values. Ramirez el al. (2012) justified this finding by explaining that, in buildings with small M_c/M_b, column hinging occurs in the bottom story, which leads to a heightened collapse probability. This single story failure mode leads to localization of demand at this level and therefore nonstructural damage is reduced, offsetting the increase in loss associated with collapse. In buildings with $M_c/M_b > 1.2$ the collapse risk is greatly reduced, and damage is more evenly distributed through the full height of the building, though this results in more nonstructural damage. Due to these tradeoffs in repair cost, M_c/M_b was not found to influence median repair cost.

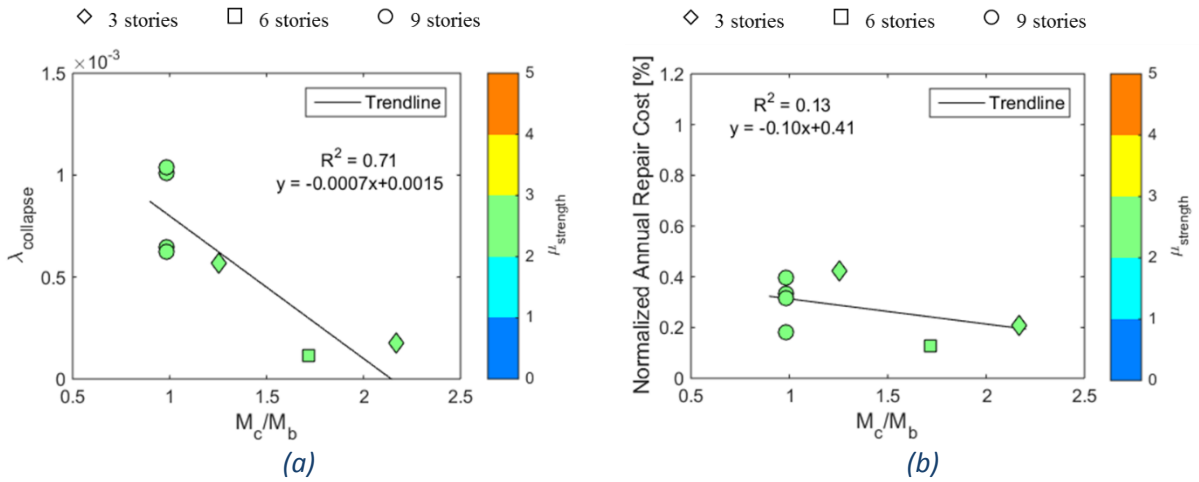

Figure 3-12 - Effect of building M_c/M_b on (a) mean annual frequency of collapse and (b) annualized repair cost. A selected subset of buildings is presented for which 2 ≤ μstrength ≤ 3.

3.10.3 Summary: Building Deficiency Indicators

The relationship between building deficiencies commonly found in 1967 buildings and decision variables measured in terms of mean annual frequency of collapse and annualized repair cost is explored. V_p/V_n provides an estimate of the expected failure mode of the columns in a building and is therefore correlated with building ductility capacity. M_c/M_b quantifies the building's ability to distribute damage to multiple floors and therefore attain a higher energy dissipation capacity. Using building deficiencies as performance indicators is effective when the decision variable is mean annual frequency of collapse. Conversely, building deficiencies are found to be poorly related to annualized repair cost.

3.11 Relationship Between Collapse Capacity and Estimated Seismic Loss

Collapse resistance in buildings has been of primary concern in design standards, especially for buildings constructed in high seismic regions (FEMA, 2015). Occupant life safety is

thought to be protected by reducing the collapse risk. However, design goals defined in terms of collapse risk may not be well correlated with good performance measured in terms of expected repair cost.

Figure 3-13 directly compares collapse probability to median repair cost at a range of hazard levels. As the collapse probability approaches one, median repair cost approaches the summation of the total building replacement cost and the cost of demolition. Therefore, at spectral levels near the collapse capacity of the structure, median repair cost and collapse capacity are correlated. However, when the collapse probability of the structure is close to zero a significant variation in median repair cost exists. In this range collapse is unlikely, yet median repair costs may vary from 1% to 50% of the building replacement cost. The large variance in repair costs at lower hazard levels signifies that collapse capacity and repair cost not highly correlated at lower shaking intensities.

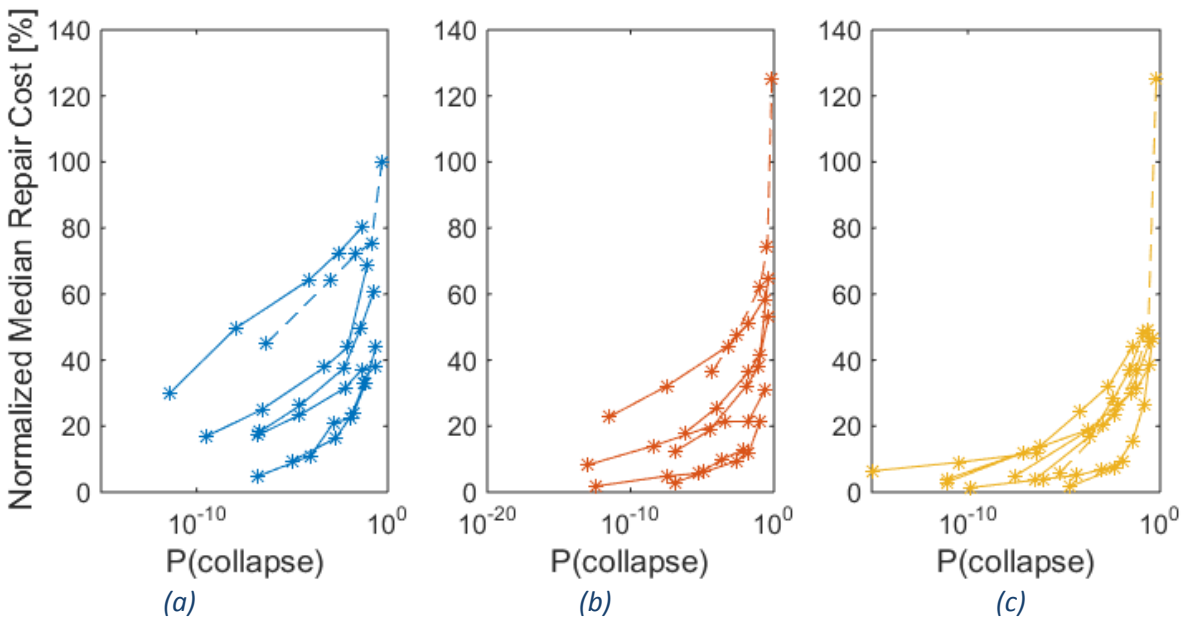

Figure 3-13 - Relationship between collapse probability and median repair cost for (a) 3-story buildings, (b) 6-story buildings, and (c) 9-story buildings at 5 different hazard levels. Dashed lines indicate original (un-retrofit) 1967 buildings. Median repair cost may exceed the building replacement cost because costs associated with demolition of the collapsed building are included in the loss analysis.

Moreover, a significant relationship does not exist between mean annual frequency of collapse and annualized repair cost (correlation coefficient, ρ = 0.38) in Figure 3-14. Low intensity earthquakes, in which collapse risk is small, have a significant contribution to annualized loss because annualized loss is obtained from a convolution of median repair cost conditioned on hazard level and the mean rate of occurrence of the hazard. This result is agreement with findings in Ramirez el al. (2012) in which mean annual frequency of collapse was found to not have a strong correlation with annualized repair cost (ρ = 0.17). Correlation between mean annual frequency of collapse and annualized repair cost is higher in this study because the building set contains structures that are high-risk by modern code standards and therefore have a higher repair costs due to collapse at spectral levels lower than the design hazard.

This results reinforces the idea that reducing the building collapse risk does not correspond to reduced repair costs. Therefore, loss and collapse must be addressed separately in performance-based design to ensure collapse risk and seismic losses are mitigated.

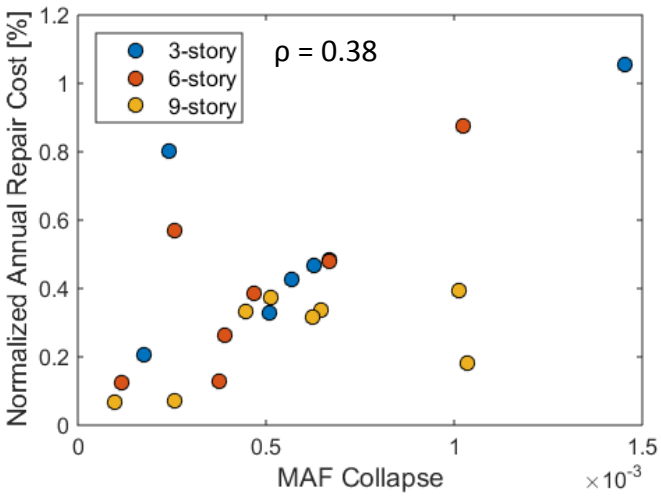

Figure 3-14 - Relationship and correlation coefficient between $\lambda_{collapse}$ and Normalized Annual Repair Cost

3.12 Conclusion

This study developed structural indicators that quantify benefits of retrofitting 1967 buildings. Structural indicators relate improvements in design parameters, possible through retrofitting, to reductions in collapse risk and earthquake-induced repair costs. A set of 3-, 6-, and 9-story buildings is designed to the Uniform Building Code of 1967 that contains building deficiencies such as shear-critical columns, weak column to strong beam arrangements, and overall weakness. 1967 buildings are retrofit to ASCE 41 Collapse Prevention, Life Safety, and Immediate Occupancy performance levels by encasing columns in steel or concrete jackets, or wrapping columns with FRP sheets.

The response of 1967 buildings and buildings that have been seismically retrofit is analyzed through performance-based engineering framework that accounts for major sources of uncertainty related to seismic hazard, building vulnerability, and earthquake-induced loss. Nonlinear, distributed plasticity models, were created that capture important response characteristics of nonductile RC buildings and takes into account changes in performance due to local seismic retrofitting. The seismic vulnerability of all buildings is assessed through IDA analysis and multiple EDPs are computed during multi-stripe analysis.

Two strength-based indicators are defined that measure improvements in strength capacity through retrofit design; normalized yield strength and normalized ultimate strength. Additionally, $\mu_{strength}$ is used as an indicator to measure the absolute strength of a building as it relates to the design spectral acceleration. Strength-based indicators identify seismic retrofit designs that improve strength as having reduced mean annual frequencies of collapse. However, retrofit designs that improve ductility capacity while having negligible effects on strength are also able to reduce building collapse risk. Therefore, combinations of strength and ductility capacity are likely better indicators of collapse risk. If the decision variable is annual repair cost strength-based indicators are able to capture general trends in building performance. Four distinct regions are defined in terms of $\mu_{strength}$ that bin buildings according to annualized repair cost. These regions are independent of retrofit type, normalized yield and ultimate strength, and number of stories, therefore providing a simple measure by which to assess benefits of retrofitting in terms of economic loss. Increasing the strength of a building by retrofitting mitigates earthquake-induced repair costs by increasing structural component capacities, reducing drift demands on

structural and drift-sensitive nonstructural components, and increasing the collapse capacity of the building.

Conflicting observations are made when using ductility capacity as an indicator of benefits from retrofitting based upon the DV of interest. While mean annual frequency of collapse can be reduced by increasing ductility capacity through retrofitting, increasing ductility without increasing strength can lead to higher annualized losses because of increased drift demands that tend to be spread throughout multiple stories. This finding highlights the importance of separately evaluating the impact of retrofitting on collapse resistance and expected loss. Prioritizing decision variables can help assist in the selection of an appropriate retrofit method. For example, if reducing collapse risk is of primary importance, retrofitting with FRP wraps may be the most suitable method of those considered, but if minimizing repair costs is of greater importance FRP wraps would not be the most effective choice.

The interaction of strength and ductility capacity was found to be strongly related to mean annual frequency of collapse. The complementing nature of strength and ductility capacity is such that deficiencies in one parameter can be mitigated through the other. However, if the DV is annualized repair cost, the interaction of strength and ductility capacity is less important, and repair costs are primarily related to strength-based indicators.

Selected design parameters, indicative of deficiencies in nonductile concrete buildings, and their impacts on multiple DVs were examined for a subset of buildings with similar strengths. V_p/V_n describes the expected failure mode of a column and average failure mode of a building. M_c/M_b relates flexural capacities of columns to beams for a given story, providing a measure for

the building's energy dissipation capacity and ability to distribute damage to multiple stories. V_p/V_n and M_c/M_b were able to describe trends in annualized frequency of collapse. Flexure controlled buildings ($V_p/V_n < 0.6$) had higher collapse capacities than shear controlled buildings. M_c/M_b was found to be inversely proportional to mean annual frequency of collapse as M_c/M_b increased from 0.4 to 1.2. Despite having strong relationships with collapse capacity V_p/V_n and M_c/M_b were found to be poorly correlated with annualized repair costs. One of the main reasons for this tenuous relation is that V_p/V_n and M_c/M_b are measures of capacity that ignore the demand side. However, damage and associated repair costs are caused when demands exceed capacities. Therefore, repair costs are better predicted by measures that compare seismic demands relative to capacities, such as δ_{DCR} and $\mu_{strength}$.

A main finding of this study is that in performance-based design, retrofits should separately consider multiple DVs. Simply designing a retrofit to mitigate collapse risk, such as ASCE 41 Collapse Prevention, tells you little about the expected repair costs of the design. DVs must be considered separately because they are not strongly correlated. For the buildings analyzed in this study, the correlation coefficient between mean annual frequency of collapse and annualized repair cost was found to be 0.38.

4 COLLAPSE ASSESSMENT OF MOMENT FRAME BUILDINGS, CONSIDERING VERTICAL GROUND SHAKING

4.1 Introduction

The vertical component of seismic motions may contribute significantly to demands imposed on structures. Building damage occurring during the Northridge, California (1994), Kobe, Japan (1995), and L'Aquila, Italy (2009) earthquakes, among others, has been attributed to intense vertical shaking (Di Sarno, Elnashai, & Manfredi, 2011). Nevertheless, the characteristics of vertical shaking and the mechanisms by which the vertical component of the ground shaking influences building response are not well understood. Vertical ground shaking, which is dominated by vertically propagating compression (P) waves, has different physical characteristics than horizontal ground shaking, which is driven by shear (S) waves. The wavelength of P-waves is much shorter that S-waves, such that vertical shaking has greater high frequency content (Kim, Holub, & Elnashai, 2011). In addition, recently developed ground motion prediction equations show that vertical shaking exhibits patterns of distance attenuation, magnitude dependence, and spectral response shape that differ from horizontal shaking (Bozorgnia & Campbell, 2003; Elnashai & Papazoglou, 1997). High seismic locations, especially sites close to faults, are thought to have the potential to experience strong vertical shaking (Bozorgnia, Niazi, & Campbell, 1995). Yet, at the same time, conventional wisdom holds that the impact of vertical ground shaking is more significant for bridges than building structures, and the vast majority of experimental and

analytical studies of building seismic response consider only the lateral component of ground shaking.

Despite the complex nature of vertical ground shaking, design approaches for dealing with this aspect of earthquake effects have been relatively simple. One of the first methods to account for vertical motions was proposed for the design of nuclear power plants (Newmark, Blume, & Kapur, 1973). In this approach, the vertical response spectrum was taken to be two-thirds of the horizontal design spectrum. This factor implies that ratio of vertical to horizontal spectra (*V/H*) is constant over all periods, site-to-source distances, site conditions, and frequency contents (Bozorgnia & Campbell, The Vertical-to-Horizontal Response Spectral Ratio and Tenative Procedures for Developing Simplified V/H and Vertical Design Spectra, 2003; Bozorgnia, Niazi, & Campbell, 1995). However, recent ground motion recordings have shown that the vertical spectra may exceed the horizontal spectra at some periods at certain sites, and, in other situations, may be substantially smaller.

Modern seismic design is based on site-specific estimation of seismic hazard. ASCE 7-10 (and, by extension, the International Building Code) uses the mapped maximum considered earthquake (MCE_R), short-period and 1-second spectral accelerations as lateral seismic design values. These "risk-targeted" seismic design maps define the MCE_R spectral accelerations to achieve a targeted collapse probability of 1% in 50 years (American Society of Civil Engineers, 2013). ASCE 7-10 quantifies the effect of vertical seismic shaking based on 20% of the short-period design value, S_{DS}, and includes this "vertical term" in two load combinations:

$$(1.2 + 0.2S_{DS})D + \rho Q_E + L + 0.2S \qquad \textit{Equation 4-1}$$

$$(0.9 - 0.2S_{DS})D + \rho Q_E + 1.6H \qquad \textit{Equation 4-2}$$

Here, *D* is the design dead load, ρ is the redundancy factor (which equals 1 or 1.3 depending on the redundancy of the load path of the lateral force resisting system), Q_E represents the effects of the horizontal seismic forces, *L* is the live load, *S* is the snow load, and *H* is the load due to lateral earth pressure and other pressures. In Equation 4-1, the vertical shaking effect amplifies the dead load, while Equation 4-2 reduces the dead load by the vertical shaking effect to consider overturning conservatively. Site-specific procedures for linear and nonlinear response analyses do not mention the vertical component of ground shaking. Moreover, at sites where $S_{DS} < 0.125g$, the vertical seismic load can be neglected altogether (American Society of Civil Engineers, 2013). Similarly, the European seismic building standard, Eurocode 8, requires the consideration of ground acceleration in the vertical direction, if the vertical acceleration exceeds 0.25g. The vertical shaking is computed as a fraction horizontal acceleration. This provision applies only to base isolated buildings or horizontal member that have long spans, are cantilevered, prestressed, or support columns directly (CEN, European Committee for Standardisation, 2003).

This study investigates how vertical ground shaking changes our estimates of structural collapse capacity for buildings. Understanding mechanisms of structural collapse is of primary importance because the primary goal of building codes and standards is to protect occupant safety and prevent collapse. Yet, recent studies examining collapse risk of code-designed buildings (e.g., (Haselton, Liel, Deierlein, Dean, & Chou, 2011)) and defining the risk-targeted mapping approach (Luco, et al., 2007) have neglected to consider vertical shaking. To quantify

the effect of vertical shaking on structural response, we focus on answering the following questions: What properties of vertical and horizontal ground motions predict trends in building response? What types of buildings are more influenced by vertical ground shaking? and, How does vertical shaking influence element level responses to affect collapse mechanisms? Nonlinear analyses of a set of low- to mid-rise buildings are conducted to shed light on the above questions.

4.2 Previous Studies of Structural Response Under Vertical Ground Shaking

This section summarizes some of the relevant previous research that examines vertical ground shaking. Most of these studies focus on a specific type of structure's (*i.e.* pre-stressed concrete structures, bridges, cantilevers, etc.) response to vertical ground shaking (Button, Cronin, & Mayes, 2002; Gulerce & Abrahamson, 2010; Gulerce, Erduran, Kunnath, & Abrahamson, 2012; Kim, Holub, & Elnashai, 2011; Papazoglou & Elnashai, 1996; Vamvatsikos & Zeris, 2008), quantify the relationship between vertical and horizontal intensities from past earthquake records (Niazi & Bozorgnia, 1990; Niazi & Bozorgnia, 1992; Bozorgnia & Niazi, 1993; Watabe, Tohido, Chiba, & Fukuzawa, 1990; Silva, 1997; Collier & Elnashai, 2001), or attempt to extract information on the implications of vertical ground shaking by examining data collected from post-earthquake reconnaissance (Abrahamson & Silva, 1997; Chang, Bray, & Seed, 1996; Papazoglou & Elnashai, 1996; Tezcan & Cheng, 2012). Selected studies are summarized below.

4.2.1 Studies Based Post-Earthquake Reconnaissance

Bozorgnia *et al.* (Bozorgnia, Niazi, & Campbell, 1995) examined the characteristics of free-field vertical ground motions that occurred during the 1994 Northridge earthquake using a database of 123 ground motion response spectra. The study found that the *V/H* ratio was strongly dependent on the period of interest and the distance from the location of interest to the seismic source. The study also concluded that the *V/H* ratio grossly exceeded the typical approximation of 2/3 at short periods for sites located near the seismic source.

The 2009 L'Aquila Italy Earthquake caused a significant amount of damage to RC structures, some of which has been attributed to intense vertical shaking. To test this theory, Di Sarno *et al.* (Di Sarno, Elnashai, & Manfredi, 2011) performed nonlinear dynamic analysis on two finite element structural models of two-story, two-bay frames designed for gravity loads. Models were subjected to a sample set of ground motion recordings from the L'Aquila Earthquake, with ratios of peak ground accelerations (PGA_V/PGA_H) ranging from 0.47 to 1.16. The study found that column compressive load increased 59% to 174% depending on the column axial load ratio. For high values of axial load, the computed axial load-bending moment interaction was greater than the threshold value, which was suggested to lead to column failure. In addition, the study found that large fluctuations in axial load adversely affected the column shear demand-to-supply ratio.

4.2.2 Analytical Studies of Effect of Vertical Ground Motions on Buildings and Bridges

Multiple studies have been conducted that examine the impact of vertical ground shaking on building seismic response. Through nonlinear dynamic analysis of a 2D model of a typical

1960's RC frame building, Vamvatsikos and Zeris (Vamvatsikos & Zeris, Influence of Uncertian Vertical Loads and Accelerations on the Seismic Performance of an RC Building, 2008) showed that vertical ground shaking's influence on building performance is dependent upon the magnitude of the gravity loads on the building. For low gravity loads vertical shaking can have a positive or negative impact on building performance, but for high levels of gravity load the impact of vertical accelerations are primarily negative. Papazoglou and Elnashai (Papazoglou & Elnashai, 1996) summarize the results of multiple nonlinear analysis of RC buildings from previous studies to demonstrate the possibility of column failure due to vertical shaking, which they conclude to be primarily attributed to high amplitude variation in column axial load demands. Based on this finding, Papazoglou and Elnashai, 1996 call attention to the need for a more advanced method of including vertical shaking in the design and analysis of RC buildings.

Much previous research has focused on the response of bridge structures, inspired in part by the damage caused by the 1971 San Fernando earthquake to these structures, some of which was attributed to vertical shaking (Saadeghvaziri & Foutch, 1991). Saadeghvaziri and Foutch conducted one of the first studies on the response of bridge structures to vertical ground shaking, using three-dimensional nonlinear models of eight RC bridges. Variation in axial force caused by combined horizontal and vertical ground shaking led to pinched hysteresis, reduced shear capacity, and amplified horizontal displacements. Based on these findings, they concluded that the damage caused by the vertical component of earthquakes was negligible when peak ground accelerations in the vertical direction were less than 0.4 g, but that for ground motions with peak ground accelerations greater than 0.7 g, the inclusion of the vertical component resulted in

considerably more damage. Kunnath *et al.* (2008) conducted nonlinear time history analysis and response spectrum analysis on a number of highway bridges. Vertical ground shaking was found to have a significant impact upon the axial force demands in the columns, the moment demands at the face of the bent cap, and the moment demand at the middle of spans, but the authors concluded that only the increase in moment demand at the middle of spans was large enough to warrant concern. The authors warned that current code specified values for vertical loads are inadequate to account for the significance of vertical ground motion in design.

4.3 Ground Motion Selection and Characteristics

For the purposes of this study, three component ground motions*, i.e.* consisting of two horizontal and one vertical component recorded at the same site from the same event, were selected from the PEER-NGA database (Ancheta, et al., 2013), with a focus on collecting a set of strong motions that could cause collapse or damaging responses. The FEMA P-695 far-field ground motion set (FEMA, 2009) which consists of 22 ground motions, provided a starting point. Nineteen other high intensity*, i.e.* large *PGA* or *Sa(T),* ground motions were added to the set, creating a final set of 41 ground motions. The ground motion set was selected such that the significance of the vertical component varies substantially among the group.

To quantify this variability, response spectra from the selected ground motions are used to calculate the ratio between the spectral acceleration of the vertical component at a period of 0.2 seconds, to the geometric mean of the horizontal components at a period of 1.0 second for all of the records, which we refer to as *V/H*. We chose fundamental horizontal and vertical periods of 1.0 sec and 0.2 sec respectively to be representative of typical building frame

structures, which are commonly much stiffer in the vertical as compared to the lateral directions. For the ground motions selected, these *V/H* ratios vary from 0.1 to greater than 1.5.

4.4 Building Designs and Models

4.4.1 Structural Designs

This study considers five reinforced concrete (RC) frame buildings, shown in Table 4-1. RC frame structures are selected for this study because they are well-understood common systems, whose primary design characteristics (*e.g.* strength and ductility capacity) are similar to other prevalent building types in high seismic areas. Our focus is on the vertical shaking impact for conventional building designs. Three of these buildings are designed in accordance with modern U.S. building codes and standards, namely ASCE 7-10 (American Society of Civil Engineers, 2013) and the 2012 International Building Code (IBC) (International Code Council, 2011). The remaining two structures are designed according to the 1967 Uniform Building Code (UBC) and are representative of older, non-ductile RC structures. Two building configurations are considered: regular geometries (Figure 4-1), and cantilever geometries (Figure 4-2). The regular structures were designed for previous studies by (Haselton & Deierlein, 2006; Haselton, Liel, Deierlein, Dean, & Chou, 2011; Raghunandan, Liel, & Luco, 2014). A frame building with cantilevers is designed by the authors to modern U.S. building standards (see Table 4-1) and included in this study because buildings containing cantilevered elements have been previously shown to be sensitive to vertical ground motions (e.g. (Dogangun, 2004; Yucemen, Ozcebe, & Pay, 2004)). The design of this building fully complies with modern U.S. standards for RC frame design

(encompassing requirements that include, but are not limited to, span-to-depth ratio requirements, shear requirements, deflection limitations, and special moment frame detailing (ACI Committee, American Concrete Institute, and International Organization for Standardization, 2008)). Furthermore, the design of the cantilever structure was conducted following the same rigorous framework (Haselton & Deierlein, 2006; Haselton, Liel, Deierlein, Dean, & Chou, 2011; Raghunandan, Liel, & Luco, 2014) that were used in designing the regular geometry structures to ensure comparability of the designs. The buildings are all designed assuming they are located at a southern California site at 33.996°N, 118.162°W.

Table 4-1 – Building designs and characteristics

Bld. ID	Governing design provisions	Num. of stories	Lateral system	Other features	Vertical seismic load included in design	V_u (kips) [1]	μ [2]	T_H (sec) [3]	T_V (sec) [4]
1	2012 IBC (ASCE 7-10)	2	RC special moment (Space) frame	None	$(0.2S_{DS})D$	233	19.3	0.44	0.06
2	2012 IBC (ASCE 7-10)	8	RC special moment (Space) frame	None	$(0.2S_{DS})D$	225	10.8	1.58	0.19
3	2012 IBC (ASCE 7-10)	2	RC special moment (Space) frame	Cantilever overhangs	$(0.2S_{DS})D$	221	24.9	0.49	0.06
4	1967 UBC	2	Older RC moment (Perimeter) frame	None	None	143	4.0	0.70	0.02
5	1967 UBC	8	Older RC moment (Perimeter) frame	None	None	207	3.0	2.02	0.20

[1] Ultimate base shear capacity of the structure, as determined from pushover analysis
[2] Ductility capacity computed as the ratio of ultimate displacement to the effective yield displacement of the structure from pushover analysis (following (FEMA, 2009))
[3] Fundamental horizontal period from eigenvalue analysis
[4] Fundamental vertical period from eigenvalue analysis

As presented in Table 4-1, the fundamental horizontal periods of these buildings range from 0.44 to 2.02 seconds, while the fundamental vertical periods range from 0.06 to 0.20 seconds. Periods are calculated from the *OpenSEES* models, which do not include floor slabs. Vertical ground shaking is typically composed of energy concentrated in a narrow high frequency

band. Such high frequency leads to large intensities in the short period range (Kim, Holub, & Elnashai, 2011), which coincides with the fundamental vertical periods of these typical building structures.

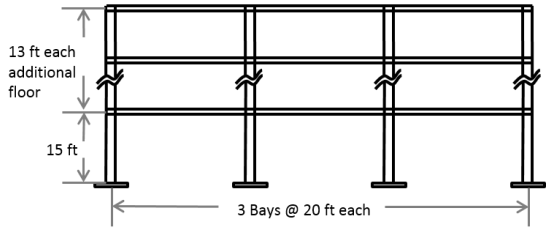

Figure 4-1 – Elevation view for regular buildings

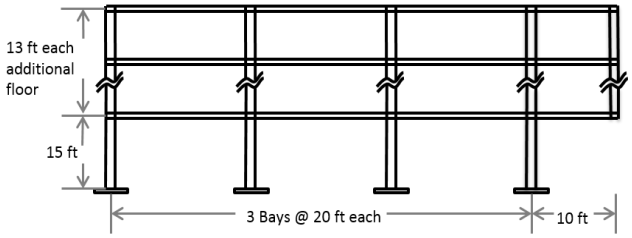

Figure 4-2 –Elevation view for cantilever building

4.4.2 Global Modeling Approach

As a starting point, this study takes the two-dimensional models of the RC frame buildings developed by (Haselton & Deierlein, 2006), which employ the lumped plasticity approach to model nonlinear behavior in beams and columns. The plastic hinge properties in these beam-column models have been calibrated to experimental data (Haselton, Liel, Lange, & Deierlein, 2008) and are capable of describing key mechanisms of strength and stiffness degradation that produce collapse. However, modifications to these models are needed in order to capture the effects of vertical seismic excitation. Crucially, the vertical component of ground shaking induces varying axial loads in columns, so models must capture the interaction of axial, flexure, and shear forces in the RC columns. In addition, the beam models are modified to capture hinging at midspan, as well as end, of the beams, and facilitate monitoring of vertical accelerations and displacements along the beam spans.

4.4.3 Modeling Approach for Modern (Ductile) Buildings

Modern frame buildings are designed to fail in flexure sidesway mechanisms due to hinging in beams and columns (Haselton, Liel, Deierlein, Dean, & Chou, 2011). The element models used to capture these phenomena in Building IDs 1, 2, and 3 are shown in Figure 4-3. Layered fiber elements, also known as distributed plasticity elements, are used to model the behavior of beams and columns until the peak load is reached. In layered fiber models, effective stress-strain response of the concrete and reinforcing materials are defined explicitly; (Applied Technology Council, 2010). The stress-strain relationship of concrete fibers is described by the modified Kent and Park model; steel fibers are modeled using the relation proposed by Giuffre-Menegotto-Pinto. These uniaxial stress-strain relationships define the nonlinear behavior of the composite fiber section with ten fibers per inch (in each direction).

Different types of fiber elements are used to model the columns versus beams, see Figure 4-3. Columns are modeled using a single force-based fiber element with four Gauss points per column (Neuenhofer & Filippou, 1998). Displacement-based fiber elements are used to describe beam members. Four elements are used to model each member in order to allow for nodes to be placed along the length of the beam at which displacements, velocities, and accelerations can be recorded during analysis.

Force-based and displacement-based fiber elements have the advantage of capturing axial-flexure interaction that is important for simulating the influence of vertical ground shaking. However, traditional fiber element formulations are limited in their ability to capture strength degradation associated with concrete spalling and bar buckling, which are an important failure

mode (Applied Technology Council, 2010; Haselton, Liel, & Deierlein, Important Issues and Suggested Best Practices in Simulating Structural Collapse Due to Earthquakes: Modeling Decisions, Model Calibration and Numerical Solution Algorithms, 2009). This limitation arises from localization caused by strain-softening behavior and nonobjectivity (response changes as a function of the number of integration points). However, recent advances have provided solutions to these issues. For example, an integration method for force-based beam-column elements has been proposed which ensures objective element response (Scott & Fenves, 2006). This method is based on modified Gauss-Radau quadrature, and confines material nonlinearity to the element ends over the expected plastic hinge length.

Here, a new approach for modeling post-capping strength degradation in flexibility-based fiber elements is presented that is objective, and also avoids the loss of solution uniqueness. In this approach, zero-length rotational springs are placed at the ends of each member to act in series with the fiber element. These springs introduce a negative stiffness to represent concrete spalling and rebar buckling phenomena (Haselton, Liel, Lange, & Deierlein, 2008). The zero-length springs are defined using a novel "limit state material". In *OpenSees*, a limit state material is a material that will update some pre-specified properties upon reaching a user-defined state (Elwood K. J., 2004). The limit state material requires the user to specify the properties describing the hysteretic response of the limit state material, the updated properties, and the state upon which the material will update these properties. As such, the limit state material differs from most other material models, which must have a predefined force-displacement hysteretic path. The state upon which the material updates its properties is defined by a "limit curve". Here, a

new flexural-based limit state material is created and assigned to the zero-length rotational springs. At low levels of deformation, the fiber element controls the response as the zero-length spring is assigned a high initial stiffness. The limit state material activates the zero-length spring once the column reaches a specified deformation, representing the rotation at which the concrete cover spalls and rebar buckling occurs. Once this deformation is reached, the stiffness of the spring is updated such that the entire column (fiber-spring) system has a negative, degrading stiffness. To determine when this activation occurs, the plastic rotation at each end of the member is calculated during every time step and is compared to the limit curve, as shown in Figure 4-4. The limit curve quantifies the unique deformation capacity, i.e. "capping" rotation, ϑ_{cap}, of each column, based on relationships for RC columns proposed by (Haselton, Liel, Lange, & Deierlein, 2008) and depending on column design and details. Once the rotation in the column exceeds the limit, the limit state material updates its stiffness. We note that ϑ_{cap}, depends on the axial load in the column (Haselton, Liel, Lange, & Deierlein, 2008). In this study, ϑ_{cap} is calculated using the design (expected) axial load for each column, and does not vary throughout the analysis, although that feature could be incorporated. Decoupling member responses such that the elastic phase and yielding phase are described with a fiber element and the strength degradation phase is associated with a zero-length element creates two elements with one-to-one mapping, leading to a unique solution, provided that the force displacement response of the fiber element is increasing under monotonic load at the time the limit curve is reached.

4.4.4 Modeling Approach for Older (Non-Ductile) Buildings

Unlike modern RC frame buildings, which largely avoid brittle shear failures through capacity design requirements, older non-ductile RC frame structures are potentially susceptible to column shear failure and subsequent loss of gravity load carrying capacity. Following (Raghunandan, Liel, & Luco, Collapse Risk of Buildings in the Pacific Northwest Region due to Subduction Earthquakes, 2014), shear and subsequent axial failure of columns are captured by the zero length springs that are assigned shear and axial limit state materials (Elwood K. J., 2004). Shear and axial springs are placed at the top of each column and describe shear and axial response over the height of the column in an average sense. The models are defined such that the shear and axial limit state materials track the column's flexural response, detecting shear or axial failure upon intersecting a predefined limit surface based on the column's properties. The shear and axial limit state material models are based on experimental data from 50 laboratory tests on RC columns (Elwood K. J., 2004). Once the response reaches the limit surface, the limit state material is updated with the expected negative stiffness associated with either shear or axial failure. The flexural response of the columns in these models is assumed not to vary substantially with axial load, and follows a bilinear force-displacement response calibrated to the expected gravity load level.

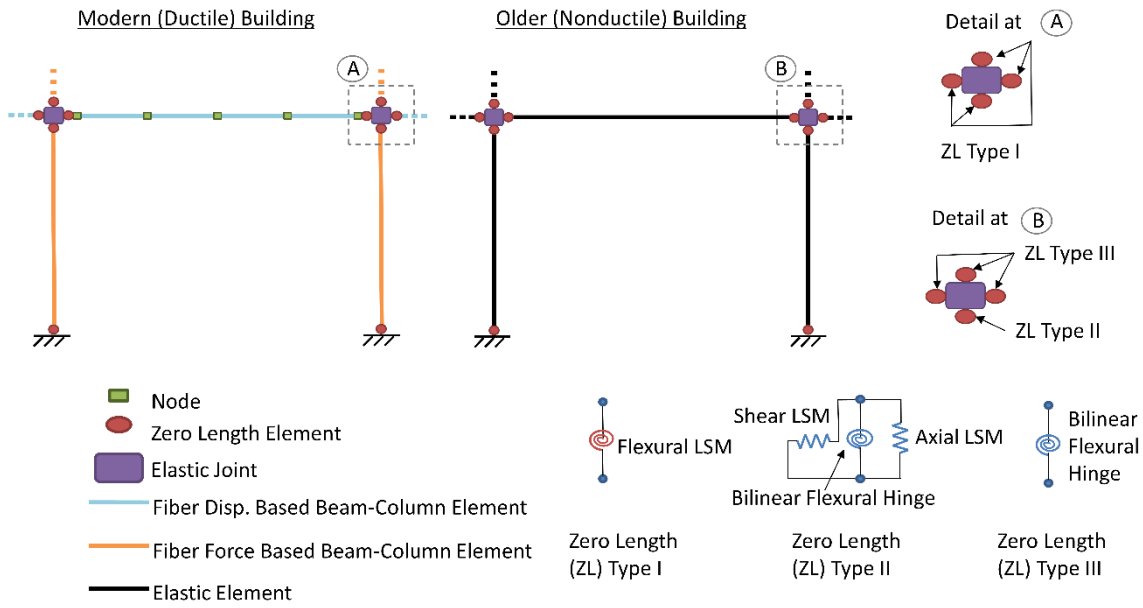

Figure 4-3 - Global modeling scheme for modern (2012 IBC) and older (1967 UBC) RC frame buildings. LSM indicates use of a limit state material and ZL shows the location of a zero length element.

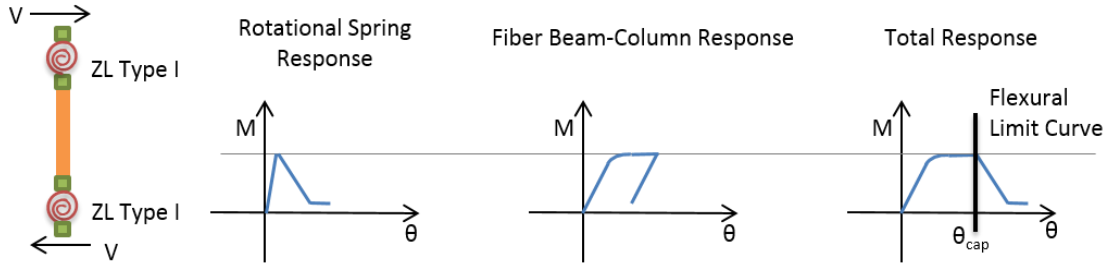

Figure 4-4 – Response of zero-length element with flexural limit state material in series with fiber force-based beam-column, as used in modern building models.

4.5 Overview of Results from Incremental Dynamic Analysis

Incremental dynamic analysis (IDA) is performed on all five nonlinear building models to quantify the collapse fragility, *i.e.* probability of collapse as a function of ground motion intensity, and the mean annual frequency of collapse (Vamvatsikos & Cornell, 2002). In the analysis, the identification of collapse occurrence depends on the model formulation and the expected failure

modes. Modern structures are expected to collapse in a sidesway mechanism. Sidesway collapse is defined as the point at which lateral deformations increase without bounds for small increases in ground motion intensity (Haselton & Deierlein, 2006), which is taken as the point at which the maximum interstory drift ratio exceeds 0.1. In the older nonductile models, collapse is defined to occur when the total story shear capacity degrades lower than the residual story shear capacity at any story, or the gravity load demand in a story exceeds the total axial capacity of columns in that story, as in (Raghunandan, Liel, & Luco, Collapse Risk of Buildings in the Pacific Northwest Region due to Subduction Earthquakes, 2014).

In the IDA, inelastic spectral displacement (S_{di}) at the building's elastic fundamental period is used as the primary ground motion intensity measure. This intensity measure is chosen because the most common ground motion intensity measures, such as elastic spectral acceleration, only capture spectral values at the building's elastic fundamental period. Yet, structural response is greatly affected by both ground motion intensity and spectral shape (Baker & Cornell, 2006). S_{di} is defined as the peak displacement of a bilinear, single degree-of-freedom (SDOF) oscillator subjected to the ground motion of interest. Because it is based on a bilinear oscillator, S_{di} accounts for period elongation, providing a measure that accounts for spectral shape and ground motion intensity (Tothong & Luco, 2007). This SDOF oscillator has period and yield displacement based on the building under consideration (where the yield displacement is taken as the effective yield displacement from a pushover analysis, as defined in (FEMA, 2009)), and a post-yield hardening stiffness ratio set to the recommended value of 5% of the elastic stiffness (Tothong & Luco, 2007).

Two sets of IDA are performed for each building model: (1) with only the horizontal component of a ground motion applied, the "unidirectional" case, and (2) with the vertical motion and a single orthogonal horizontal component simultaneously, the "bidirectional" case. Since the buildings are represented by 2D models, these two sets of IDAs are performed twice, separately involving each component from the pair of horizontal components. The median collapse capacities in Table 2 have been determined from IDA, and quantified considering the collapse capacities of all 82 ground motion pairs to account for record-to-record variability. These median collapse capacities are compared to evaluate the differences in response between unidirectional (horizontal) ground shaking and bidirectional (horizontal + vertical) shaking.

The mean annual frequency of collapse is obtained by convolving the collapse fragility with the seismic hazard curve at the site of interest. The site hazard of the design location is high seismic, site class D. To obtain the probability of collapse in 50 years, which is reported in Table 2, we use the standard Poisson probability model to convert the annual collapse rate to a 50 year probability (see *e.g.* (Eads, Miranda, Krawinkler, & Lignos, 2012)). Results show that, for each building, including the vertical component of a record in the analysis increases the probability that the building will collapse. ASCE 7-10 aims to ensure that buildings designed under its provisions will have less than or equal to 1% probability of collapse in 50 years (American Society of Civil Engineers, 2013; Luco, et al., 2007). Under purely horizontal loading, the modern structures (Bld IDs: 1, 2, 3) have 50 year collapse probabilities at, or slightly above, 1%. When vertical loading is included in the analysis, all collapse probabilities exceed 1% in 50 yrs. The most significant change occurs in the cantilever structure (Bld ID: 3), where the vertical component of

a record increases the 50-year collapse probability, to 1.2% probability of collapse in 50 years. The older models (Bld IDs: 4, 5) were designed to the 1967 UBC and therefore have 50 year collapse probabilities that are much greater than 1%, but including the records' vertical components in the analysis further increases the probability of collapse. However, we note these computed collapse risks assume that the range of *V/H* ratios for ground motions used in IDA are consistent with the considered buildings' site. For sites where a deaggregation of the hazard can be used to predict the intensity of the vertical shaking, ground motions can be selected to reflect the site-specific hazard.

The significance of the vertical component of ground shaking for the collapse assessment – the primary interest of this study – is quantified in terms of Percent Change in Collapse S_{di} or *PCSDI,* which compares the collapse capacity between the bidirectional and unidirectional analysis runs for each record:

$$PCSDI = \frac{Sdi_{uni} - Sdi_{bi}}{Sdi_{uni}} \qquad \textit{Equation 4-3}$$

Here, Sdi_{uni} is the inelastic spectral displacement corresponding to the ground motion intensity that causes collapse of the multiple degree of freedom building model when only the horizontal component of a ground motion is applied; Sdi_{bi} is the inelastic spectral displacement corresponding to the ground motion intensity that causes collapse when vertical and horizontal components of the ground motion record are applied simultaneously. Records producing positive *PCSDI* values are those in which the vertical component of a ground motion is detrimental to building response. Other records produce *PCSDI* values close to zero, showing that the vertical component has little effect on building collapse. In some cases, *PCSDI* is negative, signifying that

the inclusion of the vertical ground motion in the analysis increases the collapse S_{di} value, *i.e.* the vertical component is "beneficial" to building response. Figure 5 illustrates the range of *PCSDI* values observed in IDA for each building.

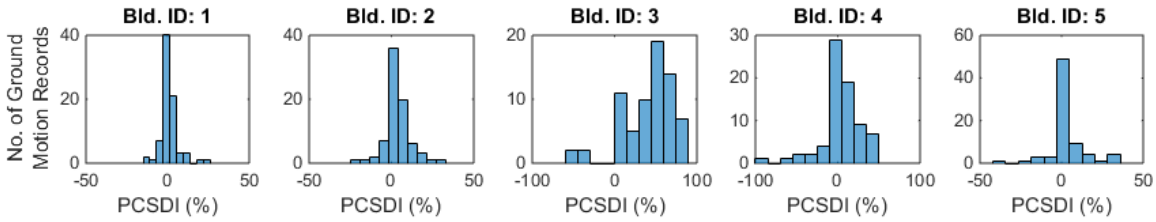

Figure 4-5 – Histograms of PCSDI plotted for all building models.

PCSDI is highly variable, as indicated by Figure 5 and the large standard deviations in *PCSDI* reported in Table 4-2. Two main drivers of variation in *PCSDI* can be identified. First is variation that exists for a single model due to record-to-record variation. This source is quantified by the magnitude of the standard deviation in *PCSDI* for a given building, and depends on ground motion features. The second source of variation relates to the building characteristics, i.e. configuration, building geometry, and design era. For example, the median *PCSDI* for Bld. ID 1 is much smaller than that of Bld. 3, suggesting that buildings with heavy cantilevered members are more susceptible to collapse influenced by vertical ground shaking than regular geometry buildings. Comparing the median *PCSDI* for modern structures (Bld. IDs 1 and 2) to older structures (Bld. IDs 4 and 5) highlights between-building variation in PCSDI due to design era, showing that, in general, PCSDI is larger for older buildings due to axial-shear interactions in shear-critical columns. Factors that influence the significance of the vertical component on collapse capacity, as measured by *PCSDI,* are investigated in more detail in subsequent sections.

Table 4-2 – Summary of IDA results

		Metrics of Collapse Capacity and Collapse Risk						Metrics of significance of vertical shaking	
		Horizontal comp only			Vertical and horizontal comp				
Bld. ID	Num. stories	Median Sdi_{uni} (in)	Log. Std. Dev. Sdi_{uni}	P[collapse] in 50 yrs (%)	Median Sdi_{bi} (in)	Log. Std. Dev. Sdi_{bi}	P[collapse] in 50 yrs (%)	Median *PCSDI* (%)	Standard deviation *PCSDI* (%)
1	2	8.5	0.58	0.99	8.3	0.56	1.03	1.2	5.4
2	8	26.5	0.55	1.5	25.8	0.54	1.6	3.2	8.0
3	2	17.9	0.47	1.0	9.1	0.47	1.2	37.2	32.1
4	2	4.1	0.24	13.5	3.8	0.30	15.4	4.4	22.8
5	8	8.5	0.25	16.9	8.2	0.25	17.0	2.4	10.8

4.6 Ground Motion Characteristics Influencing the Significance of Vertical Shaking

This part of the study focuses on analyzing ground motion parameters based on their ability to capture trends in *PCSDI*. To this end, a set of 27 ground motion parameters is quantified for both horizontal components and the vertical component of each ground motion in the set. The considered ground motion parameters include, but are not limited to: peak ground acceleration, peak ground displacement, Arias intensity, and significant duration.

4.6.1 Influential Ground Motion Parameters

4.6.1.1 Mutual Information

Mutual Information (MI) is used to quantify the relation between each ground motion parameter and *PCSDI*. *MI* is a general measure of dependence between two random variables (Moon, Rajagopalan, & Lall, 1995). *MI* is similar in concept to correlation, but the traditional correlation coefficient only captures linear relationships between two variables. *MI* is defined in Equation 4-4, where x and y are random variables, $P_{x,y}(x_i, y_i)$ is the joint probability density of x and y evaluated at (x_i, y_i) and $P_x(x_i)$ and $P_y(y_i)$ are the marginal probability densities of x and y evaluated at x_i and y_i.

$$MI_{x,y} = \sum_{i} P_{x,y}(x_i, y_i) \log_2 \left[\frac{P_{x,y}(x_i, y_i)}{P_x(x_i) P_y(y_i)} \right] \qquad \textit{Equation 4-4}$$

In this study, *x* represents one of the ground motion parameters of interest, x_i represents that ground motion parameter computed for a single ground motion record, y represents *PCSDI*, and y_i is *PCSDI* for a single record. The probability densities are estimated from the empirical distributions for x and y obtained from a kernel density estimator.

Since the magnitude of *MI* is a function of the input variables and does not have bounds, the value must be compared to the values of *MI* that result from random chance for the variables of interest, in order to quantify its significance (Moon, Rajagopalan, & Lall, 1995). The comparison is made by disrupting the pairs of data, such that x_i is now associated with y_j, where $i \neq j$, and recomputing *MI.* This process is repeated through Monte Carlo simulation, each time computing *MI*, with the results presented by a box plot, representing the range of *MI* values obtained through random chance. To determine if the value of *MI* from the true data set indicates a strong relationship between x and y, the value obtained is compared to the boxplot. This study defines a strong relationship between x and y if the *MI* is less than the 25th percentile or greater than the 75th percentile of the *MI* values obtained through random chance.

Of the 27 ground motion parameters considered, acceleration-based measures have strong mutual information with *PCSDI, i.e.* changes in collapse capacity associated with vertical shaking, for all of the buildings in this study. The acceleration-based parameters include effective design acceleration (Jack R. Benjamin and Associates, Inc, 1988), A95 parameter (Sarma & Yang, 1987), the root mean squared ground motion acceleration, peak ground acceleration, and

sustained maximum acceleration (Ye, Ma, Zhiwei, Guan, & Zhuge, 2013). These parameters all quantify the maximum acceleration of the ground acceleration, but differ in terms of the type of filter applied to the signal. Strong relationships between acceleration-based parameters of the horizontal and vertical components of a record and *PCSDI* are identified. However, the acceleration-based ground motion parameters computed for the vertical component are most informative.

Mutual information also shows a strong relationship between the ratio of the Housner Intensity (Housner, 1952) of the vertical component of a record (SI_V) to the horizontal component of the record (SI_H) and *PCSDI* for all building models with regular geometries (i.e. Bld IDs: 1, 2, 4, and 5). Housner Intensity can be used to evaluate the input energy of an earthquake and its damage potential for structures (Ye, Ma, Zhiwei, Guan, & Zhuge, 2013). The nature of the relationship between SI_V/SI_H and *PCSDI* for regular geometry buildings is further explored in the following section.

4.6.1.2 Classification and Regression Tree Analysis

Classification and Regression Tree, or *CART*[1], analysis is a useful tool for analyzing data containing many features that interact in complicated, nonlinear ways (Hastie, Tibshirani, & Friedman, 2008). *CART* organizes a set of data of *p* inputs and a response, *y*, for each of *N* observations. Classification trees are used when the response is categorical, and regression trees are used when the response is continuous. In our case, the response *y* is *PCSDI* is continuous, and the

[1] For the problem being considered, CART is sufficient to classify the differences between ground motion parameters.

inputs are the various ground motion parameters and ratios of ground motion parameters (e.g. PGA_v/PGA_h). In this process, we deliberately eliminate ground motion parameters that also include building information, *e.g.* $Sa(T_1)$, in order to enable solely ground motion based prediction of *PCSDI,* but consider all of the remaining ground motion parameters. *CART* analysis splits the data into subsets, identifying the "splitting variables" and "splitting points" that most reduce the variance in the prediction of *y*. A "tree" is used to represent the recursive partitioning, where terminal nodes, or leaves, represent a cell containing a simple prediction model. This splitting is accomplished through an algorithm of brute force, starting from one question that maximizes the information we gain about *y*, giving us two branches and two new child nodes. The same approach is then applied at the new child nodes and then continually repeated. The stopping criterion for growing a tree relies on the sum of squared error. If all binary splits of all variables at each node do not decrease the sum of squared error by a specified threshold (in our case 0.01), or the new nodes do not contain a certain number of points (5% of the full data set), the tree is fully grown. Before the regression tree is grown, the input data set is split in half at random. The first half of the data is used to grow the tree, while the second set is used to prune the tree. During pruning, the second dataset tests the accuracy of the tree. A subtree is replaced by a single leaf node when the estimated error (calculated for the pruning data) of the leaf replacing the subtree is lower than that of the subtree. The final tree can be used a predictive sense, with the values of the (input) ground motion parameters used to identify the relevant branch of the tree for a particular case, and the *PCSDI* value for that branch taken as the predictor of vertical significance for that ground motion.

To develop a CART model, *PCSDI* results for all buildings with regular geometries were combined into a single set, then a regression tree was grown based on the combined set, as illustrated in Figure 4-6. The results for the cantilever geometry model were excluded from the following tree because the magnitude of PCSDI for this building is much greater than that of the regular geometry models (as shown in Figure 5). The resulting regression tree is a function of the Housner intensity, computed as a ratio between vertical and horizontal components (SI_V/SI_H). This ground motion parameter was also found to have significant MI with *PCSDI* for the regular geometry buildings. The tree predicts that if the Housner intensity of the vertical component is at least 57% of the Housner intensity of the horizontal component, the vertical component of the record will be detrimental to building response, reducing the collapse S_{di} by an average of 9.2%. If SI_V/SI_H is less than 0.57, the vertical component of the record will have negligible effects on the collapse S_{di}.

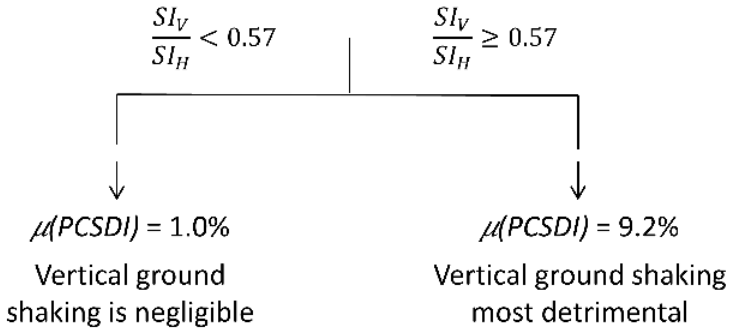

Figure 4-6 – Regression tree for all regular geometry buildings (Bld IDs: 1, 2, 4, and 5)

A regression tree such as this may serve to be useful in a number of post disaster analysis, or forensic engineering type situations. For example, an earthquake has occurred that has caused a regular (non-cantilevered) RC building to collapse. It is speculated that vertical ground shaking played a part in driving the collapse of the building. A quick, first check to give weight to this speculation would be to calculate the Housner intensities for ground motions recorded at or near the building site, and run them through the regression tree in Figure 4-6 to find the expected *PCSDI*. A similar tree could be produced for buildings with more unusual (cantilever) geometries.

4.7 Effect of Vertical Ground Shaking on Element Level Responses

The impact of vertical ground shaking on building collapse differs in severity with building design era, number of stories, and geometry. In this section, a detailed analysis of column and beam responses is conducted to identify how the effects of vertical ground shaking that drive collapse materialize at the element level, and if specific element level effects are associated with beneficial or detrimental structural level responses. Vertical shaking effects are quantified through the relationship between element responses and *PCSDI*. The relationships between element response and *PCSDI* are sorted into two categories: (1) those that exist only for individual buildings and (2) those that exist regardless of building type.

This study focuses on column response because the formation of column hinges (newer buildings) or shear failure in columns (older buildings) tends to govern collapse for RC moments frames (Liel, Haselton, & Deierlein, 2011). We examine column responses quantified by the maximum moment, maximum compressive axial load, and maximum tensile load a column experiences during ground shaking. The ratio of the time at which the maximum axial

compressive load occurs, to the time at which the maximum moment occurs, is also considered. The authors hypothesize that if this ratio is close to unity (*i.e.*, the maximum axial load and moment occur simultaneously, and if the axial load is near the balance point) under combined vertical and horizontal shaking the column's capacity will be decreased, and failure will occur prematurely. Tensile and compressive axial loads are considered separately. However, we observe that a strong correlation exists between the timing of maximum compressive force and maximum tensile force (correlation coefficient, $\rho > 0.8$ for each building) at the incipient collapse spectral level. Since trends between the maximum tensile forces and *PCSDI* are a mirror image of the trends between maximum compressive forces and *PCSDI*, only results for maximum compressive load are described hereafter.

4.7.1 Column Response Trends for All Building Models

Each building column has a controlling failure mode or mechanism, *i.e.* flexure in the modern building models, and flexure shortly followed by shear and shear-axial failure in the older building models. This section aims to identify secondary (non-governing) effects from vertical shaking that either hinder building performance by increasing column demands and expediting failure, or benefit building performance by counteracting column demands, delaying failure. The most complete picture is provided by tracing the progression of secondary forces through the ground motion intensities run in the IDA up to collapse, and comparing the progression for the unidirectional and bidirectional runs. For simplicity, and to provide a window into the element state at collapse, we focus on structural responses at a ground motion intensity referred to as the "incipient collapse spectral acceleration". This point is one spectral level before the collapse

spectral value, provides a picture of the collapse state of the structure, and avoids the nonphysical values that occur at the collapse level as the solution algorithm attempts to converge. At the incipient collapse spectral acceleration, the capacity of the elements at the critical story in the governing failure mode is exactly met (*e.g.,* moment capacity is just for an element failing in flexure) regardless of whether the shaking is uni or bidirectional. However, secondary load effects (*e.g.,* axial load demands on a column failing in flexure) do vary between the uni and bidirectional cases, and these differences provide insight into the question of how the controlling collapse mechanism is delayed or accelerated by the vertical shaking. Of course, the collapse intensity level could be different in the uni and bidirectional cases; in these cases the point of incipient collapse spectral acceleration for both cases are the scale level just before collapse, but the magnitude of the intensity levels are different. In most cases, no single secondary effect fully describes trends in collapse probability due to vertical shaking, but rather the combination of secondary effects is more important.

The most telling individual secondary effect is the change in the axial load demand on a column due to the vertical load effect. Change in axial load is taken as the percent increase in maximum axial load at collapse between the uni and bidirectional loading cases. When subjected to horizontal ground accelerations, overturning is the source of earthquake-induced column axial force. Under bidirectional loading, the column's axial load becomes the sum of the effects due to overturning and due to vertical ground acceleration. Vertical ground shakings contributions to the axial load may add to or counteract axial load from overturning.

The average change in maximum compressive load in the critical story columns at the incipient collapse spectral acceleration is examined for: (1) the 10% most beneficial vertical records, *i.e.* records producing the lowest *PCSDI* values, (2) the full earthquake set, and (3) the 10% most detrimental vertical records, *i.e.* records producing the highest PCSDI values. The most detrimental ground motions impose the largest axial load demands on column elements, as shown in Figure 4-7, leading to an increase in moment demand (the governing failure mode for these buildings) through P-Δ effects. The additional flexural column demand from vertical shaking exceeds the flexural capacity of the columns before their capacity is exceeded under solely horizontal ground shaking. This finding aligns with results from (Di Sarno, Elnashai, & Manfredi, 2011), in which vertical shaking increased column compressive load 59% to 174% on average depending on building type, causing the axial load-bending moment interaction to exceed the threshold value, which lead to column failure. If the column axial load is near the balance point, this effect may be combined with a reduction in flexural capacity associated with the axial-flexural (P-M) interaction. For shear-critical members in older RC frames, increased axial compressive load reduces the drift capacity at which shear failure is expected to occur (Elwood K. J., 2004). In contrast, the most beneficial ground motions induce lower than average axial load demands under bidirectional loading and, in turn, lower than average flexural demands on the columns for a given spectral level, thus contributing to improved structural level performance under combined shaking. Note that Building ID: 4 does not align with this general pattern, and this discrepancy is addressed in the following section.

The timing of the occurrence of maximum load is also an important factor in explaining trends in *PCSDI*. Of particular importance is the idea that if the timing of the maximum column compressive load becomes more coincident with the timing of the maximum moment when vertical shaking is included in the analysis (*i.e.,* the maximum axial and flexural load effects occur in close proximity), and the axial load on the column is close to the balance point, the column capacity will be reduced, triggering failure at a lower spectral acceleration. The axial load increase due to vertical shaking is large enough that it passes the balance point on the axial-flexure interaction curve for the 8 story modern model, entering the range of response where increase in axial load reduces column flexural capacity. A visual representation of this concept is presented in Figure 4-8, which shows how the timing ratio of axial and flexural loads shifts between the uni and bidirectional loading for Building ID: 1. Quadrants A or C indicate a shift away from unity in the ratio of maximum compressive force to time of maximum moment when vertical shaking is included in the analysis; quadrants B or D indicate a shift toward unity; any points falling along either 45 degree line indicate no shift in timing. The impact of vertical shaking on structural response is indicated by the color and shape of the plotted markers. In an average sense, the more detrimental vertical ground motions shift the timing of maximum compressive load and maximum moment such that they occur in close proximity (regions B and D) (more of the detrimental red markers are in those regions than in B and D). Conversely, beneficial vertical ground motions shift the timing of maximum compressive load and maximum moment such that they occur at more different times (regions A and C). These observations do not hold for all individual data points, but, when combined with the information about the magnitude of the

load variations, explain many of the patterns in *PCSDI*. Similar findings are observed for the other buildings.

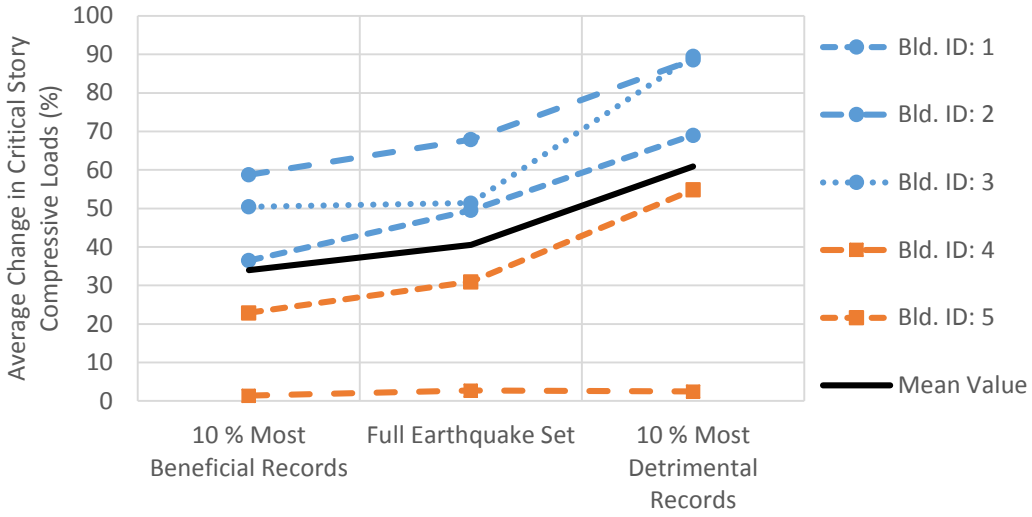

Figure 4-7 – Average percent increase in maximum compressive demand between unidirectional and bidirectional analyses for each building. Calculated for columns in the critical story at the incipient collapse acceleration.

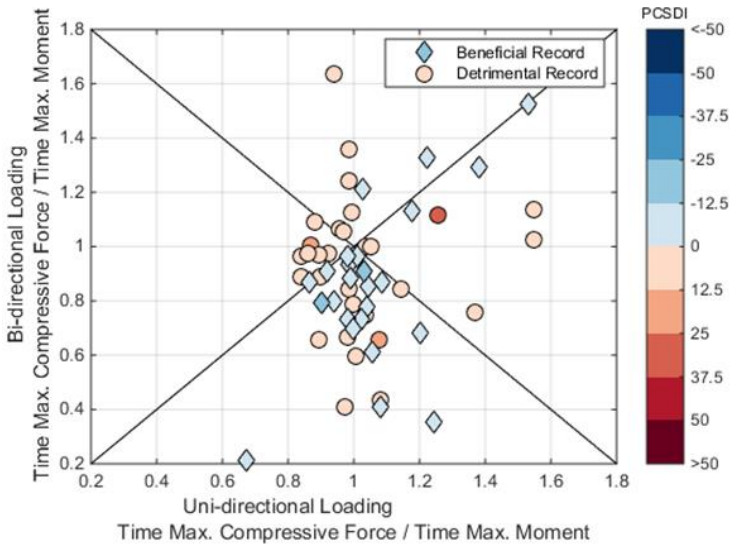

Figure 4-8 – Ratio of timing of maximum compressive force to time of maximum moment plotted for the bidirectional loading case vs. the unidirectional loading case. Results are averaged for columns in the critical story in, shown Building ID: 1.

4.7.2 Column Responses Trends in PCSDI that are Unique to Certain Buildings

On average, the most detrimental vertical ground motions place the largest axial load demands on critical columns. However, this trend is not apparent for the two story older building (Building ID: 4) in Figure 4-7. For this building, the nonlinear simulation model indicates that column failure, and by extension building collapse, is controlled by the column axial response (represented by an axial spring in the model). Since the building always fails in the vertical or column axial mode, the axial load level at collapse does not depend on the occurrence of unidirectional or bidirectional shaking. To demonstrate that axial load from vertical shaking still controls the element response in Building ID: 4, Figure 4-7 is recreated for a spectral level (S_a(T=0.7) = 0.2 g) that does not correspond with collapse. At this lower shaking intensity, it is more apparent that the most detrimental vertical records produce the largest increases in

maximum axial load. The increased axial demands exceed the axial capacity of the columns, leading to axial failure at a lower level of ground motion intensity. Unlike Building ID: 4, the other non-ductile building, Building ID: 5, is an 8-story building and collapse is governed by a sidesway (shear) mechanism, not only the axial failure criterion, so these trends were apparent at the collapse level.

For the buildings with shear-critical columns (Building IDs 4 and 5), it is also interesting to look at how flexural demands capture trends in the influence of vertical shaking on structural performance at the incipient collapse level. As indicated in Figure 4-10, in these buildings, vertical ground motions that benefit structural response tend to decrease the average maximum column moment that occurs under purely horizontal loading and detrimental vertical ground motions increase the average maximum column moment. Significant past research has shown that flexure-shear interaction contributes significantly to element response (Vecchi & Collins, 1988). The outcome of vertical ground shaking counteracting moment demand from horizontal shaking at collapse is to effectively increase shear capacity by reducing the deformation demand on the column. Conversely, vertical ground motions that add to the flexural, and therefore drift, demand from horizontal shaking effectively decrease column shear capacity. The increase or decrease in shear capacity of these older models is of primary importance as the shear capacity of the element dictates failure, effectively altering structural performance.

4.8 Examination of Nominal Vertical Earthquake Load for design

In the interest of comparing the ASCE 7-10 specified nominal vertical earthquake load with the recorded vertical earthquake action, each of the modern buildings (Bld. IDs: 1, 2, and 3)

is analyzed at the ASCE 7-10 specified horizontal design ground shaking level ($S_D(T_1)$) for the site of interest. This analysis is carried out using the same ground motion set used for IDA, but providing a stripe of data relating ground shaking at the design level to building response.

To quantify the nominal vertical earthquake load, we recall the ASCE 7-10 load combinations (Equation 4-1 and Equation 4-2) pertaining to vertical ground shaking. The horizontal earthquake load is the primary load in the combinations in Equation 4-1 and Equation 4-2; all other loads in the combinations are taken as their expected value of the load at the time of maximum horizontal earthquake loading, *i.e.* treated as arbitrary point-in-time (APT) loads (Ellingwood, Galambos, MacGregor, & Cornell, 1980). This idea is expressed directly in the discussion of the code development, wherein it states that "the concurrent maximum response of vertical accelerations and horizontal accelerations, direct and orthogonal, is unlikely and, therefore, the direct addition of responses was not considered appropriate" (Building Seismic Safety Council, 2004). Following the rationale of APT loads, the vertical earthquake load effect (axial force) in the columns in the analysis in this study is extracted at the time of maximum horizontal earthquake loading. Here, the maximum horizontal earthquake loading is identified by the time step at which the column shear force is at its peak. In beams, the vertical earthquake effect is taken as the moment caused by vertical shaking. This force is extracted at the time of maximum horizontal earthquake loading in the beams, which is taken as the time at which the axial load in the beam is at its peak. Dead (182 psf) and live loads (12 psf) in the models are taken as the expected loads from ASCE 7-10, with no reduction factor applied to the live load. The snow

load, *S,* and the load due to lateral earth pressure, *H*, are ignored in this analysis because these loads are not explicitly represented in dynamic analysis.

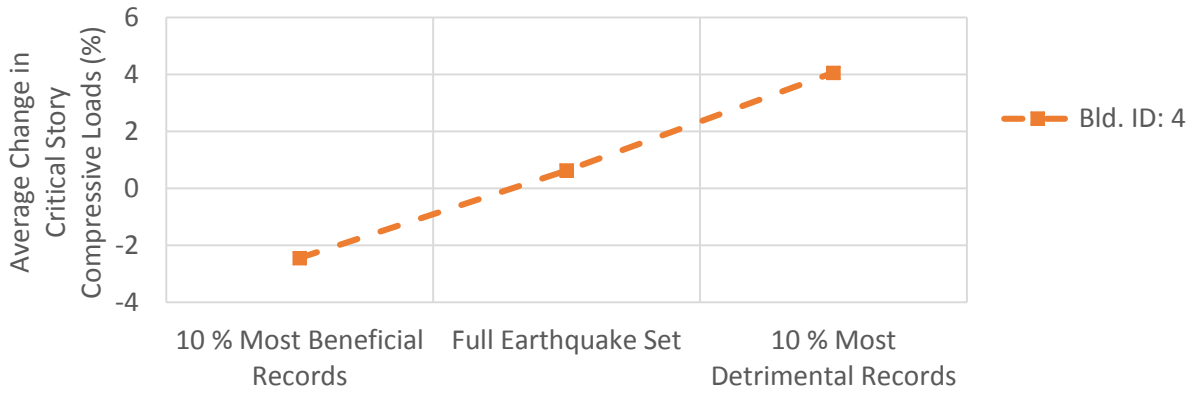

Figure 4-9 - Average percent increase in maximum compressive demand between unidirectional and bidirectional analysis for Building ID: 4. Results shown for columns in the critical story.

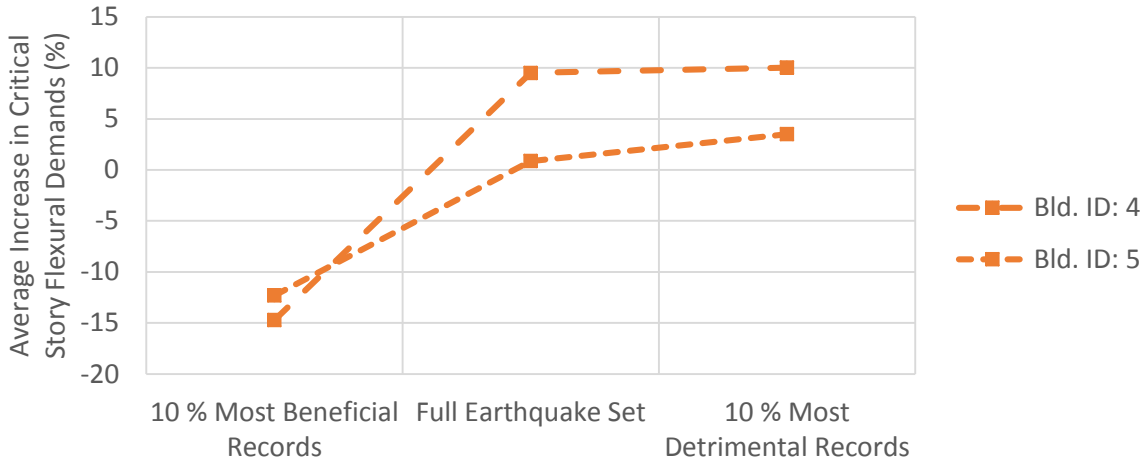

Figure 4-10 - Average percent increase in maximum flexural demand between unidirectional and bidirectional analysis. Results shown for columns in the critical story in at the incipient collapse spectral acceleration for shear-critical buildings.

To obtain the mean vertical earthquake action for each member in each building, the load effects are deaggregated into the contributions from the horizontal earthquake, vertical earthquake, dead, and live loads. For column members, the axial load due to dead and live loads

is subtracted first from the total axial load recorded in the analysis. Separating the axial load contribution from horizontal loading due to overturning is less straightforward. Here, we assume that the axial load due to overturning is negligible compared to the axial load due to vertical shaking. This assumption is reasonable for columns located near the centroid of the structure or in upper floors where the effects of overturning are the smallest, and therefore only columns in these locations are considered in the results. For beams, identifying the APT moment from vertical shaking involves decoupling the total recorded moment. To do so, the contribution from dead and live loads to the total APT moment is found by assuming a semi-fixed beam, with two inflection points each located a distance one-tenth of the beam span length from either end of the member. The contribution to the total beam moment from horizontal loading is estimated using the portal frame method. Responses are separated into two categories based on Equation 4-1 and Equation 2, *i.e.* separating the cases in which the APT vertical load effect is additive with the dead and live loads, and the case in which the vertical load effect counteracts the other load effects. Once decoupled for both beams and columns for every ground motion record, the recorded APT vertical earthquake action in each element is compared to its corresponding nominal action from ASCE 7-10, which is taken as the load effect (moment or shear) from $0.2S_{DS}D$ applied in the positive and negative gravity directions.

Probability distributions are fitted to histograms of a random variable which represents the ratio of (i) the vertical earthquake effect observed in the dynamic analysis to (ii) the load effect from nominal earthquake load. Best-fit distributions in Table 4-3 are selected on the basis of Bayesian information criterion (Schwarz, 1978). This criterion is similar to the likelihood

function in that it minimizes lost information, but also avoids overfitting by introducing a penalty factor for the number of parameters in the fitted model. This penalty factor is higher in the Bayesian information criterion than in the Akaike information criterion. Of 16 probability models considered, the Extreme Value Type II distribution is selected as the best-fit for both categories of vertical loading (additive and counteracting). Many meteorological and hydrological phenomena have been modeled using this distribution (Gumbel, 1958) as well as horizontal ground shaking (Ellingwood, Galambos, MacGregor, & Cornell, 1980).

The maximum vertical load effect observed during design level shaking in numerical simulation is on average 10.3 and 7.3 times greater than the ASCE 7-10 nominal vertical load effect for the additive and counteracting effects, with coefficients of variation 0.85 and 0.72 respectively. These results indicate that the vertical impacts of ground shaking are highly variable, and that the APT load effects are substantially higher than those represented by the $0.2S_{DS}D$ design load. Although these results are at this time based only a limited number of buildings, these findings nevertheless suggest a need to reexamine vertical loads used for design and to clarify what the design load is intended to represent. Although $0.2S_{DS}D$ is referred to as a vertical earthquake action in (American Society of Civil Engineers, 2013), documentation of code changes over time makes it clear that part of the rationale for the load was to counteract a decrease in design dead load that occurred at the same time that this factor was introduced (Heausler, 2004). The timing of a reconsideration of vertical earthquake load may be ideal given the proposals to map the vertical component of seismic hazard, eliminating the need for the $0.2S_{DS}$ assumption, which are currently under consideration by the Building Seismic Safety Council.

Table 4-3 – Probability distribution parameters for arbitrary point-in-time vertical earthquake load effect normalized by nominal vertical earthquake load

Vertical Earthquake Effect	*Best-Fit Distribution*	*Scale Parameter*	*Shape Parameter*
Additive	Type II Extreme Value	0.34	0.43
Counteracting	Type II Extreme Value	0.07	3.73

4.9 Conclusions

The vertical component of ground shaking has fueled a long debate among structural engineers about their significance and appropriate methods for inclusion in design and analysis. The complex phenomena controlling vertical shaking make simple, yet robust methods for incorporating their effects into analysis and design difficult. Therefore, more advanced methods are needed to adequately capture the effect of vertical ground motions and to understand the mechanisms by which vertical shaking can substantially alter seismic response.

In this study, five buildings are analyzed using 82 pairs of ground motions. The influence of vertical shaking is evaluated by comparing the change in collapse capacity when the vertical shaking is included, versus when horizontal shaking alone is considered. Including the vertical component in the dynamic analysis produces large variations in building response. In some cases, building response benefits from vertical shaking while, in other cases, response is significantly worsened, or there may be little to no change.

The study shows that certain ground motion parameters are effective predictors of trends in building collapse due to vertical shaking. Through the use of Mutual Information and Classification and Regression Tree analysis, the ratio of the Housner intensity computed for the vertical component of a record to the Housner intensity of the horizontal component of a record is identified as the most telling ground motion parameter for regular geometry buildings. If SI_V/SI_H

is at least 0.57, the vertical component of the record will likely be detrimental to building response, reducing the collapse S_{di} by an average of 9.2%. Conversely, if SI_V/SI_H is less than 0.57, the vertical component of the record will likely have a negligible effect on the collapse S_{di}.

Of the five considered buildings, the building with large structural cantilevers is most impacted by vertical ground shaking. The vertical response of the cantilever sections induces large moment demands on the neighboring columns, serving as the catalyst for collapse. In addition, the models representing older nonductile buildings are more severely impacted than ductile models due to the reduced shear capacity stemming from flexure-shear and axial-flexure interactions under combined shaking. An investigation into element level response shows that no single response dictates the severity of vertical ground shaking. Nevertheless, the severity of vertical ground shaking on structural performance can be attributed, in part, to the records' increase on column axial loads due to service and horizontal earthquake shaking. On average, the most detrimental vertical ground motions increase column axial load by 60% at incipient collapse. Furthermore, vertical ground motions that produce a shift in the timing of maximum column axial load and moment such that they occur at similar times are found to be detrimental to structural response in an average sense. Finally, the load effect from vertical ground motions is found to be significantly larger than the nominal value used in U.S. building design.

5 SUMMARY AND CONCLUSIONS

5.1 Overview

Performance-based earthquake engineering (PBEE) has advanced to a point where its application in practice is increasing. This marks an important shift in seismic design and analysis that places value on the performance desired by relevant stakeholders. However, the relative youth of PBEE, and its implantation in practice, drives us to study the efficacy of standards that mold the PBEE framework into standardized form, specifically as applied to retrofit buildings (Chapter 2). While PBEE-based standards attempt to provide consistency in design, the cost of designing or retrofitting to satisfy a standard-based performance objective may not fully consider the relative costs and benefits of specific retrofit decisions and actions (Pekelnicky & Poland, 2012). This study further identifies dimensionless indicators, indicative of improvements in structural characteristics from seismic retrofitting, that have strong relationships with performance improvements (Chapter 3). Retrofit indicators highlight areas of retrofit design that contribute to reductions in building collapse risk and/or earthquake induced repair cost. Lastly, PBEE methods are used to assess the vulnerability of reinforced-concrete (RC) buildings to combined horizontal and vertical ground shaking (Chapter 4).

5.2 Performance Outcomes Achieved from Retrofitting to Standardized Levels (Chapter 2)

FEMA 356 (FEMA and ASCE, 2000) and 273 (Applied Technology Council, 1997) were some of the first documents to standardize PBEE for use in practice (Porter, 2003). ASCE 41 is based on

these initial efforts, and has become the most commonly used standard for seismic evaluation and retrofit of existing buildings in the U.S. (Pekelnicky & Poland, 2012; Sattar & Hulsey, 2015). While ASCE 41 applies PBEE concepts by defining performance objectives in terms of global performance, adherence to the selected performance objective is governed by the response of individual components, analyzed independently.

The performance achieved through retrofitting to a standardized level was studied by evaluating the performance of 3-, 6-, and 9-story RC buildings retrofit to multiple ASCE 41 performance levels. First, a set of buildings is designed to the Uniform Building Code of 1967 (International Conference of Building Officials, 1967). Buildings are then retrofit with FRP wraps, steel jackets, or concrete jackets to comply with ASCE 41 CP, LS, and IO performance levels. ASCE 41 defines these performance levels in terms of approximate global, structural, and nonstructural damage. Next, the performance of each retrofit buildings are assessed through a rigorous PBEE framework developed by the Pacific Earthquake Engineering Research (PEER) Center. Results from the PBEE provide quantifiable metrics by which to gauge the performance obtained through retrofitting to an ASCE 41 level.

Overall, the results show that the component-based retrofit procedures in ASCE 41 produce retrofit designs that behave similarly to the approximate global behavior from ASCE 41. Furthermore, damage during design level shaking decreases as the design PL is increased from CP to LS and IO, indicating that PLs are internally consistent. Nevertheless, retrofit designs that comply with CP and LS performance levels typically sustain less damage, as estimated through the PBEE framework, than is estimated by ASCE 41. The study also showed that buildings

designed to CP or LS levels have a larger possible range of estimated repair costs than buildings designed to comply with IO. This occurs because acceptance criteria for CP and LS are more relaxed than in IO, allowing for a broader range of retrofit design solutions.

Damage to structural components in buildings retrofit to ASCE 41 standards is studied using two approaches. First, damage to the entire structural system resulting from design level shaking was assessed through nonlinear dynamic analysis. After shaking ceased, a pushover analysis is run on the buildings in their post-dynamic states. Capacities of the damaged buildings are calculated from the pushover results and compared to capacities of the un-damaged buildings. For buildings retrofit to the LS level, on average, a building retains 75%-85% of its original strength and stiffness after a design level event, and buildings designed to IO retain all their original strength, and 80% of the stiffness. These reductions in building stiffness and strength indicate that ASCE 41 damage estimates for LS and IO compliant buildings are in good agreement with median damage observations from buildings in this research. On average, buildings designed to CP level retain 60% of their original stiffness, 80% of its yield strength, and 70% of its ultimate strength. ASCE 41 approximate damage estimate that states buildings designed to CP will have "little residual stiffness and strength to resist lateral loads". Buildings designed to CP levels from this research show less damage than predicted by ASCE 41.

Additionally, damage to structural components is evaluated and compared to approximate damage patterns from ASCE 41 conditioned on the design PL. In buildings retrofitted to CP and LS levels, damage concentrates in structural components of moment frames that have not been seismically retrofit. This observation differs from the ASCE 41 approximate damage

patterns, in which damage is estimated to concentrate in ductile components. The undesirable damage pattern observed during simulation may not warrant extreme concern if the strength and stiffness provided by the retrofit design sufficiently reduces the building collapse risk. Damage in buildings designed to IO levels concentrates in beams of retrofit, ductile, moment frames, which matches the ASCE 41 approximate damage pattern.

Nonstructural performance levels, defined by ASCE 41, and considered in this study include: Position Retention and Not Considered. While nonstructural components are not explicitly considered during the retrofit design process or modeled during numerical simulation in this study, nonstructural component fragilities are updated to seismically-rated components whenever possible in buildings designed to the Position Retention level. Nonstructural component fragilities in buildings designed to the Not Considered level are representative of nonstructural components found in 1967 buildings. Differences in nonstructural component fragilities are important during the loss analysis and affect multiple decision variables.

Building designs that are designed to the Not Considered nonstructural performance level have annualized repair costs (losses) from nonstructural components that equal repair costs in buildings that have not been seismically retrofit. This finding applies to buildings designed to CP or LS structural performance levels. Therefore, a designer cannot expect nonstructural performance, measured in terms of annualized repair cost, to improve in retrofits that strengthen structural performance if nonstructural performance is not explicitly considered in the design, despite benefits to system-level structural performance. Furthermore, buildings designed to Position Retention standards had annualized repair costs due to nonstructural components equal

to the un-retrofit 1967 buildings. Recall that the buildings designed to Position Retention standards are also designed to the IO structural performance level. The increased floor accelerations and multi-story damage patterns resulting from designing to the IO level are found to negate improvements in nonstructural repair costs from seismically rated fragilities and reduced drift demands.

5.3 Evaluation of Improvements in Performance Achievable Through Retrofit: Development of Dimensionless Retrofit Indicators (Chapter 3)

In Chapter 3, the PBEE framework is used to quantify benefits of retrofitting 1967 buildings. Results from RC building designs and models developed in Chapter 2 are utilized to identify dimensionless indicators that describe improvements due to retrofitting with respect to two Decision Variables (DV). DVs included in this study are mean annual frequency of collapse and annualized repair cost quantify earthquake-induced losses. Retrofit indicators are intended to be simple measures that are easily calculated during the retrofit design process. The suitability of retrofit indicators to identify trends in building performance improvements is dictated by the DV of interest. Therefore, the following results are separated by DV.

Improvements in mean annual frequency of collapse are best described by a combination of strength-based and ductility-based indicators. While either strength-based, or ductility-based indicators are able to capture general trends in mean annual frequency of collapse independently, they are not able to accurately represent the response improvements of all retrofit methods. The complementing nature of strength and ductility capacity is such that

deficiencies in one parameter can be mitigated through the other. Therefore, this study suggests that improvements in mean annual frequency of collapse due to retrofit are best described by the combination of $\mu_{stregnth}$ and ductility capacity, where $\mu_{stregnth}$ quantifies the building strength in relation to the design spectral acceleration computed at the fundamental period of the building. Buildings with the lowest mean annual frequencies of collapse are shown to have large ductility capacities (i.e. > 8) and small $\mu_{stregnth}$ values (i.e. < 2). Conversely, 1967 buildings that have not been seismically retrofit have low ductility capacities and high $\mu_{stregnth}$ values; these structures pose the highest risk of collapse. These results align with modern seismic code philosophies, which attempt to provide strength and ductility capacity to a structure such that collapse risk is mitigated. Additionally, indicators such as M_c/M_b and V_p/V_n, which measure RC building deficiencies, are shown to be meaningful predictors of mean annual frequency of collapse for a group of buildings with similar $\mu_{stregnth}$ values.

When the DV of interest is annualized repair cost, indicators that provide information on building capacities and seismic demands (such as $\mu_{strength}$ and δ_{DCR}), best capture improvements in performance achieved by seismic retrofitting. $\mu_{strength}$ quantifies the design spectral acceleration computed at the fundamental period of the structure to the base shear capacity and seismic weight of the building. $\mu_{strength}$ is able to describe general trends in annualized repair costs reductions from retrofitting. Four regions are defined in terms of $\mu_{strength}$ that bin buildings according to annualized repair cost. Regions are independent of retrofit type, normalized yield and ultimate strengths, and number of stories, therefore providing a simple measure by which to assess benefits of retrofitting in terms of economic loss. δ_{DCR} is another indicator that captures

trends in reductions to annualized repair cost from retrofitting (R^2 = 0.76). δ_{DCR} compares the expected seismic drift demand during design level shaking to the effective yield drift capacity of the building. Interestingly, ductility capacity is found be a poor indicator of annualized repair cost, as the two variables are shown to be weakly related. Lower intensity events, in which the structural response remains elastic or exhibit slight nonlinear behavior, contribute significantly to annualized repair cost. In these regions of response, ductility capacity is unimportant because the response is elastic. Furthermore, drift demands and repair costs from drift-sensitive components will be larger in retrofit designs that improve ductility capacity without significantly impacting strength than in designs that improve both strength and ductility.

This study shows the importance of separately considering multiple DVs during performance-based design. Mean annual frequency of collapse and annualized repair cost are found to be weakly correlated, ρ = 0.38. Therefore, designs that only address collapse risk does not necessarily produce designs that mitigate earthquake-induced repair costs.

5.4 Evaluating the Seismic Vulnerability of RC Buildings to Vertical Ground Shaking (Chapter 4)

The influence of vertical ground shaking on the collapse capacity of modern and 1967 RC buildings is evaluated using probability-based methods. Incremental dynamic analysis (IDA) is run using set of 82 ground motion pairs. First, the ground motion set is run using only the horizontal shaking components. Next, vertical and horizontal components are run simultaneously. The inclusion of vertical ground shaking in dynamic analysis is shown to produce a range of effects on

structural collapse; in some cases, vertical ground shaking caused collapse at spectral levels that are much lower than when the horizontal component as run independently, while other cases produced structural collapse at higher spectral levels.

Certain ground motion parameters are shown to be useful in describing the impact a vertical record will have on building collapse capacity. Both Mutual Information and Classification and Regression Tree analysis show that the ratio of the Housner intensity computed for the vertical component of a record to the Housner intensity of the horizontal component of a record (SI_V/SI_H) is the most telling ground motion parameter for regular geometry buildings. Records with SI_V/SI_H greater than 0.57 reduced the collapse level by 9.2% on average, while records with SI_V/SI_H less than 0.57 had negligible effects on the collapse level observed when the horizontal component is run independently.

Buildings containing cantilevered sections are shown to be more sensitive to vertical ground shaking than regular geometry structures. Additionally, 1967 buildings are more severely impacted than modern, ductile models due to the reduced shear capacity stemming from flexure-shear and axial-flexure interactions under combined shaking. On average, the most detrimental vertical ground motions increase column axial load by 60% at incipient collapse.

5.5 Limitations

Structural designs, numerical model development, and evaluation methods are performed in a systematic manner to mitigate errors and sources of bias that would influence

the results of this study. Nevertheless, certain simplifications were made and uncertainties exist that are addressed herein.

In Chapters 2 and 3, this work analyzed buildings that were seismically retrofit using local methods; namely, steel jacketing, concrete jacketing, and wrapping members in FRP sheets. Local retrofit strategies are selected because they lend themselves nicely for implementation in a systematic retrofit design process. Global retrofit measures and mixed retrofit designs are not considered. However, these retrofit strategies are commonly used in practice. For example, retrofit designs often wrap deficient members in FRP and add shear walls, improving system strength and ductility. While the local retrofit strategies implemented in this research do not cover the broad spectrum of possible retrofit designs, the impact of local retrofits on system characteristics (i.e. strength, stiffness, ductility capacity) are expected to be common to all retrofit designs. Nevertheless, more variation in seismic performance may exist when analyzing additional retrofit strategies. Therefore, results from this work should be compared with studies that analyze additional retrofit strategies.

Advanced modeling techniques are used to estimate structural response, however, certain limitations in the capability of element and material models to capture all possible responses exist. Limitations in numerical modeling include, but are not limited to:

- 2-dimensional models, representative of a single frame line, are used to describe the behavior of the complete, 3-dimensional building. Therefore, torsional effects are neglected in this research. Torsional effects for the studied buildings are not expected to be significant because considered designs are space frame buildings

that are symmetric in plan. Furthermore, retrofits are designed to be symmetric in plan, mitigating the effects of torsion. However, torsional effects may be significant in other structures.

- Numerical models for members retrofit using FRP wraps in this study are not able to capture fracture of the FRP laminate. Research on modeling this response is currently ongoing (Megalooikonomou, Monti, & Santini, 2012; Papavasileiou & M egalooikonomou, 2015). A major difficulty in modeling this failure mode is appropriately describing the change lateral confining stress provided by the FRP wrap to the concrete after FRP fracture occurs. For this reason, FRP laminates are not explicitly modeled in this study, and therefore failure of FRP wrapped columns is governed by rebar bucking and concrete crushing of the original RC member.
- The interface between concrete or steel jackets and the encased RC member are not modeled. Such detailed finite element modeling is outside the scope of this study.
- Effects of soil structure interaction on structural performance is outside the scope of this research, though these effects are not likely to be important for ductile moment frames or taller non-ductile buildings.
- Uncertainty related to structural modeling was not included in predictions of collapse risk. Research has shown that modeling uncertainty can significantly impact building fragilities, however, more research needs to be done to develop

an accepted method for quantifying such uncertainties (Haselton, Liel, Deierlein, Dean, & Chou, 2011).

- Fragility functions for components that have been seismically retrofit using steel jackets, concrete jackets, and FRP wraps are currently unavailable. Therefore, fragility functions for Ordinary Moment Frames (OMF) with weak joints and flexurally controlled beams are used as a substitute. In these systems, columns are flexurally-governed and damage tends to concentrate in beams and joints. Therefore, damage states for OMFs are reasonable substitutes for RC subsystems where the columns have been jacketed because the damage patterns are similar. However, the cost associated with repair of OMF systems and locally retrofit systems may differ.

A method employed in this research to minimize the impacts of the discussed modeling limitations is to frame conclusions in terms of relative performance as opposed to absolute measures whenever possible. For example, the performance of buildings retrofit to CP, LS, and IO levels is compared with modern buildings (designed using similar assumptions) to evaluate the efficacy of ASCE 41. In the development of retrofit indicators, relative improvements in seismic performance are used as opposed to absolute reductions in DVs. Framing conclusions in terms of relative comparisons helps to minimize systematic errors because the results for different models are subject to the same set of limitations.

This research analyzes RC buildings ranging from 3- to 9-stories in height. Therefore, many building types are not explicitly considered, such as timber, masonry, infilled RC and RC shear

walls, braced frames, and steel buildings. However, a wide range of design characteristics (i.e. strength, stiffness, and ductility) are represented in the RC buildings analyzed by this research. Therefore, the author hypothesizes that design characteristics of many other building types will covered by the range of properties considered herein. Furthermore, conclusions presented by this research are based on trends that are consistent for all variations of the researched RC buildings. Based on the assumption that other building types have design characteristics covered by the building set considered herein, the author expects results to be applicable to other structural systems. However, it would not be appropriate to extend results from this study to building types with design characteristics much different from the researched RC building set, such as masonry buildings and buildings containing tuned mass dampers.

5.6 Future Work

Further work is needed to fully integrate local retrofit design and PBEE. Specifically, fragility functions and loss function, representative of the unique damage states and associated repair costs for seismically retrofit components, are currently unavailable. In the future, the author would like to assemble a database of experimental tests on retrofit components, from which fragility and loss functions could be derived. The derivation of such fragility and loss functions would lead to more accurate loss estimation for retrofit buildings.

Currently, ASCE 41 does not provide acceptance criteria for locally retrofit members. Therefore, judgement must be used by the analyst in order to prove a retrofit member complies with the desired performance objective. Work is ongoing to develop modeling parameters for jacketed members (Alvarez & Brena, 2014). However, analysts would benefit from the creation

of acceptance criteria for retrofit members. The author would like to work towards developing such acceptance criteria once a database of experimental tests on retrofit components is assembled. Acceptance criteria should be of a similar form as criteria for existing RC members.

Additionally, there is a disconnect between component damage states used in loss estimation methods such as FEMA P-58, and acceptance criteria in ASCE 41. Once possible way to connect ASCE 41 with other PBEE procedures such as FEMA P-58 would be to develop acceptance criteria based upon component damage states, effectively, linking ASCE 41 PLs with measurable component damage states. This would help to provided consistency between buildings designed and analyzed to different standards.

6 REFERENCES

Aboutaha, R., Engelhardt, M., Jirsa, J., & Kreger, M. (1996). Retrofit of Concrete Columns with Inadaquate Lap Splices by the Use of Rectangular Steel Jackets. *Earthquake Spectra, 12*(4), 693-714.

Aboutaha, R., Engelhardt, M., Jirsa, J., & Kreger, M. (1999). Rehabilitation of Shear Critical Concrete Columns by Use of Rectangular Steel Jackets. *ACI Strucutral Journal, 96*(1), 68-78.

Abrahamson, N. A., & Silva, W. J. (1997). Empirical response spectral attenuation relations for shallow crustal earthquakes. *Seismological Research Letters, 68*, 94–127.

ACI Comittee 440. (2008). *Guide for the Design and Construction of Externally Bonded FRP Systems for Strengthening Concrete Structures.* Farmington Hills: American Concrete Institute.

ACI Committee 318. (1963). *Building code requirements for reinforced concrete (ACI 318-63).* Detroit, Michigan: American Concrete Institute.

ACI Committee 318. (2014). *ACI 318-14: Building Code Requirements for Structural Concrete and Commentary*. Farmington Hills, MI: American Concrete Institute.

ACI Committee 440. (2008). *Guide for the Design and Construction of Externally Bonded FRP Systems for Strengthening Concrete Structures.* Farmington Hills, MI: American Concrete Institute.

ACI Committee, American Concrete Institute, and International Organization for Standardization. (2008). *Building code requirements for structural concrete (ACI 318-08) and commentary.* American Concrete Institute.

Alvarez, J. C., & Brena, S. F. (2014). Non-linear Modeling Parameters for Jacketed Columns Used in Seismic Rehabilitation of RC Buildings. *SP-297 Seismic Assessment of Existing Reinforced Concrete Buildings*, 6.1-6.22.

American Society of Civil Engineers. (2013). *Minimum Design Loads for Buildings and Other Structures (ASCE/SEI 7-10).*

Ancheta, T. D., Darragh, R. B., Stewart, J. P., Seyhan, E., Silva, W. J., Chiou, B. S., . . . Donahue, J. L. (2013). *PEER NGA-West2 Database.* Berkeley: Pacific Earthquake Engineering Research Center.

Applied Technology Council . (1997). *FEMA 273: NEHERP Guidelines for the Seismic Rehabilitation of Buildings.* Washington, D.C.: Federal Emergency Management Agency.

Applied Technology Council. (2010). *Modeling and acceptance criteria for seismic design and analysis of tall buildings.* Redwood City: Applied Technology Council.

ASCE. (2013). *Minimum Design Loads for Buildings and Other Structures (ASCE/SEI 7-10).* American Society of Civil Engineers: Reston, Virginia.

ASCE. (2013). *Seismic Evaluation and Upgrade of Existing Buildings (ASCE/SEI 41-13).* Reston, Virginia: American Society of Civil Engineers.

ATC. (2015). *ATC 78-3: Seismic evaluation of older concrete frame buildings for collapse*

potential. Redwood City, California: Applied Technology Council.

Baker, J. W. (2011). Conditional Mean Spectrum: Tool for ground motion selection. *Journal of Structural Engineering, 137*(3), 322-331.

Baker, J. W., & Cornell, C. A. (2006). Spectral shape, epsilon and record selection. *Earthquake Engineering and Structural Dynamics, 35*, 1077–1095. doi:10.1002/eqe.571

Bakis, C. E., Bank, L. C., Brown, V. L., Cosenza, E., Davalos, J. F., Lesko, J. J., . . . Triantafillou, T. C. (2002). Fiber-Reinforced Polymer Composites for Construction—State-of-the-Art Review. *Journal of Composites for Construction, 6*(2), 73-87.

Baradaran Shoraka, M., Yang, T. Y., & Elwood, K. J. (2013). Seismic loss estimation of non-ductile reinforced concrete buildings. *Earthquake Engineering and Structural Dynamics, 42*(2), 297–310.

Bett, J., Klinger, R., & Jirsa, J. (1988). Lateral Load Response of Strengthened and Repaired Reinforced Concrete Columns. *ACI Strucutral Journal, 85*(5), 499-508.

Bousias, S., Biskinis, D., Fardis, M., & Spathis, A.-L. (2007). Strength, Stiffness, and Cyclic Deformation Capacity of Concrete Jacketed Members. *ACI Structural Journal, 104*(5), 521-531.

Bousias, S., Spathis, A.-L., & Fardis, M. (2004). Seismic Retrofitting of Columns with Lap-Splices via RC Jackets. *13th World Conference on Earthquake Engineering.* Vancouver.

Bozorgnia, Y., & Campbell, K. W. (2003). The Vertical-to-Horizontal Response Spectral Ratio and Tenative Procedures for Developing Simplified V/H and Vertical Design Spectra. *Journal of Earthquake Engineering*, 175-207. doi:10.1080/13632460409350486

Bozorgnia, Y., & Niazi, M. (1993). Distance scaling of vertical and horizontal response spectra of the Loma Prieta earthquake. *Earthquake Engineering and Structural Dynamics, 22*(8), 695–707. doi:10.1002/eqe.4290220805

Bozorgnia, Y., Niazi, M., & Campbell, K. (1995, November). Characteristics of Free-Field Vertical Ground Motion during the Northridge Earthquake. *Earthquake Spectra, 11*(4), 515-525.

Brena, S. F., & Alcocer, S. M. (2009). Seismic Performance Evaluation of Rehabilitated Reinforced Concrete Columns through Jacketing. *ATC & SEI 2009 Conference on Improving the Seismic Performance of Existing Buildings and Other Structures* (pp. 572-583). ASCE.

Building Seismic Safety Council. (2004). *NEHRP Recommended Provisions for Seismic Regulations for New Buildings and Other Strucutres* (FEMA 450-3/2003 ed.). Washington, D.C.: FEMA.

Button, M., Cronin, C., & Mayes, R. (2002). Effect of Vertical Motions on Seismic Response of Highway Bridges. *Journal of Structural Engineering, 128*(12), 1551-1564. doi:10.1061/(ASCE)0733-9445(2002)128:12(1551)

CEN, European Committee for Standardisation. (2003). *Eurocode 8: Design Provisions for Earthquake Resistance of Structures, Part 1.1: General rules, seismic actions and rules for buildings.*

Chalioris, C., Thermou, G., & Pantazopoulou, S. (2014). Behaviour of rehabilitated RC beams with self-compacting concrete jacketing – Analytical model and test results. *Construction*

and Building Materials, 55, 257–273.

Chang, S., Bray, J., & Seed, R. (1996). Engineering Implications of Ground Motions from the Northridge Earthquake. *Bulletin of the Seismological Society of America, 86*(1B), S270-S288.

City of Los Angeles. (2015). *Ordinance No. 183893, Amending Divisions 93 and 95 of Article I of Chapter IX of the Los Angeles Municipal Code.*

Collier, C. J., & Elnashai, A. S. (2001). A Procedure for Combining Vertical and Horizontal Seismic Action Effects. *Journal of Earthquake Engineering, 5*(4), 521 — 539. doi:10.1080/13632460109350404

Dhakal, R., & Maekawa, K. (2002). Modeling for Postyield Buckled of Reinforcement. *Journal of Structural Engineering, 128*(9), 1139-1147.

Di Sarno, L., Elnashai, A., & Manfredi, G. (2011). Assessment of RC columns subjected to horizontal and vertical ground motions. *Engineering Structures*, 1514–1535.

Dogangun, A. (2004). Performance of reinforced concrete buildings during the May 1, 2003 Bingo ̈l Earthquake in Turkey . *Engineering Strucutres*, *26*, 841-856.

Eads, L., Miranda, E., Krawinkler, H., & Lignos, D. (2012). Improved Estimation of Collapse Risk for Structures in Seismic Regions. *15th World Conference on Earthquake Engineering.* Lisbon.

Ellingwood, B., Galambos, T., MacGregor, J., & Cornell, C. (1980). *Developement of a Probability Based Load Criterion for American National Standard A58.* Washington, D.C.: National Bureau of Standards.

Elnashai, A., & Papazoglou, A. (1997). Procedure and Spectra for Analysis of RC Structures Subjected to Strong Vertical Earthquake Loads. *Journal of Earthquake Engineering*, 121-155.

Elwood, K. J. (2004). Modelling failures in existing reinforced concrete. *Canadian Journal of Civil Engineering, 31*(5), 846-859. doi:10.1139/L04-040

Elwood, K. J. (2004). Modelling failures in existing reinforced concrete columns. *Canadian Journal of Civil Engineering, 31*, 846–859.

Elwood, K. J., Marquis, F., & Kim, J. H. (2015). Post-Earthquake Assessment and Repairability of RC Buildings: Lessons from Canterbury and Emerging Challenges. *Proceedings of the Tenth Pacific Conference on Earthquake Engineering*, (p. 9p). Sydney, Australia.

Elwood, K. J., Matamoros, A. D., Wallace, J. W., Lehman, D. E., Heintz, J. A., Mitchell, A. D., . . . Moehle, J. P. (2007). Update to ASCE/SEI 41 Concrete Provisions. *Earthquake Spectra, 23*(3), 493-523.

Fakharifar, M., Chen, G., Dalvand, A., & Shamsabadi, A. (2015). Collapse Vulnerability and Fragility Analysis of Substandard RC Bridges Rehabilitated with Different Repair Jackets Under Post-mainshock Cascading Events. *International Journal of Concrete Structures and Materials, 9*(3), 345–367.

FEMA. (1997). *NEHRP Commentary on the Guidelines for the Seismic Rehabilitation of Buildings.* Federal Emergency Management Agency.

FEMA. (2009). *Quantification of Building Seismic Performance Factors* .

FEMA. (2012). *Seismic Performance Assessment of Buildings, Volume 1 – Methodology.* Washington, D.C.: Federal Emergency Management Agency.

FEMA. (2015). *NEHRP Recommended Seismic Provisions for New Buildings and Other Structures Volume I: Part 1 Provisions, Part 2 Commentary.* Washington, D.C.: Building Seismic Safety Council.

FEMA and ASCE. (2000). *FEMA 356: Prestandard and Commentary for the Seismic Rehabilitation of Buildings.* Washington, D.C.: Federal Emergency Management Agency.

Filippou, F. C., Popov, E. P., & Bertero, V. V. (1983). *Effects of Bond Deterioration on Hysteretic Behavior of Reinforced Concrete Joints.* University of California, Berkeley. Earthquake Engineering Research Center.

Galanis, P. H., & Moehle, J. P. (2015). Development of Collapse Indicators for Risk Assessment of Older-Type Reinforced Concrete Buildings. *Earthquake Spectra, 31*(4), 1991–2006.

Goel, R. K., & Chadwell, C. (2008). Evaluation of ASCE-41 Nonlinear Static Procedure Using Recorded Motions of Reinforced-Concrete Buildings. *Structures Congress 2008: Crossing Borders.* Vancouver, Canada: ASCE.

Gulerce, Z., & Abrahamson, N. A. (2010). Vector-Valued Probabilistic Seismic Hazard Assessment for the Effects of Vertical Ground Motions on the Seismic Response of Highway Bridges. *Earthquake Spectra, 26*(4), 999–1016. doi:10.1193/1.3464548

Gulerce, Z., Erduran, E., Kunnath, S., & Abrahamson, N. A. (2012). Seismic demand models for probabilistic risk analysis of near fault vertical ground motion effects on ordinary highway bridges. *Earthquake Engineering and Strucutral Dynamics, 41,* 159-175. doi:10.1002/eqe.1123

Gumbel, E. (1958). *Statistics of Extremes.* New York: Columbia University Press.

Harrington, C. C., & Liel, A. B. (2016). Collapse assessment of moment frame buildings, considering vertical ground shaking. *Earthquake Engineering and Strucutral Dynamics*.

Harris, J. L., & Speicher, M. S. (2015). *Assessment of First Generation Performance- Based Seismic Design Methods for New Steel Buildings, Volume 2: Special Concentrically Braced Frames.* NIST Technical Note, National Institute of Standards and Technology, Gaithersburg, MD.

Harris, J. L., & Speicher, M. S. (2015). *Assessment of First Generation Performance-Based Seismic Design Methods for New Steel Buildings, Volume 1: Special Moment Frames.* NIST Technical Note , National Institute of Standards and Technology, Gaithersburg, MD.

Haselton Baker Risk Group. (n.d.). *Seismic Performance Prediction Program (SP3)*. Retrieved from www.hbrisk.com

Haselton, C. B., & Deierlein, G. G. (2006, December). *Assessing Seismic Collapse Saftey of Modern Reinforced Concrete Moment Frame Buildings.* Racific Earthquake Engineering Research Center. Stanford University.

Haselton, C. B., Liel, A. B., & Deierlein, G. G. (2009). Important Issues and Suggested Best Practices in Simulating Structural Collapse Due to Earthquakes: Modeling Decisions, Model Calibration and Numerical Solution Algorithms. *CompDyn2009.* Greece.

Haselton, C. B., Liel, A. B., Deierlein, G. G., Dean, B. S., & Chou, J. H. (2011). Seismic Collapse Safety of Reinforced Concrete Buildings: I. Assessment of Ductile Moment Frames.

American Society of Civil Engineers Journal of Structural Engineering, 137(4), 481-491.

Haselton, C. B., Liel, A. B., Lange, T., & Deierlein, G. G. (2008). *Beam-Column Element Model Calibrated for Predicting Flexural Response Leading to Global Collapse of RC Frame Buildings.* Berkeley: Pacific Engineering Research Center.

Hastie, T., Tibshirani, R., & Friedman, J. (2008). *The Elements of Statistical Learning - Data Mining, Inference, and Prediction.* Springer.

Heausler, T. (2004, Sept.). Practical use of the new load combinations. *Structure Magazine*.

Housner, G. W. (1952). Spectrum intensities of strong motion earthquakes. *Proceedings of the Symposium on Earthquakes and Blast Effects on Structures* (pp. 20-36). Earthquake Engineering Research Institute.

International Code Council. (2011). *2012 international building code.* Country Club Hills, Ill, ICC.

International Conference of Building Officials. (1967). *Uniform building code.* Pasadena, California: International Conference of Building Officials.

Jack R. Benjamin and Associates, Inc. (1988). *A criterion for determining exceedance of the operating basis earthquake.* Palo Alto, California: Electric Power Research Institute.

Jalayer, F., & Cornell, C. A. (2009). Alternative Nonlinear Demand Estimation Methods for Probability-Based Seismic Assessments. *Earthquake Engineering And Structural Dynamics, 38*(8), 951-972.

Kent, D. C., & Park, R. (1971). Flexural members with confined concrete. *ASCE Journal of the Structural Division, 97*(7), 1969–1990.

Kim, I., & Hagen, G. (2014). Seismic Assessment and Retrofit of Existing RC Buildings: Case Studies from Degenkolb Engineers. *SP-297 Seismic Assessment of Existing Reinforced Concrete Buildings,* 9.1-9.12.

Kim, S., Holub, C. J., & Elnashai, A. S. (2011). Analytical Assessment of the Effect of Vertical Earthquake. *Journal of Structural Engineering*, 252-260.

Kunnath, S. K., Erduran, E., Chai, Y. H., & Yashinsky, M. (2008). Effect of Near-Fault Vertical Ground Motions on Seismic Response of Highway Overcrossings. *Journal of Bridge Engineering*, 282-290.

Lam, L., & Tang, J. G. (2003). Design-oriented stress–strain model for FRP-confined concrete. *Construction and Building Materials, 17*(6-7), 471–489.

Li, Y., Elwood, K. J., & Hwang, S. J. (2014). Assessment of ASCE/SEI 41 Concrete Column Provisions using Shaking Table Tests. *ACI Structural Journal, 297*, 1-22.

Liel, A. B., & Deierlein, G. G. (2013). Cost-Benefit Evaluation of Seismic Risk Mitigation Alternatives for Older Concrete Frame Buildings. *Earthquake Spectra*, *29*(4), 1391-1411.

Liel, A. B., Haselton, C. B., & Deierlein, G. G. (2011). Seismic Collapse Saftey of Reinforced Concrete Buildings: II. Comparative Assessment of Non-Ductile and Ductile Moment Frames. *Journal of Strucutral Engineering, 137*(4), 492-502.

Liel, A., Haselton, C., & Deierlein, G. (2011). Seismic Collapse Safety of Reinforced Concrete Buildings: II. Comparative Assessment of Non-Ductile and Ductile Moment Frames. *Journal of Structural Engineering, 137*(4), 492-502.

Lin II, R.-G., Xia, R., & Smith, D. (2014, January 25). For Los Angeles, list is a first step toward improved quake safety. *Los Angeles Times*. Retrieved from http://www.latimes.com/local/la-me-adv-earthquake-concrete-list-20140126-story.html

Luco, N., Ellingwood, B., Hamburger, R., Hooper, J., Kimball, J., & Kircher, C. (2007). Risk-Targeted versus Current Seismic Design Maps for the Conterminous United States. Structural Engineers Association of California.

Maison, B. F., Kasai, K., & Deierlein, G. (2009). ASCE-41 and FEMA-351 Evaluation of E-Defense Collapse Test. *Earthquake Spectra, 25*(4), 927–953.

Mander, J. B., Priestley, N. M., & Park, R. (1988). Theoretical Stress-Strain Model for Confined Concrete. *Journal of Structural Engineering, 114*(8), 1804-1826.

Megalooikonomou, K. G., Monti, G., & Santini, S. (2012). Constitutive Model for Fiber – Reinforced Polymer - and Tie – Confined Concrete. *ACI Structural Journal, 109*(4), 569-578.

Mirmiran, A., & Shahawy, M. (1997). Behavior of Concrete Columns Confined by Fiber Composites. *Journal of Strucutal Engineering, 123*(5), 583-590.

Moehle, J. (2000). State of Research on Seismic Retrofit. *US-Japan Symposium and Workshop on Seismic Retrofit of Concrete Structures—State of Research and Practice.*

Moehle, J. P., Hooper, J. D., & Lubke, C. D. (2008). *Seismic Design of Reinforced Concrete Special Moment Frames: A Guide for Practicing Engineers.* Gaithersburg, MD: National Institute of Standards and Technology.

Moon, Y.-I., Rajagopalan, B., & Lall, U. (1995, September). Estimation of mutual information using kernel density estimators. *Physical Review E, 52*(3), 2318--2321.

Neuenhofer, A., & Filippou, F. (1998, June). Geometrically Nonlinear Flexibility-Based Frame Finite Element. *Journal of Structural Engineering, 124*(6), 704-711.

Newmark, N. M., Blume, J. A., & Kapur, K. (1973). Seismic Design Spectra for Nuclear Power Plants. *Journal of the Power Division, 99*(2).

Niazi, M., & Bozorgnia, Y. (1990). Observed ratios of PGV/PGA and PGD/PGA for deep soil sites across SMART-1 array, Taiwan. *Fourth US National Conference on Earthquake Engineering, 1*, pp. 367–374. Palm Springs.

Niazi, M., & Bozorgnia, Y. (1992). Behavior of near-source vertical and horizontal response spectra at SMART-1 array, Taiwan. *Earthquake Engineering and Structural Dynamics, 21*, 37–50.

Palieraki, V., & Vintzileou, E. (2009). Cyclic Behaviour of Interfaces in Repaired/Strengthened RC Elements. *ARCHITECTURE CIVIL ENGINEERING ENVIRONMENT* , 97-108.

Papavasileiou , G. S., & M egalooikonomou, K. G. (2015). Numerical Simulation of FRP-Confined Circular Bridge Piers Using Opensees. *Opensees Days Italy (OSD), Second International Conference.* University of Salerno, Fisciano, Salerno, Italy.

Papazoglou, A. J., & Elnashai, A. S. (1996). Analytical and field evidence of the damaging effect of vertical earthquake ground motion. *Earthquake Engineering and Structural Dynamics, 25*, 1109-1137.

Paulay, T., & Priestley, M. N. (1992). *Seismic Design of Reinforced Concrete and Masonry*

Buildings. New York: John Wiley and Sons.

Pekelnicky, R., & Poland, C. (2012). ASCE 41-13: Seismic Evaluation and Retrofit of Existing Buildings. *SEAOC 2012 Convention.* Strucutral Engineers Association of California.

Petersen, M. D., Frankel, A. D., Harmsen, S. C., Mueller, C. S., Haller, K. M., Wheeler, R. L., . . . Rukstales, K. S. (2008). *Documentation for the 2008 Update of the United States National Seismic Hazard Maps.* U.S. Geological Survey.

Porter, K. A. (2003). An Overview of PEER's Performance-Based Earthquake Engineering Methodology. *Ninth International Conference on Applications of Statistics and Probability in Civil Engineering (ICASP9).* San Francisco.

Porter, K. A. (2003). An Overview of PEER's Performance-Based Earthquake Engineering Methodology. *Ninth International Conference on Applications of Statistics and Probability in Civil Engineering (ICASP9).* San Francisco: PEER.

Priestley, M. N., Seible, F., & Calvi, G. M. (1996). *Seismic design and retrofit of bridges.* New York: John Wiley & Sons, Inc.

Priestley, N. M., Seible, F., Xiao, Y., & Verma, R. (1994). Steel Jacket Retrofitting of Reinforced Concrete Bridge Columns for Enhanced Shear Strength Part 1: Theoretical Considerations and Test Design. *ACI Structural Journal, 91*(4), 394-405.

Raghunandan, M., Liel, A., & Luco, N. (2014). Collapse Risk of Buildings in the Pacific Northwest Region due to Subduction Earthquakes. *Earthquake Spectra*. doi:http://dx.doi.org/10.1193/012114EQS011M

Raghunandan, M., Liel, A., & Luco, N. (2015). Collapse Risk of Buildings in the Pacific Northwest due to Subduction Earthquakes. *Earthquake Spectra, 31*(4), 2087 -2115.

Ramirez, C. M., Liel, A. B., Mitrani-Reiser, J., Haselton, C. b., Spear, A. D., Steiner, J., . . . Miranda, E. (2012). Expected earthquake damage and repair costs in reinforced concrete frame buildings. *Earthquake Engineering and Strucutral Dynamics, 41*(11), 1455–1475.

Saadeghvaziri, M. A., & Foutch, D. A. (1991). Dynamic behaviour of R/C highway bridges under combined effects of vertical and horizontal earthquake motions. *Earthquake Engineering and Structural Dynamics, 20*, 535–549.

Sarma, S. K., & Yang, K. S. (1987). An evaluation of strong motion records and a new parameter A95. *Earthquake Engineering and Structural Dynamics, 15*(1), 119–132.

Sattar, S., & Hulsey, A. M. (2015). Assessment of First Generation Performance-Based Seismic Design Methods: Case Study of a 4-Story Reinforced Concrete Special Moment Frame Building. *Structures Congress* (pp. 984-994). Portland, Oregon: ASCE.

Sattar, S., & Liel, A. B. (under review). Collapse Indicators for Existing Nonductile Concrete Frame Buildings with Varying Column and Frame Characteristics. *Engineering Structures*.

Schwarz, G. (1978). Estimating the Dimension of a Model. *Annals of Statistics, 6*(2), 461-464.

Scott, M. H., & Fenves, G. L. (2006, February). Plastic Hinge Integration Methods for Force-Based Beam–Column Elements. *Journal of Structural Engineering*.

Scott, M. H., & Hamutcuoglu, O. M. (2008). Numerically consistent regularization of force-based. *International Journal for Numerical Methods in Engineering, 76*(10), 1612–1631. doi:10.1002/nme.2386

SEAOSC. (under review). *SEAOSC Design Guide — City of Los Angeles NDC Building Ordinance.* Los Angeles, CA: Structural Engineers Association of Southern California.

Searer, G. R., Paret, T. F., & Freeman, A. S. (2008). ASCE-31 and ASCE-41: What Good Are They? *Structures 2008: Crossing Borders.* Vancouver, British Columbia, Canada: American Society of Civil Engineers.

Silva, W. (1997). Characteristics of vertical strong ground motions for applications to engineering design. *FHWA/NCEER Workshop on the National Representation of Seismic Ground Motion for New and Existing Highway Facilities, Burlingame, CA, Proceedings.* Buffalo: National Center for Earthquake Engineering Research.

Smyth, A. W., Altay, G., Deodatis, G., Erdik, M., Franco, G., Gulkan, P., . . . Yuzugullud, O. (2004). Probabilistic Benefit-Cost Analysis for Earthquake Damage Mitigation: Evaluating Measures for Apartment Houses in Turkey. *Earthquake Spectra, 20*(1), 171–203.

Sun, Z., Seible, F., & Priestley, M. N. (1993). *Flexural Retrofit of Rectangular Reinforced Concrete Bridge Columns by Steel Jacketing.* University of California, San Diego.

Takahashi, N., & Shiohara, H. (2004). Life Cycle Economic Loss Due to Seismic Damage of Nonstructural Elements. *13th World Conference on Earthquake Engineering.* Vancouver, B.C., Canada.

Tesfamariam, S., & Goda, K. (2015). Loss estimation for non-ductile reinforced concrete building in Victoria, British Columbia, Canada: effects of mega-thrust Mw9-class subduction earthquakes and aftershocks. *Earthquake Engineering & Structural Dynamics, 44*, 2303-2320.

Tezcan, J., & Cheng, Q. (2012). A nonparametric characterization of vertical ground motion effects. *Earthquake Engineering and Strucutral Dynamics, 41*, 515–530. doi:10.1002/eqe.1142

Thermou, G. E., & Elnashai, A. S. (2006). Seismic retrofit schemes for RC structures and local–global consequences. *Earthquake Engineering and Structural Dynamics, 8*, 1-15.

Tothong, P., & Luco, N. (2007). Probabilistic seismic demand analysis using advanced ground motion intensity measures. *Earthquake Engineering & Structural Dynamics, 36*(13), 1873-1860.

Tu, Y.-H. (2016). *Reconnaissance Report: 2016/02/06 Meinong Earthquake, Kaohsiung, Taiwan Main damage area: Tainan.* Berkeley, CA: PEER.

Vamvatsikos, D., & Cornell, C. (2002, March). Incremental Dynamic Analysis. *Earthquake Engineering and Strucutral Dynamics, 31*(3), 491-514.

Vamvatsikos, D., & Zeris, C. (2008). Influence of Uncertian Vertical Loads and Accelerations on the Seismic Performance of an RC Building. *3rd Panhellenic Conference on Earthquake Engineering and Engineering Seismology.* Athens.

Vandoros, K. G., & Dritsos, S. E. (2006). Axial preloading effects when reinforced concrete columns are strengthened by concrete jackets. *Prog. Struct. Engng Mater.*(8), 79–92.

Vecchi, F., & Collins, M. (1988). Prediciting the Response of Reinforced Concrete Beams Subjected to Shear Using Modified Compression Field Theory. *ACI Structural Journal* , 258-268.

Watabe, M., Tohido, M., Chiba, O., & Fukuzawa, R. (1990). Peak accelerations and response

spectra of vertical strong motions from near-field records in USA. *Eighth Japan Earthquake Engineering Symposium, Proceedings, 1*, pp. 301–306.

Welsh-Huggins, S. J., & Liel, A. B. (under review). Is hazard resilience sustainable? Evaluating multi-objective outcomes from enhanced seismic design decisions.

Ye, L., Ma, Q., Zhiwei, M., Guan, H., & Zhuge, Y. (2013). Numerical and comparative study of earthquake intensity indices in seismic analysis. *The Structural Design of Tall and Special Buildings, 22*(4), 362–381.

Yucemen, M. S., Ozcebe, G., & Pay, A. C. (2004). Prediction of potential damage due to severe earthquakes. *Structural Safety, 26*(3), 349–366. doi:10.1016/j.strusafe.2003.09.002